CELLULAR TRANSPORT, METABOLISM AND TOXICITY OF SELENIUM IN RAINBOW TROUT (*Oncorhynchus mykiss*)

A Thesis Submitted to the College of

Graduate Studies and Research

In Partial Fulfillment of the Requirements

For the Degree of Doctor of Philosophy

In the Department of Biology

University of Saskatchewan

Saskatoon

By

Sougat Misra

PERMISSION TO USE

In presenting this thesis in partial fulfilment of the requirements for a Postgraduate degree from the University of Saskatchewan, I agree that the Libraries of this University may make it freely available for inspection. I further agree that permission for copying of this thesis in any manner, in whole or in part, for scholarly purposes may be granted by the professor or professors who supervised my thesis work or, in their absence, by the Head of the Department or the Dean of the College in which my thesis work was done. It is understood that any copying or publication or use of this thesis or parts thereof for financial gain shall not be allowed without my written permission. It is also understood that due recognition shall be given to me and to the University of Saskatchewan in any scholarly use which may be made of any material in my thesis.

DISCLAIMER

The name of company, corporation, brand name and website were exclusively created to meet the thesis and/or exhibition requirements for the degree of Degree of Doctor of Philosophy at the University of Saskatchewan. Reference in this thesis/dissertation to any specific commercial products, process, or service by trade name, trademark, manufacturer, or otherwise, does not constitute or imply its endorsement, recommendation, or favoring by the University of Saskatchewan. The views and opinions of the author expressed herein do not state or reflect those of the University of Saskatchewan, and shall not be used for advertising or product endorsement purposes.

Requests for permission to copy or to make other use of material in this thesis in whole or part should be addressed to:

Head of the Department of Biology

University of Saskatchewan

Saskatoon, Saskatchewan, S7N 5E2

Canada

ABSTRACT

The present research was designed to investigate the mechanisms of cellular transport, metabolism and toxicity of selenium [inorganic (selenite) and organic (selenomethionine)] in a model teleost, rainbow trout (*Oncorhynchus mykiss*), using both *in vitro* and *in vivo* experimental approaches. The transport properties of selenite and its thiol (glutathione and cysteine) reduced forms were examined in isolated enterocytes and hepatocytes. The kinetics of selenite uptake revealed a linear profile in both cell types, suggesting a low affinity transport process. However, the uptake kinetics was different between the two cell types in the presence of extracellular glutathione, since a concentration-dependent Hill uptake kinetics was recorded in enterocytes, while a linear kinetics persisted in hepatocytes. Both cysteine and glutathione augmented cellular selenium accumulation in these cells. The selenium transport was found to be energy independent, but sensitive to the extracellular pH and inorganic mercury. The pharmacological examination suggested that the cellular transport of selenite is primarily mediated by anion transport systems (e.g., sulphite transporters and/or bicarbonate transporters), although cell-specific differences in transport efficiency was apparent. The metabolism of selenite, selenate and selenomethionine in hepatocytes was examined using X-ray absorption near edge structure spectroscopy (XANES). Inorganic and organic forms of selenium appeared to be metabolized *via* different cellular pathways, as both selenite and selenate were found to be metabolized into elemental selenium, whereas selenocystine constituted the primary metabolite of selenomethionine. My findings also suggested direct enzymatic transformation of selenomethionine into methylselenol at high exposure level, a process that leads to enhanced intracellular reactive oxygen species generation because of the redox-reactive properties of methylselenol. To validate the metabolite profile of selenium observed in *in vitro* studies, the

tissue-specific differences in selenium metabolism *in vivo* was analyzed in fish exposed to elevated dietary selenomethionine for two weeks. Similar to the observation in hepatocytes, selenocystine and selenomethionine were found to be the major selenium species across tissues, although there were differences in their relative proportion in different tissues. In addition, a good correlation between the total selenium burden and selenocystine fraction was recorded among all the major tissues except gonads. To understand the role of oxidative stress in cellular toxicity of selenium, isolated trout hepatocytes were exposed to increasing dosage of selenite and selenomethionine over a period of 24h. Selenite was found to be 10 times more toxic than selenomethionine to the hepatocytes. Both selenite and selenomethionine induced rapid generation of reactive oxygen species, which subsequently triggered an upregulation of enzymatic antioxidants. Interestingly, a sharp dose-dependent decrease in intracellular thiol redox (reduced to oxidized glutathione ratio) was recorded with exposure to both selenite and selenomethionine, indicating that glutathione plays an important role in mediating selenium toxicity. At the high exposure dosage, both selenium compounds compromised membrane and DNA integrity, disrupted intracellular calcium homeostasis, and induced enzymatic apoptosis pathway, ultimately leading to cell death *via* aponecrosis. These findings suggested that high selenium exposure causes cellular toxicity by inducing a rapid loss of the intracellular reducing milieu. Overall, the findings from the present study provided novel information on the transport, metabolism and toxicity of selenium in fish. This fundamental information will be useful in understanding the chemical species-specific toxicity of selenium in fish, and may help in identifying cellular biomarkers for assessing the health of selenium-impacted natural fish populations.

Acknowledgements

I thank Dr. Som Niyogi, my mentor, for his support and guidance throughout my Ph.D. His commitment to science and encouragement were inspiring. I extend my special thanks to him for allowing me to pursue my Ph.D. work with 'selenium'.

I am thankful to my committee members, Drs. Derek Peak, David M. Janz and Jack Gray for their valuable advice and important contribution in the present work.

This acknowledgement is incomplete without extending my cordial thankfulness to all the teachers in my life, starting from the elementary school to the university. I could not have done this without their immense encouragement, guidance and sharing of the serendipitous joy of education.

I extend my gratitude to all the faculty, staff, and graduate students members in the Department of Biology. I am especially thankful to Diedre Wasyliw, Joan Virgl, Shirley Hleck, Guosheng Liu, Marlyn Mierau, Drs. Steve Wiseman (Toxicology Centre), Ning Chen (CLS), Vipen Sawhney, Doug Chivers, Neil Chilton, Yangdou Wei, Ken Wilson and Chris Todd for their support when it needed most. A very special thank goes to Sheri and Glyn for being very good friends over the years.

I thank Dr. Peta Bonham-Smith for her unconditional encouragement, thoughtful insights and mentorship.

I am thankful to fellow graduate students Aditya, Jake, Charmain, Prasad, Eric, Shaun, Graham and Chad. Amongst my many wonderful friends and colleagues, Jitabrata, Malay, Raymond, Naveen and Bidraha encouraged me to think critically, to grow and to appreciate science – all of which were important in the pursuit of science as a graduate student.

Most deeply, I am delightful to thank my parents, Shefali and Chitta Ranjan Misra, who believe that I can always excel irrespective of the situation. It is my great honor and pride to acknowledge both of you that it has added an invaluable responsibility in my way life. It is not only your love and affection that has been a continuous driving force, but also you have taught me to ask the question with confidence "Why".

Very special thanks go to my wife, Beauti, for her love, support and encouragement, ever since she has joined me. My apology to her for all the sacrifices she has suffered over the years while I remained busy with 'my' work. I am also grateful to my sisters Krishna, Samita and Mitali for their love, fight and support. I will be ever indebted to my uncle, Mr. Mihir Misra, for everything that he has done for me.

I acknowledge the financial contributions of the NSERC (Natural Sciences and Engineering Research Council), CFI (Canadian Foundation for Innovations) and the University of Saskatchewan College of Graduate Studies and Research. I am thankful to the University of Saskatchewan College of Graduate Studies and Research, SETAC (Society of Environmental Toxicology and Chemistry) and SOT (Society of Toxicology) for the travel awards that helped me attending the meetings and conferences. The research described in this thesis was performed at the Canadian Light Source, which is supported by NSERC, NRC (National Research Council, Canada), CIHR (Canadian Institutes of Health Research), and the University of Saskatchewan.

Dedication

I dedicate this thesis to my late grandfather, Mr. Nabagopal Misra, who was a farmer and lived most of his life at a remote village in India, yet always dreamt that one of his grandsons will receive his education in abroad.

Table of Contents

List of Figures

List of abbreviations

$[Ca^{2+}]_i$	Intracellular calcium
°C	Degree Celsius
µg	Microgram
µl	Microliter
µm	Micrometer/Micron
µM	Micromolar
AE1	Anion exchanger protein 1
AI	Anterior intestine
ANOVA	Analysis of variance
ATRF	Aquatic Toxicology Research Facility
Bmax	Maximum rate of uptake
Ca^{2+}	Calcium ion (divalent)
CAT	Catalase
CH_3SeH	Methyl-selenol
cm^2	Centimeter square
cpm	Count per minute (radioactivity)
DCCD	Dicyclohexylcarbodiimide
DFO	Dimethylformamide
DIDS	4,4′-Diisothiocyanostilbene-2,2′-disulfonic acid
DIO	Deiodinases
DNA	Deoxyribonucleic acid
EC_{50}	Median (or half-maximal) effective concentration
EDTA	Ethylenediaminetetraacetic acid

eV	Electron volt
Fe	Iron
g	Gram
Ge	Germanium
GeV	Giga-electron volt
GFAAS	Graphite furnace atomic absorption spectroscopy
GPx	Glutathione peroxidase
GSH	Reduced glutathione
$GSSe^{-}$	Selenopersulfide
GSSeSG	Selenotrisulfide
GSSG	Oxidized glutathione
$GSSG^{\cdot -}$	Glutathione disulfide radical
h	Hour
H_2O_2	Hydrogen peroxide
H_2Se	Hydrogen selenide
HCO^{3-}	Bicarbonate anion
Hg^{2+}	Divalent mercury
HPLC-ICPMS	High-performance liquid chromatography coupled with inductively coupled plasma mass spectrometry
Kb	Kilobases
K_d	Concentration at which half of maximal transport rate is attained
KEGG	Kyoto Encyclopaedia of Genes and Genomes
Kg	Kilogram
K_m	Michaelis-Menten constant

K-S test	Kolmogorov-Smirnov test
L^{-1}	Per liter
LDH	Lactate dehydrogenase
LSM	Laser scanning microscopy
MBTH	3-methylbenzthiazolinone-2-hydrazone
MCT	Monocarboxylate transporter proteins
mg	Milligram
$mg.L^{-1}$	Milligram/litre
min	Minute
MS-222	Tricaine methanesulfonate
mU	Milliunit
N_2	Nitrogen
NADPH	Nicotinamide adenine dinucleotide phosphate
PI	Posterior intestine
R^2	Regression coefficient
RFU	Relative fluorescent unit
ROS	Reactive oxygen species
S	Sulphur
s	Second
SCB	Sodium-cacodylate buffer
Se	Selenium
Se^0	Elemental selenium
Sel	Selenoprotein
S.E.M.	Standard error of the mean

SEM	Scanning electron microscopy
SeMetO	Methionine selenoxide
SeO_3^{2-}	Selenite
SeO_4^{2-}	Selenate
SLC16	Solute carrier family proteins 16
SLC26	Solute carrier family proteins 26
SLC26A1	Solute carrier protein 26A1
SLC26A3	Solute carrier protein 26A3
SOD	Superoxide dismutase
SPS	Selenophosphate synthases
T3	Triiodothyronine
T4	Thyroxine
TBARS	Thiobarbituric acid reactive substances
TCA	Trichloroacetic acid
TrxR	Thioredoxin reductases
UV	Ultraviolet
V_{max}	Maximum rate of uptake
XANES	X-ray absorption near-edge structure

CHAPTER 1: General Introduction

1.1 A historical preview

Selenium was discovered in 1818 at the laboratory of a Swedish scientist, Dr. Jöns Jacob Berzelius. The discovery was first reported in the journal *Annales De Chimie Et De Physique* in the form of a letter to the editor by Dr. Berzelius (Berzelius, 1818). The original letter was published in French. Here is the translated form in English, stating the discovery of the new metalloid.

> *"This new alkali was discovered by M. Arfredson, a very clever young chemist, who had worked in my lab for a year. He had found this alkali in a rock already discovered by M. d'Andrada, in the mine d'Uto, which he named Petalite. This rock consisted of, neglecting the fractions, 80pc of silica, 17pc of alumina, and 3pc of the new alkali. To remove it, we used the ordinary methods to calcinate the stone to a powder with barium carbonate, and to separate all the land."*

Since the discovery of selenium, there was little or no use of selenium until 1883, when Dr. Charles Fritts first used selenium as a semiconductor material in the solar cell that he invented. Subsequently, the use of selenium in various industrial and agricultural processes led to its elevated exposure to biota and emergence as a toxic contaminant. The first authentic report on selenium toxicity in livestock was reported by Madison (1860). Later in 1930's, a detailed description of selenium toxicity was reported in farm animals (Dudley, 1936a) and humans working in copper mines (Dudley, 1936b). Byers and Lakin (1939) reported that some plants that grow naturally in the cretaceous soils (both in USA and Canada) were toxic to farm animals. At the time this report was published, both of these authors were working in the Department of Agriculture of the United States of America. The authors stated that they conducted the research in west-central Canada (province of Saskatchewan, Alberta and Manitoba) following the suggestion of Dr. L.E. Kirk (University of Saskatchewan), and were accompanied by J.L. Bolton from the Dominion Agricultural Experiment Station at Swift Current, Saskatchewan (Byers and Lakin, 1939). They expressed their concern about the loss of livestock in some of the

experimental areas. Affected animals showed signs of 'frozen feet'- typically associated with the malformation of hoofs and even the loss of hoofs in certain cases. By this time, it was known that selenium can cause teratogenicity in chickens (Franke et al., 1936). Later studies by Thorvaldson and Johnson (1940) reported elevated level of selenium in wheat grown in Saskatchewan, and suggested that wheat grown in certain areas might be harmful if ingested in large quantities. The toxicity of selenium in fish was discovered around the same time, based on the laboratory studies conducted by Ellis et al. (1937). The authors observed mortality in goldfish (*Carassius auratus auratus*) when exposed to 2 $mg.L^{-1}$ of sodium selenite for 18-46 days. Moreover, when the fish were exposed to 5 $mg.L^{-1}$ of sodium selenite, mortality occurred within 4-10 days. Thus, it was certainly known around 1940's that selenium at an elevated exposure level can be harmful to animals as well as humans.

At the time the concept of selenium as a toxicant was still emerging, an interesting observation by Dr. Jane Pinsent revolutionized our understanding about the role of selenium in biological systems by suggesting selenium as an essential constituent. While she was studying the activity of formic dehydrogenase, she found that selenium was essential for maintaining its high activity (Pinsent, 1954). Her insightful discussion led to the conclusion that selenium does not bind to this enzyme loosely, and a later study proved that to be correct as it was found that selenocysteine is an integral component of this enzyme molecule (Zinoni et al., 1986). Since the seminal work by Dr. Pinsent, it has been proved subsequently that selenium, considered therein as a component of α-factor 3, is an essential trace element that prevents necrotic liver disease in rat (Schwarz and Foltz, 1957). Thus, it took about 140 years since the discovery of selenium to prove the fact that selenium is an essential micronutrient for vertebrates.

1.2 Physiological basis of selenium essentiality

An essential trace element participates in several important biochemical pathways that translate into the functionality of cells and tissues. Thus, it is important to understand what confers the biological essentiality of selenium. In 1973, two independent research groups reported that selenium is an essential constituent of glutathione peroxidase (Flohé et al., 1973;

Rotruck et al., 1973), an enzyme previously reported to be involved in preventing oxidative breakdown of haemoglobin (Mills, 1959). This observation deciphered the link between selenium and oxidative stress, and led to the proposition that selenium has potential antioxidant properties. A plethora of scientific investigations have subsequently shown that selenium can protect biological systems against oxidative stress. This protective effect is mediated by the up-regulated synthesis of selenoproteins that can scavenge toxic free radicals. Selenium is also an integral component of the deiodinase enzymes, which play a critical role in thyroid hormone metabolism (Arthur et al., 1990; Behne et al., 1990). Using genomic tools, recent research has shown that mammals contain 23-25 selenoproteins (Lobanov et al., 2008). The physiological role of many of these selenoproteins is yet to be fully understood. Although a comprehensive appraisal of the physiological functionality of these selenoproteins is out of scope for this thesis, a synopsis of human selenoproteins and their critical role in cellular physiology is represented in Figure 1.1 (modified representation from Papp et al., 2007).

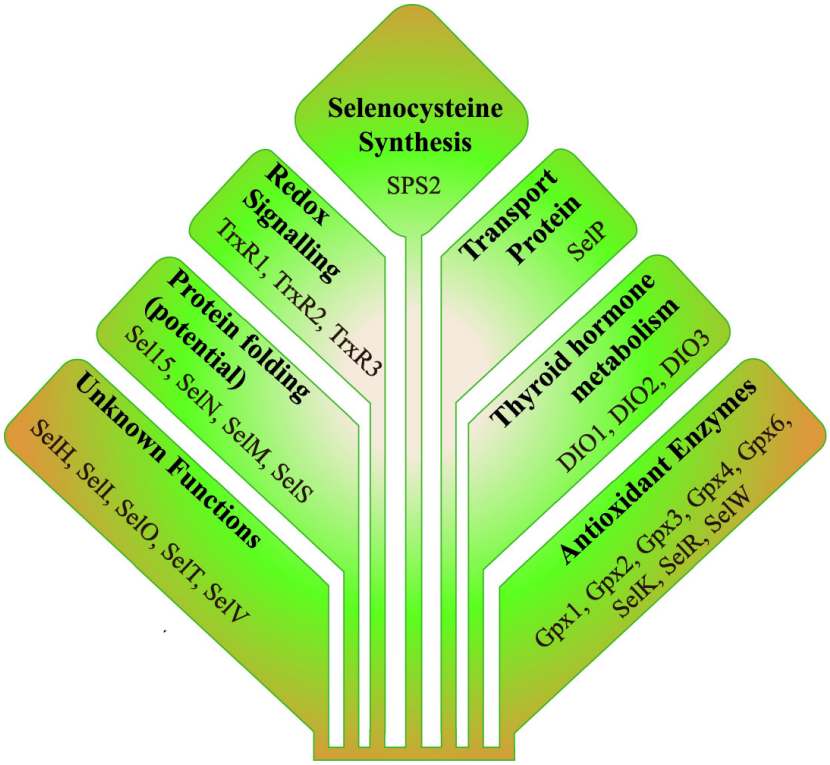

Figure 1.1: Graphical representation of human selenoproteins and their functionality. Abbreviations: SPS – Selenophosphate synthases, TrxR – Thioredoxin reductases, DIO – Deiodinases, GPx – Glutathione peroxidases, Sel – Selenoprotein.

Although selenium is essential for the functionality of many proteins that have important physiological roles, recent research indicates that the degree of essentiality vary across animal taxa. Lobanov et al. (2008) suggested that as life moved from the sea into the terrestrial environment, selenocysteine residues in some selenoproteins of terrestrial animals were replaced by its sulphur analog, cysteine. This observation is an indicator of reduced reliance on selenium in terrestrial vertebrates compared to their aquatic counterparts. For example, fish are known to have 32-34 selenoproteins, whereas terrestrial mammals contain only 23-25 selenoproteins (Lobanov et al., 2008). It would be unrealistic to think that these additional selenoproteins in fish do not serve any physiological functions. Otherwise, why would fish carry such an array of selenoproteins during their evolution that lasted over millions of years? The greater number of selenoproteins in fish may translate into a higher nutritional requirement of selenium in fish relative to that in humans. Interestingly, a comparative assessment of the daily selenium requirement between humans and fish supports this proposition. The daily requirement of selenium in an adult human is 55µg.day^{-1} (Institute of Medicine, 2000). Considering the body weight of 60 kg of an average human being, the daily required dose of selenium is 0.92 µg.day^{-1}.kg^{-1} body weight. In contrast, selenium requirement in fish is about 5-25 µg.day^{-1}.kg^{-1} body weight (Janz, 2011).

The basic understanding on the nutritional requirement of a micronutrient is incomplete without the information about the effects of its deficiency. Similar to many other micronutrients, experimental evidences on the deficiency syndromes in rats led Professor Klaus C. Schwarz to suggest that selenium is an essential micronutrient (Schwarz and Foltz, 1957). Selenium deficiency has been found to be either the cause of or at least a contributor to the exudative diathesis (oozing of fluid as a result of inflammation or injury) in chicken (Patterson et al., 1957; Schwarz et al., 1957), white muscle disease in calves, lamb, sheep and bird (Gill et al., 1980; Muth et al., 1958; Muth et al., 1959; Whanger et al., 1977), myopathy of cardiac and skeletal muscles in pig (Vanvleet et al., 1970) and infertility in rat (Wu et al., 1973). Early epidemiological studies indicated that selenium might have protective effects against cancer (Shamberger and Frost, 1969) and cardiovascular diseases (Frost and Olson, 1972) in humans, and therefore humans can become more susceptible to these diseases during selenium deficiency. To date, the effects of selenium deficiency in fish are extremely limited. It has been suggested

though that in the absence of vitamin E and selenium, Atlantic salmon (*Salmo salar*) show deficiency symptoms that are quite similar to those observed in mammals (Poston et al., 1976).

1.3 Selenium as a potential environmental toxicant

The cretaceous soil is a significant depository of selenium in the natural environment. Due to weathering effects, a substantial amount of selenium can thus be leached out from this seleniferous soil into the aquatic environment, the ultimate sink of contaminants. This phenomenon was first reported in the Colorado river that carried significant amount of selenium to the Gulf of California, although no adverse effects on resident fish populations were reported at that time (Williams and Byers, 1935).

Unfortunately, soil deposits are not the only source of selenium contamination into the aquatic environments. With the advent of science and technology, there is ever increasing use of selenium in different industries including, but not limited to, glass, pigment (plastic colouration), electronics, electrical rectifiers, photocopier and metallurgy (Butterman and Brown, 2004). Mining activities (e.g., uranium, coal, bentonite, phosphate, gold, silver, nickel etc.) are also significant sources of selenium contamination in the environment (Lemly, 2004; Muscatello et al., 2006). In addition, smelting of ore (especially copper) can potentially be a major source of selenium, leading to its release into the air (volatile form) as well as into the natural water bodies *via* drainage systems. A report from the United States Geological Survey suggests that total world refinery production of selenium in 2000 was about 1800 metric tons (Butterman and Brown, 2004). This, along with an estimation suggesting 90% of domestically used selenium is dissipated (unrecoverable) into the environment (Butterman and Brown, 2004), poses a serious risk of selenium becoming a major environmental toxicant. It is also important to note here that the margin of essentiality and toxicity of selenium is quite narrow (Janz et al., 2010), which can also enhance its potential to cause toxicity in exposed biota.

The effects of selenium exposure in natural fish populations are quite well documented. It has been reported that toxicity symptoms appear in fish when dietary selenium concentration exceeds 7-30 times to that of the daily requirement (Hilton et al., 1980; Hilton and Hodson,

1983). The case studies conducted at Belews Lake, North Carolina, receiving effluents from ash ponds of a coal fired power plant, provided a classic example of selenium toxicity in wild fish populations, which showed pathology of multiple organs (gill, liver, heart and ovary) and teratogenic deformities (Lemly, 1993b; Lemly, 2002). The effluents of similar type have been also reported to cause toxicity in fish from the Hyco Reservoir, North Carolina and the Sweitzer Lake in Western Colorado (reviewed by Hamilton, 2004). In addition, input of selenium from the irrigation water has been reported to affect the fish populations residing in Kesterson Reservoir, California (Hamilton, 2004). Some of the agricultural sumps in the region of San Joaquin valley in California have been reported to contain selenium as high as 4200 $\mu g.L^{-1}$ – the primary cause of adverse consequences to resident fish populations in these natural aquatic habitats (Presser and Barnes, 1984). Larval deformities have been implicated to maternal exposure to selenium in rainbow trout (*Oncorhynchus mykiss*) and northern pike (*Esox lucius*), collected from selenium-impacted natural waters of western Canada (Holm et al., 2005; Muscatello et al., 2006).

1.4 Implications of selenium exposure on fish

1.4.1 The diversity of chemical speciation of selenium

In the context of characterizing selenium toxicity in fish, it is important first to understand the chemical speciation of selenium, which influences its toxicity (discussed later). Selenium can be present in four different oxidation states (i.e., +6, +4, 0 and - 2). Higher oxidation states are mostly found in inorganic forms (i.e., selenate, +6; selenite +4). Elemental selenium with zero oxidation state (Se^0) is usually considered to be unreactive. Selenium in organic selenium compounds (e.g., selenomethionine, selenocysteine) is predominantly in -2 oxidation state. In the water column, dissolved inorganic selenium compounds constitute a major part of the total selenium, however different organic forms constitute the major fraction of selenium found in the diets (Maher et al., 2010). Since the information on the chemical speciation of selenium in natural fish diet is relatively limited, few selenium species of toxicological importance from different food sources are presented in Figure 1.2 (modified from Gammelgaard et al., 2011).

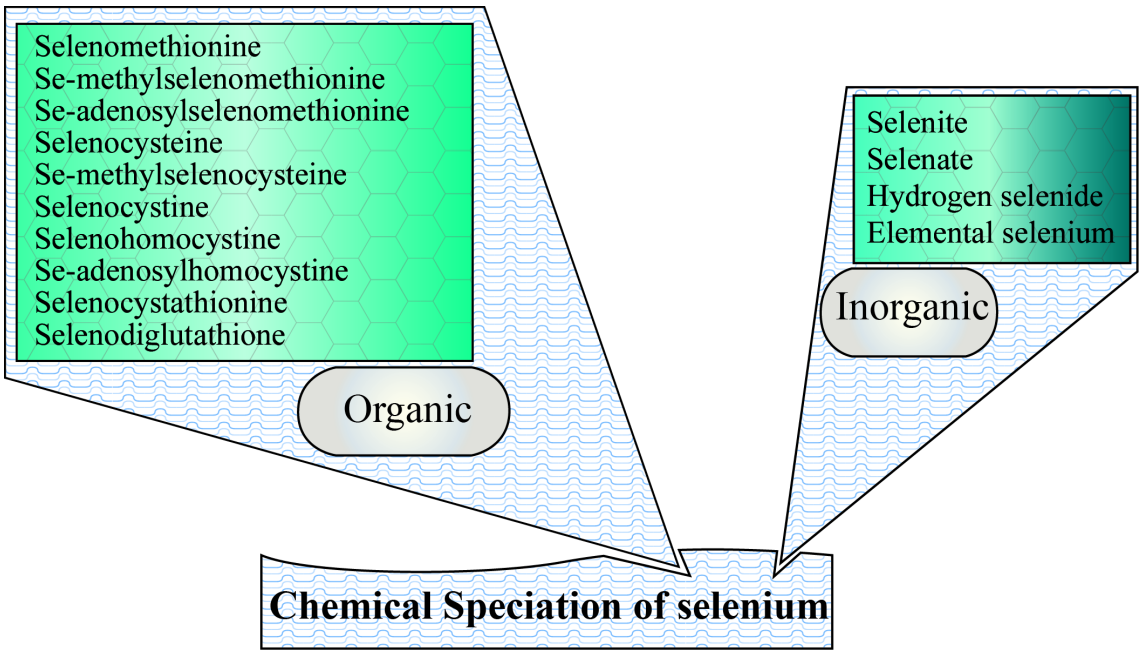

Figure 1.2: Various inorganic and organic species of selenium generally found in different food sources and selenium species of toxicological importance.

1.4.2 Implications of selenium speciation for its toxicity

The toxicity of selenium varies greatly depending on its chemical form, as some of the seleno-compounds are toxic at a low level, whereas others are relatively less toxic. For example, selenate was found to be 3-7 fold less toxic to fish than selenite (Hamilton and Buhl, 1990). In juvenile rainbow trout, the 96 h LC_{50} for sodium selenite and sodium selenate ranges from 4.2 to 9.0 mg $Se.L^{-1}$ and 32 to 47 mg $Se.L^{-1}$, respectively (Buhl and Hamilton, 1991; Hodson et al., 1980a). However, the water quality criterion of selenium for the protection of aquatic biota in many jurisdictions ranges from 1-5 µg dissolved $Se.L^{-1}$ (Janz, 2011). This is primarily because dietary, not the waterborne, exposure plays the most significant role in overall selenium toxicity. In the natural environment, the primary producers take up dissolved selenium from the water column (bioconcentration), and selenium accumulates in greater concentration at higher trophic levels (biomagnification). The bioconcentration factor is so high for selenium that primary producers can accumulate up to 1,000,000-fold higher selenium relative to that in the water column, depending on the diversity of algal community and hydrodynamics of water bodies (Stewart et al., 2010). In this regard, it is important to understand the toxicity of organic selenium compounds (e.g., selenomethionine) that are biotransformed from inorganic selenium compounds. Diet is the primary source of selenium accumulation in aquatic organisms belonging to the higher trophic levels (Luoma and Presser, 2009). Selenomethionine is considered to be the major form of selenium in the diet and often constitutes greater than 80% of the total available selenium (Maher et al., 2010). Significant growth retardation has been observed in larval rainbow trout when fed with diet containing 4.6 µg $Se.g^{-1}$ (dry weight) in the form selenomethionine (Vidal et al., 2005). In addition, chinook salmon swim-up larvae and fingerlings have been reported to display signs of toxicity when fed with a diet spiked with selenomethionine at a concentration of 3-5 µg $Se.g^{-1}$ (dry weight) (Hamilton et al., 1990). The same study also reported that the early life stages of this species are more sensitive to dietary selenomethionine than the juveniles.

In selenium contaminated aquatic systems, it is expected that both water and diet would constitute the exposure routes of selenium to fish, albeit in different degrees. In spite of the overwhelming evidence of greater bioavailability of dietary selenium, there remains a dearth of

knowledge regarding the relative contribution of waterborne exposure in selenium accumulation by fish during a combined-exposure (water plus diet). Besser et al. (1993) suggested that the bioaccumulation of selenomethionine is generally higher than inorganic selenium compounds (selenite and selenate) in bluegill (*Lepomis macrochirus*). Interestingly though, they also observed that the slow accumulation of selenite was accompanied by the slow turnover (depuration), resulting in high selenium accumulation in fish during long-term waterborne exposure to selenite. These findings are important from the perspective of understanding the differences in chemical species-specific selenium toxicity (inorganic versus organic) in fish as well as the implications of different exposure routes.

1.4.3 Physiological effects of selenium exposure in fish

Exposures to both organic and inorganic selenium have been reported to cause damage to the major organs in fish, both in the laboratory and field-based studies. It has been suggested that the liver is the major site of selenium accumulation (Hicks et al., 1984; Hodson et al., 1980b), and morphological changes and structural degeneration of liver tissues have been observed in fish following selenium exposure. In green sunfish (*Lepomis cyanellus*) collected from selenium-contaminated Belews Lake, increased occurrences of vacuolar degeneration of liver cells and increased numbers of Kupffer cells, the characteristics that are not normal to fish liver architecture, have been reported (Sorensen et al., 1984). Similarly, megalocystosis (increased size of nuclei and cells) of hepatocytes were observed in chinook salmon fed with selenium contaminated mosquitofish (*Gambusia affinis*) (Hamilton et al., 1986). In a similar study, nuclear degeneration, glycogen depletion, fat vacuoles and basophilic cytoplasm in the liver cells were observed in striped bass (*Morone saxatilis*) fed with selenium-contaminated red shiners (*Cyprinella lutrensis*) (Coughlan and Velte, 1989). Juvenile splittail (*Pogonichthys macrolepidotus*) fed with an experimental diet spiked with selenium also showed severe glycogen depletion and moderate fatty vacuolar degeneration in the liver tissue (Teh et al., 2004). In addition to liver, kidney also accumulates significant amount of selenium during exposure to elevated levels of selenium (Hodson et al., 1980a). In green sunfish, environmental selenium exposure resulted in focal intra-capillary proliferative glomerulonephritis of kidney,

characterized by abnormal matrix and increased proliferation of mesanglial cells (Sorensen et al., 1984). The functional implications of such pathological changes suggest compromised blood flow through the capillary in the kidney. In addition, tubular cell necrosis and blood stasis was also observed in the kidney of redear sunfish (*Lepomis microlophus*) exposed to environmental selenium (Sorensen, 1988). Coughlan and Velte (1989) reported hydropic vacuolation, degeneration and lymphocyte infiltration in the renal proximal tubules of striped bass following dietary exposure to selenium. In rainbow trout, nephrocalcinosis has been observed upon feeding with selenite spiked diet (Hicks et al., 1984). Degeneration of the endothelial cells of the glomerular capillary loop has been reported in chinook salmon exposed to dietary selenium (Hamilton et al., 1986).

In addition to the pathology of liver and kidney, selenium exposure has also been reported to alter the blood parameters and causes damage to the gill tissue. Sorensen and Bauer (1983) observed reduced number of immature erythrocytes along with increased erythrolysis in sunfish residing in a selenium-contaminated lake. Erythrocytes from the exposed fish were microcystic (smaller than normal) and poikilocytic (abnormally shaped). Sorenson and Bauer (1983) reported reduced packed cell volume and hematocrit values in selenium-impacted redear sunfish. In a subsequent study, Sorenson et al. (1984) reported histopathological changes of the gill in selenium-exposed green sunfish exhibiting swollen lamellae and extensive cellular vacuolation. Hamilton et al. (1986) also observed hypertrophy, hyperplasia and dissociation of the gill epithelium in chinook salmon (*Oncorhynchus tshawytscha*) following dietary selenium exposure. Similar to the observations of Sorenson and Bauer (1983), changes in blood parameters were reported later in juvenile bluegill following a combined exposure to waterborne (4.8 µg Se/L, mixture of selenite and selenate in a 1:1 ratio) and dietary (5.1 µg Se/g as L-selenomethionine, dry weight) selenium (Lemly, 1993a). This study also documented swelling of blood sinuses in the secondary gill lamellae upon prolonged exposure. The studies described above highlight the toxic effects of selenium at the tissue level in juvenile and adult fish.

Miller et al. (2007) reported that waterborne selenite exposure induces physiological stress response (increased plasma cortisol) and elevates plasma thyroxin (T3 and T4) levels in rainbow trout. Although they did not observe any activation of the physiological stress-response

in selenium-impacted wild fish, elevated plasma glucose level was recorded, indicating energy mobilization in fish during environmental selenium exposure (Miller et al., 2009a, b). Thomas and Janz (2011) recently documented compromised swimming performance in adult zebrafish (*Danio rerio*) following dietary exposure to environmentally relevant concentrations of selenomethionine. Similar impairment of swimming performance was also observed in juvenile splittail and white sturgeon (*Acipenser transmontanus*), exposed to elevated dietary selenium (Teh et al., 2004; Tashjian et al., 2006). Interestingly, Wiseman et al. (2011) recently reported upregulation of gonadal steroidogenesis in rainbow trout exposed to selenomethionine, indicating the possible endocrine disrupting effects of selenium in fish. Moreover, larval fish have been found to be quite sensitive to selenium exposure, which causes edema and teratogenic deformities (reviewed by Janz et al., 2010). Overall, these findings indicate that selenium contamination in the aquatic ecosystems can have long-term adverse implications for the recruitment and sustainability of feral fish populations.

1.5 The toxicokinetics and toxicodynamics of selenium

Fundamental knowledge on the toxicokinetics and toxicodynamics are important to decipher how a toxicant causes toxicity in organisms. Toxicokinetics describes how the bioavailable fractions of a toxicant are absorbed, distributed, metabolized and excreted by the organisms. Toxicodynamics describes the interaction of toxicants with vital biological components that leads to the onset of adverse physiological effects. A schematic diagram, representing a connection between the two, is presented in Figure 1.3.

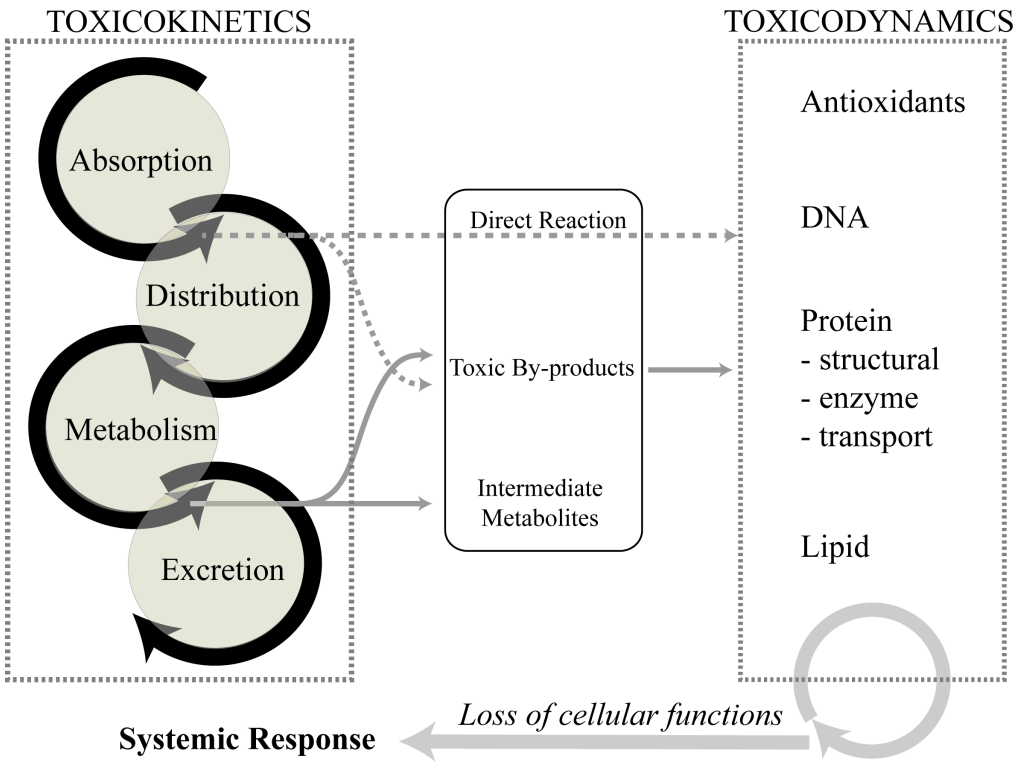

Figure 1.3: A schematic diagram of toxicokinetics and toxicodynamics of a toxicant. Once a toxicant is absorbed into the biological systems, it is distributed throughout the body depending on the route of exposure. This is followed by metabolism in the respective organs and subsequent excretion from the body. However, a toxicant can spontaneously react with vital biomolecules immediately after absorption (the dotted arrow) before being metabolized. Similarly, the intermediate metabolites and toxic by-products can also exert their undesirable effects on cellular macromolecules, eventually resulting into systemic toxicity.

As indicated previously, the route of exposure plays a major role on subsequent systemic toxic effects. Unlike in terrestrial animals, fish can be exposed to toxicants *via* both the gills and intestine, and the toxic effects may differ depending on the exposure route. Hodson and Hilton (1983) proposed an interesting model for selenium toxicity *in vivo*, which suggested that waterborne selenium is taken up by the gill and subsequently distributed to all the major tissues before reaching the liver (receives blood *via* hepatic portal system). In contrast, selenium absorbed from the diet first passes through the liver before reaching the systemic circulation and subsequently to other organs (See Figure 1.4). In general, this model indicates that the inorganic selenium compounds are mainly distributed to various organs other than the liver, whereas the organic forms of selenium accumulate primarily in the liver. However, this model does not account for any possible metabolism of inorganic selenium in the uptake epithelium or blood, and the transport efficiency of individual organs. Also, this model cannot explain why the liver accumulates the highest amount of selenium relative to other organs during water-borne selenium exposure. In any case, the underlined concept may be important in understanding the progression of tissue specific toxic effects of selenium in fish.

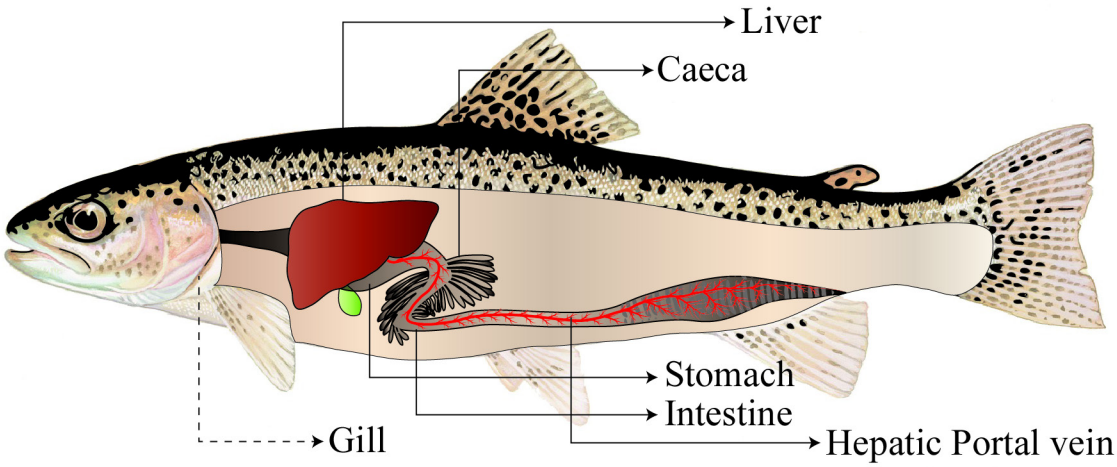

Figure 1.4: A schematic diagram of the hepatic-portal circulation in rainbow trout. Upon digestion of food, nutrients as well as dietborne toxicants are absorbed by the gastro-intestinal tract and subsequently transported *via* the hepatic portal vein directly to the liver, before being distributed to other organs. However, waterborne toxicants are taken up *via* the gills and subsequently distributed to various organs including the liver. Trout image: Courtesy of United States Department of Interior.

Absorption: The mechanisms of selenium absorption in fish are largely unknown, and much of the information on the transport processes involved comes from mammalian studies. McConnell and Cho (1965) first reported that selenite is transported passively in the rat intestine. However, their experimental results supported an active transport of selenomethionine – a process inhibited by its sulphur analog, methionine. Several subsequent studies have examined selenite transport in the intestine of various mammalian and avian species including rat, pig, sheep and chicken. In rat and sheep intestine, the transport of selenite was found to be sodium-dependent and inhibited by thiosulfate (Ardüser et al., 1986). Interestingly, the transport of selenate was faster than selenite in the rat ileum. There were also species-specific (rat versus sheep) differences in the intestinal transport profile of inorganic selenium (Ardüser et al., 1986). Later studies reported that the uptake of selenite is pH-dependent; with higher tissue accumulation at pH 7.0 compared to that at pH 5.0 in the sheep mid-jejunum (Würmli et al., 1989). The same study also reported that the selenite transport was increased by 5-fold in the presence of L-cysteine. They suggested that selenite is reduced by cysteine to form selenodicysteine and selenopersulfide, which are more bioavailable than selenite. Increased selenium uptake has also been reported in rat intestine in the presence of other thiols such as cysteamine, thioglycolate, and mercaptopyruvate (Scharrer et al., 1992). Using brush border membrane vesicles prepared from chicken duodenum, Mykkanen and Wassermen (1989) showed that selenite transport was vitamin D-dependent. Increased selenite uptake was believed to be due to the increased binding sites at the membrane vesicles upon *in vivo* Vitamin D supplementation to the chicken. Mykkanen and Wassermen (1989) also found that the selenite uptake reaches a steady state within 60-120 minutes, however the dose-dependent uptake of selenite showed a linear profile. Interestingly, they did not find any sodium-dependent component of the intestinal selenite transport. Park and Whanger (1995) also reported that the dose-dependent selenite transport was linear in rat hepatocytes up to the supra-physiological dose level. In transformed human keratinocytes, the time-dependent selenite transport was found to be saturable, energy-dependent and sensitive to anionic transporter inhibitor (DIDS) (Ganyc and Self, 2008). The general consensus among these studies discussed above is that the cellular transport of selenite is mediated by multiple types of anionic transporters. Using a heterologous

expression system in *Xenopus* oocytes, it has recently been shown that selenomethionine shares the same transport pathway as methionine, however the capacity of selenomethionine transport varies among different methionine transporters (Nickel et al., 2009). Using the everted gut sacs of green sturgeon (*Acipenser medirostris*), Bakke et al. (2010) has recently demonstrated the existence of similar transport processes for selenomethionine in the fish intestine. These studies provide important insights into the cellular transport of both inorganic and organic forms of selenium, however further studies are required to understand the roles of specific transporters involved.

Distribution: Tissue distributions of selenium in fish are well-characterized. Liver is the primary organ for selenium accumulation, although significant accumulation also occurs in the kidney, gonads, muscle and gill (Hodson et al., 1980a; Sato et al., 1980). However, distribution of selenium at the cellular level is not very well understood in fish. In the insect *Corcyra cephalonica*, it has been found that a significant amount of selenium accumulates in the mitochondria and nucleus (Lalitha et al., 1994). A similar trend of organelle-specific selenium distribution has also been reported in the hepatopancreas and gill tissues of mussel (*Mytilus galloprovincialis*) (Znidaric et al., 2006) as well as in human liver (Chen et al., 1999). Weekley et al. (2011) recently reported elevated selenomethionine localization around the perinuclear region in human cancer cells following exposure to selenomethionine. In all of these studies, it is not clear though whether selenium fractions were protein-bound or in their free form. Nevertheless, these studies provide useful information that has important implications for understanding selenium toxicity.

Metabolism: The chemistry of selenium and sulphur is quite similar, and for most of the biologically relevant sulphur compounds, there are selenium analogs. However, some selenium compounds are much more reactive than their sulphur counterparts (Jacob et al., 2003; Moroder, 2005). Recent research indicates that the metabolism of inorganic and organic selenium compounds occurs through different pathways. In mammalian systems, rapid biotransformation of some inorganic selenium compounds (e.g., selenite) has been reported because of their strong reactivity with endogenous bioactive molecules such as glutathione and cysteine (Ganther, 1968, 1971; Nuttall, 1985; Spallholz, 1994; Spallholz et al., 2001; Suzuki et al., 1995; Suzuki and Itoh,

1997; Suzuki et al., 1997; Suzuki et al., 2006a; Suzuki et al., 2006b; Suzuki et al., 2006c; Suzuki et al., 2007). For example, selenite is rapidly reduced by glutathione to hydrogen selenide (Ganther, 1968; Kice et al., 1980). In contrast, the metabolism of organic seleno-compounds occurs more slowly since most of these compounds are known to undergo enzymatic biotransformation. For example, selenomethionine is metabolized to methylselenol either via the *trans*-sulfuration pathway or directly by the enzyme methioninase (Spallholz, 1994). Interestingly, the metabolism of both inorganic and organic selenium produces a common intermediate metabolite hydrogen selenide, which is incorporated into the selenoproteins (Lu and Holmgren, 2009; Xu et al., 2007). It is also important to note here that the metabolism of selenium (inorganic as well as organic) leads to the generation of redox-active metabolites, which often facilitate the generation of intracellular reactive oxygen species (ROS) (See below for a more in-depth discussion of this aspect). It is yet to be investigated whether similar pathways of selenium metabolism exist in fish - information that is critical for unravelling the mechanistic underpinnings of chemical species-specific selenium toxicity in fish.

Excretion: The common routes of selenium excretion in mammals are through the urine and the breath, in the form of selenosugars (Gammelgaard et al., 2008) and methylated volatile compounds (Kremer et al., 2005), respectively. At present, information on selenium excretion in fish is quite limited. In fathead minnows (*Pimephales promelas*) exposed to selenite administered by gavage, urinary elimination was found to be the predominant pathway of selenium excretion followed by the gill and biliary secretion (Kleinow and Brooks, 1986b). Interestingly, using a similar experimental approach, they found that biliary excretion played a more significant role in selenium excretion when minnows were exposed to selenite and selenomethionine (Kleinow and Brooks, 1986a, b). However, the relative importance of these pathways in regulating selenium homeostasis during elevated waterborne or dietary selenium exposure to fish is yet to be understood.

1.6 Biochemical basis of selenium toxicity – a link to redox biochemistry

In order to delineate the biochemical basis of systemic selenium toxicity, an in-depth analysis of the biochemical pathways involved in selenium metabolism is required. Extensive

investigations in mammalian systems indicate that oxidative stress plays a critical role in selenium toxicity. However, the role of oxidative stress in mediating selenium toxicity has rarely been explored in fish, and this particular aspect has been identified as a pressing need for future investigations (Janz et al., 2010).

Although it has long been established that selenium is a potential toxicant, the biochemical basis of its toxicity was unclear until recently. Initially, it was hypothesized that the resemblance in the chemical properties between sulphur and selenium could be the basis of selenium toxicity (Moxon and Rhian, 1943). Sulphur in methionine and cysteine molecules is replaced by selenium resulting in the formation of selenomethionine and selenocysteine, respectively. This process can have important biological implications. For example, the protein synthesis machinery may not distinguish between methionine and selenomethionine and thus selenomethionine can be incorporated into the protein structure. Several authors postulated that the replacement of the sulphur-containing amino acids with the seleno amino acids might result in improper protein folding (loss of tertiary structure due to the replacement of S-S bond with Se-Se bond) or dysfunctional proteins such as enzymes (Diplock, 1976; Maier and Knight, 1994; Sunde, 1997). It is important to note that the incorporation of selenomethionine in place of methionine may not necessarily result in misfolded proteins because neither of these participates in the tertiary structure of protein *via* diselenide (Se-Se) or disulphide (S-S) bonding. The formation of diselenide (Se-Se) linking in protein structure is only possible when cysteine is replaced by selenocysteine. In β-galactosidase enzyme, replacing 80 of the 150 methionine residues with selenomethionine was found to have no effect on its kinetic parameters (measured as K_m and V_{max}) (Huber and Criddle, 1967). Orme-Johnson et al. (1968) reported that the replacement of sulphur with selenium in iron-sulphur [2Fe-2S] protein has little effect on its functions. A similar observation with ferredoxin enzyme has also been reported upon replacement of methionine by selenomethionine (Moulis and Meyer, 1982). In addition, no changes in the tertiary structure of ribonuclease A was found when cysteine was replaced with selenocysteine, even with the additional substitution of methionine by selenomethionine (Moulis and Meyer, 1982). These observations suggest that selenomethionine and selenocysteine substitutions may not seriously impair the structure and functionality of enzymes or proteins. Nevertheless, such generalizations are inconclusive in the absence of any broad array of

observations with multiple types of proteins, and further research is required to determine whether the selenium substitution of sulphur is a key factor for selenium toxicity at the cellular level. Interestingly, Phibbs et al. (2011a) recently suggested increased substitution of sulphur by selenium in wild lake chub (*Couesius plumbeus*) collected from the selenium-impacted natural waters of Northern Saskatchewan, however its physiological implication remains to be investigated.

The interaction between selenium and cellular antioxidants was first reported by Painter (1941), when he observed instant oxidation of thiols (e.g., glutathione, cysteine) by selenite. Ganther (1968) later reported the detailed reactions between thiols and selenite, with the formation of intermediate selenotrisulfide (RSeSSeR). However, it was not known how such reactions could lead to the impairment of cellular functions except altered redox status. The finding, that the reactions of selenite with glutathione lead to the generation of ROS, was a major breakthrough that explained the toxic effects of selenite, at least partially (Seko et al., 1989). Several subsequent studies have documented selenite-induced oxidative stress effects in mammalian systems, including elevation of intracellular ROS generation (Yan and Spallholz, 1992) and enzymatic antioxidants activity (Stewart et al., 1999), alteration of cellular thiol redox and metabolism (Kiersztan et al., 2007; Kuchan et al., 1990), DNA damage (Garberg et al., 1988) and cell death (Kim et al., 2002). Miller et al. (2007) observed decreased hepatic glutathione level in rainbow trout acutely exposed to waterborne selenite, indicating that selenite exposure may induce oxidative stress in fish as well. Miller and Hontela (2011) also suggested recently that selenite impairs cortisol secretion by the adrenocortical cells of salmonid fish by inducing oxidative damage.

Exposure to organic selenium compounds can also induce oxidative stress in cells since some of the organic selenium compounds (e.g., selenocysteine, selenocystamine) are redox-active and generate ROS following reaction with thiols (Spallholz, 1997; Spallholz et al., 2001; Terada et al., 1999). In addition, methylselenol, an intermediate metabolite of selenomethionine, has been reported to undergo glutathione facilitated redox cycling, leading to the generation of intracellular ROS (Chaudiere et al., 1992). In the context of selenium toxicity, it is interesting to note that cellular thiols act as pro-oxidants instead of functioning as the natural antioxidants. It is

also important to note here that mammalian cells have been found to be much more sensitive to inorganic selenium compounds such as selenite or selenate compared to common organic selenium species like selenomethionine (Hoefig et al., 2010). Similarly, Miller and Hontela (2011) reported that the adrenocortical cells of salmonid fish are markedly more sensitive to selenite than selenomethionine. This differential sensitivity to inorganic and organic selenium occurs probably due to the differences in the rate of uptake and metabolism.

1.7 XANES spectroscopy for selenium speciation

Since the toxicity of selenium is dependent on its chemical form, the characterization of selenium speciation in biological systems is important. At present, several advanced techniques are available for characterizing selenium speciation (Gammelgaard et al., 2011; Lobinski et al., 2000). In my project, XANES (X-ray absorption near edge structure) spectroscopy is sought over the other techniques because it requires minimum pre-analytical sample treatment. This technique also reduces the possibility that the speciation of the analyte may alter during sample preparation and thus may not reflect the original speciation in the sample (Roberge et al., 2003). Some selenium compounds can react with intracellular thiols, and the possibility of occurrence of such process is exceedingly higher in other techniques that require sample extraction procedures.

XANES spectroscopy relies on the principle that a high energy incident ionizing radiation can eject a core electron from an atom, thereby generating a characteristic absorbance or X-ray fluorescence (Penner-Hahn, 2003). Such high energy X-ray is only available in a synchrotron facility. The element specificity of the process arises from the characteristic binding energy of a core electron of an element. When a core electron absorbs an ionizing radiation greater than its binding energy, it is ejected out from its shell as a photoelectron, leaving a highly excited core-hole state (Figure 1.5). The relaxation of excited state can happen *via* different mechanisms, however the most important of those are the emissions of Auger electron and X-ray fluorescence (Penner-Hahn, 2003). The dominant relaxation process is usually emission of an Auger electron for lower-energy excitation, whereas X-ray fluorescence is the primary relaxation process for high energy excitation. Upon scanning with high energy X-ray (in the region of the binding

energy of core shells), an increase in the absorption cross-section occurs, which is called the absorption edge, representing a different core electron binding energy (Penner-Hahn, 2003). Depending on the shell from which the core electron is ejected, the absorption edges are called as L-edge, M-edge etc. The oxidation state of an element is determined based on the characteristic absorption spectra. From the extended region of the available spectra, it is also possible to extract information about the bond length and coordination number. The chemical forms of an element in the target sample are usually determined using the representative spectra obtained from standard compounds.

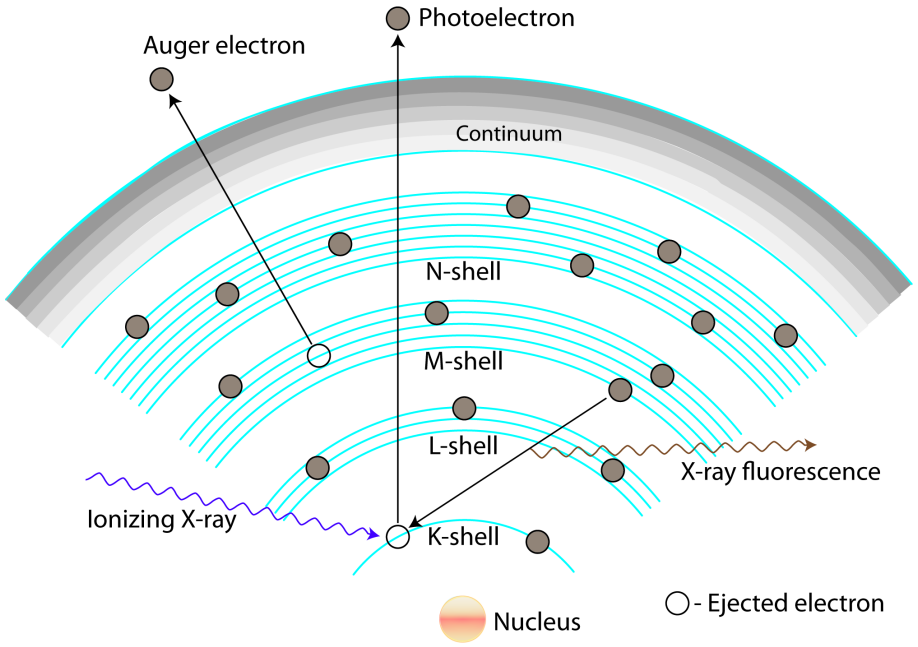

Figure 1.5: A schematic diagram showing the interaction of high energy ionizing radiation with an atom and the subsequent cascades of relaxation events (Adapted from George and Pickering, 2007; Heald, 1988; Penner-Hahn, 2003).

Recent studies have successfully used XANES spectroscopy technique to study selenium speciation in bacteria (Sarret et al., 2005), yeast (Yu-Feng et al., 2010), insects (Andrahennadi et al., 2007; Franz et al., 2011; Vickerman et al., 2004), fish (Phibbs et al., 2011a; Phibbs et al., 2011b), and plants (Pickering et al., 2000). This approach has been highlighted as a promising analytical tool for investigating the oxidation state of metals/metalloids in biological systems – information that has often critical implications in toxicology (Gunter et al., 2002).

1.8 Isolated cells as model *in vitro* system in toxicology

Toxicokinetics and toxicodynamics of contaminants are often studied *in vivo* at the organ level. However, such approaches often do not allow the manipulation of the experimental conditions without systemic inferences, posing a major challenge in determining a precise cause and effect relationship. When the focus of an experiment pertains to a specific cell type or a cellular structure (e.g., membrane), the existence of multiple cell types within the organ architecture may confound the experimental observations. In addition, complex physiological interactions among organs can also complicate distinguishing the primary toxic consequences from the secondary effects of a toxicant *in vivo* (Guillouzo, 1998). A simple and practical solution to address such problems is the use of *in vitro* experimental systems.

Considering the fact that toxic effects always occur first at the cellular level, isolated cells are useful models for investigating the mode of action of a toxicant. This often necessitates the use of primary cells isolated from the key organs involved in the uptake and/or metabolism of a toxicant. Since liver is the major site of selenium accumulation and metabolism in fish, the isolated hepatocytes (the functional units of liver) can be an appropriate experimental system for investigating the cellular basis of selenium toxicity. Isolated fish hepatocytes in primary culture have been widely used as a model system for toxicity assessment as well as for examining the toxic mechanisms for various types of environmental contaminants (Gagné et al., 1999; Pesonen and Andersson, 1997; Segner, 1998; Zahn and Braunbeck, 1993). Similarly, isolated enterocytes are also a useful model for examining the intestinal transport properties of essential nutrients

and/or contaminants. Since diet is the primary source of selenium in fish, this experimental system can be particularly useful in characterizing selenium absorption pathways in fish intestine. Recent studies have successfully used this approach to characterize the kinetic and pharmacological properties of intestinal iron and cadmium transport in fish (Kwong et al., 2010).

1.9 Research objectives

Rationale: Fish are an interesting model to study selenium transport, metabolism and toxicity because of their higher nutritional requirement of selenium than mammals. Fish have higher number of selenoproteins compared to mammals, and there are also differences in the number of selenocysteine residues in selenoproteins (e.g., selenoprotein P) between fish and mammals. Overall, these observations suggest that the uptake and handling of selenium in fish may have important similarities as well as significant differences with mammals. Current understanding of selenium transport pathways in mammals suggest that the anionic transporters are involved in transporting selenite and selenate in different cell types. However, there are no experimental evidences suggesting the existence of comparable pathways in fish. Similarly, the biochemical pathways involved in selenium metabolism in fish are virtually unknown. Although the organismal and population level effects of selenium exposure in fish are quite well documented, the cellular basis of selenium toxicity is poorly understood. Mammalian studies suggest that both inorganic and organic forms of selenium cause toxicity by inducing oxidative stress; however the role of oxidative stress in mediating chemical species-specific selenium toxicity in fish has not been investigated with great insights. Selenium is rapidly emerging as a priority aquatic pollutant across the world, and a comprehensive knowledge of the toxicokinetics and toxicodynamics of selenium in aquatic organisms including fish are required for understanding the implications of selenium contamination. Keeping this in view, I have investigated the cellular transport, metabolism and toxicity of selenium in a model freshwater fish, rainbow trout, using both *in vitro* and *in vivo* experimental approaches.

Hypotheses: I hypothesized that: (i) the cellular transport of selenium (selenite and its reduced forms) is mediated by anionic transporters in hepatocytes and enterocytes; (ii) there are differences in the hepatocellular metabolism of organic and inorganic selenium forms; (iii) in

spite of the differences in their metabolism, the cytotoxicity of both inorganic (selenite) and organic (selenomethionine) selenium occurs *via* a common mechanism of oxidative stress in hepatocytes; and (iv) there are organ specific differences in the accumulation and metabolism of selenomethionine upon *in vivo* dietary exposure.

Research objectives: The overall goal of my research was to elucidate the cellular mechanisms of selenium transport, metabolism and toxicity in fish. The specific research objectives and experimental approach employed are outlined below.

1. ***Characterization of selenium (selenite and its reduced forms) transport in isolated hepatocytes and enterocytes (Chapter 2)***

The cellular transport of selenite and its reaction products with thiols were characterized using isolated rainbow trout hepatocytes and enterocytes. The kinetic properties of transport were evaluated in both cell types. The effects of extracellular proton gradient was evaluated to characterize the influence of pH on the transport process. Pharmacological treatments were employed to understand the energy dependency of the uptake process and transporter specificity. Additionally, the influence of extracellular inorganic mercury on the transport of selenite and its reduced forms were examined.

2. ***Characterization of the hepatic pathways involved in selenium (both inorganic and organic) metabolism using isolated hepatocytes (Chapter 3)***

The temporal metabolic profile of selenite, selenate and selenomethionine in hepatocytes were assessed by XANES spectroscopy available at the synchrotron facility of the Canadian Light Source (Saskatoon, Canada). The time-dependent intracellular ROS generation during selenomethionine exposure was measured by confocal microscopy. The possibility of redox-active methylselenol formation *via* direct enzymatic catalysis of selenomethionine in hepatocytes was also examined.

3. Investigation of the role of oxidative stress in mediating selenite toxicity in isolated hepatocytes (Chapter 4)

The involvement of oxidative stress in dose- and time-dependent selenite toxicity was evaluated using isolated hepatocytes in primary culture. To evaluate selenite-induced oxidative stress, several cellular endpoints including the intracellular ROS generation, antioxidant enzyme (catalase, superoxide dismutase and glutathione peroxidase) activities, cellular thiol redox (reduced to oxidized glutathione) and peroxidation of membrane lipid were measured. To understand the consequences of oxidative stress on cell viability, the integrity of genomic DNA, intracellular calcium homeostasis, induction of enzymatic apoptosis, and alterations in cell morphology were examined.

4. Investigation of the role of oxidative stress in mediating selenomethionine toxicity in isolated hepatocytes (Chapter 5)

The role of oxidative stress in dose- and time-dependent toxicity of selenomethionine in cultured primary hepatocytes was evaluated using the same experimental approach outlined above for selenite. An identical set of cellular endpoints was also analyzed to examine the consequences of selenomethionine exposure on cell viability.

5. Examination of in vivo accumulation and metabolism of dietary selenomethionine (Chapter 6)

To examine the differences in organ-specific accumulation and metabolism of selenomethionine, adult fish were fed with normal and selenomethionine-spiked diets for 14 days. At the end of the exposure, the total selenium accumulation in tissues was measured by graphite atomic absorption spectroscopy. Metabolic profiling of selenium in different tissues was carried out using XANES spectroscopy as described previously. A comparative assessment of the *in vivo* and *in vitro* findings was carried out to determine whether the *in vitro* approach validates the observations of selenomethionine metabolism *in vivo*.

CHAPTER 2: Characterization of selenium (selenite and its reduced forms) transport in isolated hepatocytes and enterocytes[1]

2.1 Introduction

Selenium is an essential micronutrient for all eukaryotes (Schwarz and Foltz, 1957). From an indispensable constituent of selenoproteins (Kryukov et al., 2003) to its role in cancer prevention (Rayman, 2005), the diverse biological functionality of selenium is unfolding. To date, the physiological roles of many selenoproteins remain unknown. Beyond essentiality, selenium can be toxic when the concentration marginally exceeds its nutritional requirement. Therefore, the maintenance of selenium homeostasis is of critical physiological importance from both nutritional and toxicological perspectives.

The current knowledge on the mechanisms of cellular selenium transport systems is limited and much of the information comes from mammalian studies. Like its functionality, the chemical speciation of selenium (e.g., organic and inorganic forms in different oxidation states) in biological systems is also diverse. This adds to the complexity in the understanding the cellular transport of selenium. Diverse speciation of selenium suggests that the cellular uptake of selenium occurs *via* multiple membrane transporters, depending on its discrete chemical forms. Early work by McConnell and Cho (1965) suggests passive transport of inorganic selenite in everted intestinal sacs of golden hamster. Further investigation with human lymphocytes also indicates that the transport of selenite is a passive process and sensitive to sulfhydryl inhibitors (Porter et al., 1979). In human erythrocytes, anion exchanger 1 (AE1) has been suggested to be involved in selenite transport (Galanter et al., 1993; Haratake et al., 2009). However, apart from selenite, AE1 can also transport multiple substrates (phosphate, sulphate and its target substrate bicarbonate) with high efficiency (Galanter et al., 1993). This raises an alternate possibility that phosphate, sulphate and other bicarbonate transporters can also transport selenite. A recent study

---

[1] This chapter of the thesis has been communicated for publication under joint authorship with W.M. Raymond Kwong and Som Niyogi (University of Saskatchewan).

suggests another type of molecular mimicry where the monocarboxylate transporter, *Jen1P*, can transport selenite in yeast (McDermott et al., 2010). All this evidence indicates the possible involvement of multiple transporters in cellular transport of selenite. Interestingly, it was reported that selenite exhibits a lower transport rate than its reduced form(s) in yeast (Tarze et al., 2007) and in transformed keratinocytes (Ganyc and Self, 2008).

To date, the mechanisms of selenite transport in fish, particularly at cellular level, are largely unknown. Fish are an interesting organism to study selenium transport given that their selenium requirement is much higher (5-25 µg/day/kg body weight) (Janz, 2011) than humans (0.67 µg/day/kg body weight, considering 60kg of body weight) (Brown and Arthur, 2001). This suggests that fish need to acquire selenium efficiently to fulfill the requirement. Diet is the primary source of selenium in fish, and selenomethionine is considered to be the major chemical form in the natural fish diets (Maher et al., 2010). Recent evidence suggests that the uptake of selenomethionine in fish intestine occurs *via* the methionine transporter(s) (Bakke et al., 2010). Interestingly, an inorganic form of selenium such as selenite constitutes a substantial fraction (up to 15%) of the total selenium in the natural aquatic invertebrate prey species (Andrahennadi et al., 2007). In addition, detritivorous fish may absorb a significant amount of selenite since the sediment selenite concentration can exceed over 20% of total selenium depending on the redox state of the system (Martin et al., 2011). Selenite can also be used as a supplement in commercial fish diet with no differences in growth or muscle selenium content when compared to its organic counterpart, selenomethionine (Cotter et al., 2008). Following absorption in the intestine, selenite can be transported to the liver (the primary organ of selenium metabolism) *via* hepatic portal circulation with or without first pass metabolism by enterocytes. The cellular systems involved in the transport of selenite and its interactions with other dietary/physiological components (e.g., thiols) need to be examined in fish, which will allow us to understand whether the transport mechanisms in fish are similar to those of mammals. Moreover, such fundamental knowledge on the physiology of selenium transport in fish has important environmental implications since selenium has been categorized as one of the priority pollutants in aquatic ecosystems and selenite is known to be the most toxic inorganic form of selenium to aquatic life (Hamilton, 2004). Thus, the present study was designed to investigate the kinetic and pharmacological transport

properties of selenite and its reduced form(s) in isolated hepatocytes and enterocytes of a model teleost, rainbow trout (*Oncorhynchus mykiss*).

2.2 Methods

2.2.1 Fish

Rainbow trout weighing 200–300 g were obtained from the Saskatchewan Government Fish Farm, Saskatchewan. All fish were acclimated for at least 2 weeks prior to their use in the experiments. The experimental protocol was in accordance with the Canadian Council for Animal Care Guidelines and was approved by the animal research ethics board at the University of Saskatchewan.

2.2.2 Chemicals

^{75}Se as selenous acid was purchased from the University of Missouri Research Reactor (UMRR). Selenite, GSH, cysteine, collagenase, cell dissociation solution, 4,4′-diisothiocyanostilbene-2,2′-disulfonic acid (DIDS) and dicyclohexylcarbodiimide (DCCD) were obtained from Sigma-Aldrich, Canada. High purity propionic acid, phloretin and acetazolamide were obtained from Acros Organics, Canada. L-15 media was purchased from Invitrogen, Canada. All other chemicals used were of analytical grade and purchased from VWR, Canada, unless mentioned otherwise.

2.2.3 Cell Culture

Hepatocytes were isolated and cultured using a standard methodology as outlined elsewhere (Misra et al., 2010). Cells were plated on to 100 mm BD Primaria™ plate to form monolayer. All of the transport studies were carried out after 24h of cell isolation. Non-enzymatic cell dissociation solution was used for harvesting cells to avoid any unsought cellular

injury following the manufacturer instruction. Upon harvesting, cells were washed twice in freshly prepared L-15 media and kept at 15°C until used for experimentation.

Enterocytes were isolated following the previously established protocol in our laboratory (Kwong et al., 2010). Isolated cells were suspended in Modified Cortland saline [in mM: NaCl 133.0, KCl 5.0, $CaCl_2$ 1.0, $MgSO_4$ 1.9, $NaHCO_3$ 1.9, NaH_2PO_4 2.9, glucose 5.5, HEPES 10.0, pH 7.4]. All the experiments with enterocytes were conducted within 4h of isolation. For both cell types, cells showing ≥ 90% viability (trypan blue exclusion test) were only used for the experimental purpose.

2.2.4 Kinetics experiments

The uptake of selenite as well as the reaction products of selenite with GSH or L-cysteine (both within the regime of physiologically relevant concentration) was examined. All flux experiments were carried out either in L-15 media or modified Hanks' media (in mM: NaCl 136.9, KCl 5.4, $MgSO_4 \cdot 7H_2O$ 0.8, $Na_2HPO_4 \cdot 7H_2O$ 0.33, KH_2PO_4 0.44, HEPES 5.0, Na-HEPES 5.0, $CaCl_2$ 1.5, pH 7.63) for hepatocytes and in Modified Cortland saline for enterocytes at 15°C (thermostatic water bath, Linberg Blue M, Thermo Scientific, USA). Four hundred microliters of cell suspension containing 1-1.2 × 10^6 cells/ml was used for all experiments. When different media was used, cells were washed with excess of the representative media and resuspended. Radiolabeled stock solution of selenite was prepared by adding ^{75}Se to cold selenite stock and diluted accordingly to achieve the target selenium exposure concentrations and specific activity (final activity – 14.9 μCi/ml for hepatocytes and 16.25 μCi/ml for enterocytes).

For hepatocytes, I examined the concentration dependent (0.0125-5 μM) accumulation of [^{75}Se]-selenite, both in the absence and presence of GSH (30 μM), over an exposure period of 0-60 min. Similarly, I evaluated the accumulation of 0.0125 μM [^{75}Se]-selenite, in the absence and presence L-cysteine (25-100 μM), over 30 min of exposure. For enterocytes, I examined the concentration dependent (0.5-20 μM) uptake of [^{75}Se]-selenite for 30 min in the absence of GSH and for 10 min in the presence of GSH (30 μM). In addition, I evaluated the time-dependent accumulation of 3.5 μM [^{75}Se]-selenite with (for 0-30 min) or without (0-60 min) GSH in the

exposure media. Similarly, accumulation of 0.5 and 3.5 μM of [^{75}Se]-selenite were also recorded in the absence as well as the presence of L-cysteine (30 μM), over 30 min. Furthermore, to examine whether the reducing equivalent or sulfhydryl group (GSH or L-cysteine) facilitates reduced selenium uptake, the effect of NADPH (30 μM) on the cellular [^{75}Se]-selenite accumulation was also examined under identical experimental conditions.

The effect of GSH and L-cysteine (final concentration = 30 μM each) on [^{75}Se]-selenite influx was assessed upon incubating these compounds with radiolabeled stock solution of selenite for 10 minutes at 15°C. To examine whether the reducing equivalent or sulfhydryl group (GSH or L-cysteine) facilitates reduced selenium uptake, the effect of equimolar concentration of NADPH to that of GSH and L-cysteine under identical conditions was also examined.

Each experimental treatment was run at least in triplicate, using cells isolated from individual fish at each time [sample size (n) for the data corresponds to the number of individual fish used for each treatment]. The uptake experiment was initiated by adding the required ^{75}Se stock volume at time '*zero*'. At the end of the exposure period, uptake was terminated using the respective ice-cold media containing 100 μM of selenite and the cells were washed 3-times (centrifuged at 1000*g* for 1 minute at each time) at 4°C to remove any adsorbed ^{75}Se. The radioactivity of the cell pellet was counted by the Wallac 1480 Wizard 3" Gamma Counter (Perkin Elmer, USA). The protein content of a reference cell pellet (equal cell number and treated alike except no radiolabelled ^{75}Se was added) was measured by the Bradford method (Bradford, 1976) using a commercial kit (Sigma-Aldrich, Canada) and BSA as the standard. The cellular accumulation of selenium was normalized with the protein content of cell pellet and calculated as follows:

$$Cellular\ accumulation\ (picomoles/mg\ protein) = \frac{Count\ from\ the\ cell\ pellet\ (cpm)}{Specific\ activity\ (cpm/picomoles) \times protein\ content\ (mg)}$$

The rate of cellular selenium uptake (picomoles/mg protein/time) was determined by dividing the cellular accumulation with exposure time.

2.2.5 Pharmacological experiments

The effects of several inhibitors/antagonists on the cellular accumulation of selenite were investigated, both in the presence and absence of GSH (30 μM). The final [^{75}Se]-selenite concentration in the transport media was 0.0125 μM (physiologically relevant) for hepatocytes and 3.5 μM for enterocytes in all of these experiments. In all of these experiments, cells were pre-incubated with the inhibitors/antagonists for 20 minutes at 15°C prior to the initiation of uptake analysis, unless mentioned otherwise. Since most of the inhibitors are very toxic, parallel quality control experiments were conducted to ensure that cell viability was not compromised during the course of the experiments. In each run, control experiments were performed concurrently for a better comparison. Some of the experiments were carried out only with hepatocytes because of comparatively much lower yield of isolated enterocytes from the trout intestine.

2.2.6 Effects of anionic transport inhibitor

Based on the previous report that selenite may be transported *via* anion exchangers (Galanter et al., 1993), DIDS (0.0125-62.5 μM for hepatocytes and 0-100 μM for enterocytes) was used as an inhibitor of anionic transporters. Initial screening experiments showed that DIDS lost its inhibitory effect when stored at -20°C. Therefore, DIDS (as well as other antagonists used in this study) was prepared fresh, just prior to their use in experiment.

2.2.7 Effects of ATPase inhibitor and uncoupler of ATP synthesis

The majority of cellular anion transport processes are energy independent. Based on that, it is hypothesized that selenite transport is also energy independent, both in the presence and absence of GSH. Orthovanadate (a P-type ATPase inhibitor) and DCCD (an uncoupling agent of ATP synthesis) were used to examine whether the transport process is energy independent. The concentration of orthovanadate and DCCD in the exposure media ranged from 0.0125-125μM for experiments with hepatocytes and 0-100μM for enterocytes.

2.2.8 Effects of sulphite and monocarboxylates on selenite transport

To study the inhibitory effect of a structurally similar compound on selenite transport, the effect of sulphite (0.0125-125μM) was examined. To evaluate the possible roles of monocarboxylate(s) transport system in selenite transport, the inhibitory effects of Na-pyruvate and propionic acid (each at 1 and 5 mM) on selenite transport were investigated in both hepatocytes and enterocytes. Experiments with propionic acid indicated a possible influence of pH on the cellular uptake of selenite (See the results for details). Therefore, the effects of pH (6.5-8.5) on selenite transport were also studied, both in the presence and absence of GSHEffects of mercury and aquaporin inhibitors

It is well known that mercury is a potential inhibitor of several carrier-mediated transport systems (Pritchard and Renfro, 1983). Thus, the effects of possible extracellular complexation of Hg^{2+} with selenium, and interaction of Hg^{2+} with selenium transporter(s), as well as a combination of both were investigated. For these experiments, cells were either pre-incubated with Hg^{2+} or radiolabeled selenite stock was spiked with Hg^{2+} and pre-incubated together, prior to the initiation of selenite uptake analysis with or without GSH. The concentration of Hg^{2+} ranged from 0–10 μM. DIDS (62.5 μM) was used in combination with Hg^{2+} to investigate whether a component of selenite uptake was DIDS insensitive.

The effects of two different aquaporin inhibitors, phloretin (10 and 20 μM) and acetazolamide (100 and 200 μM) were investigated, in addition to propionic acid (described previously).

2.2.9 Data Analysis

All statistical analyses and curve-fitting was performed using SigmaPlot® (Version 11.0; Systat Software, Inc., Point Richmond, CA, USA). Kinetics and inhibition data were fitted with equations which provided the best fit. For the determination of the transport kinetics parameters for reduced form of selenium in enterocytes, the data were fitted with the three parameters sigmoid Hill equation:

$$f = \frac{B_{max} * X^h}{[K_d]^h + X^h}$$

where, B_{max} is the maximum rate of uptake, K_d is the substrate concentration at which half of maximum velocity is attained and 'h' is known as Hill coefficient.

Comparison among the different treatment groups was carried out using one-way ANOVA (followed by Tukey's posthoc test) or by t-test, as appropriate. Data that did not follow the assumptions of ANOVA, were analyzed by Kruskal-Wallis test. All the data are presented as mean ± S.E.M. (n). A p-value of ≤ 0.05 was considered to be significant while comparing different treatments.

2.3 Results

2.3.1 Kinetic properties of selenium transport and the effects of thiols on the transport process

Data in Figures 2.1A and 2.1B depict the dose dependency of [^{75}Se]-selenite accumulation in the absence and presence of GSH by hepatocytes at 15ºC. Cellular accumulation showed a linear pattern in both cases. The linear transport profile was persistent up to 50µM of [^{75}Se]-selenite exposure dose. Time-course studies revealed that [^{75}Se]-selenite cellular accumulation reached saturation within 30 min, whereas the saturation occurred at 10 min in the presence of GSH [see Appendix, Figure C2.S1A – B]. The initial rate (first 2 min) of selenium (from [^{75}Se]-selenite) uptake in the presence of GSH was about 8 times (5.66±0.66 picomoles/min/mg protein) higher than that of the selenite alone (0.69±0.13 picomoles/min/mg protein).

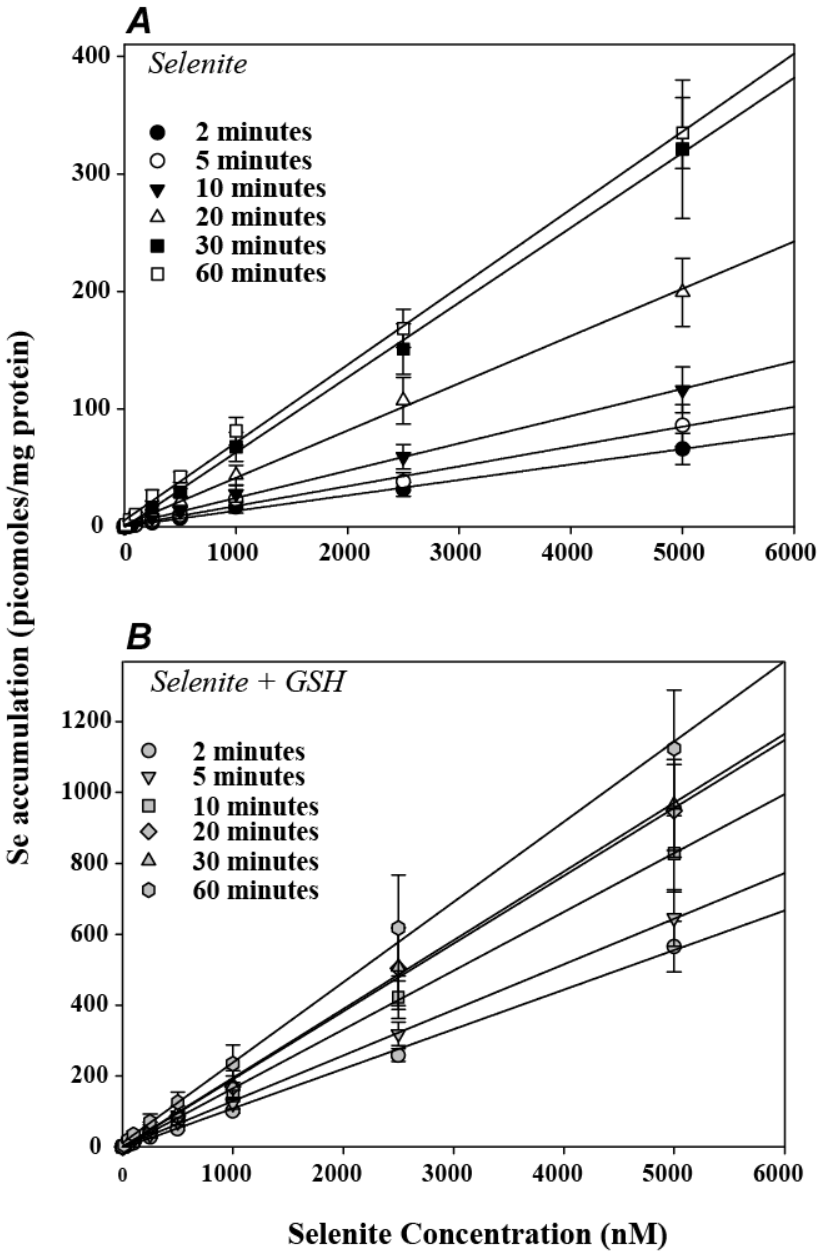

Figure 2.1: Kinetic characterization of selenium transport in hepatocytes. Dose-dependent selenium accumulation in isolated hepatocytes, either in the absence (Figure 2.1A) or presence (Figure 2.1B) of 30μM GSH. Accumulation data are expressed as picomoles/mg of protein. Data are presented as mean ± S.E.M. (n=6), where n represents the number of independent measurements using cells from as many fish.

In enterocytes, the rate of [^{75}Se]-selenite uptake was linear over the concentration range tested (Figure 2.2A). However, the uptake followed high-affinity Hill kinetics in the presence of GSH, as opposed to the hepatocytes (Figure 2.2B). The maximum rate of uptake was 6.661±0.279 picomoles/mg protein/min. The kinetic analysis of uptake is indicative of two substrate interaction sites (Hill coefficient = 1.911±0.23), with a substrate concentration corresponding to the half of maximal uptake rate being 3.612±0.283 μM. The time-dependent uptake data indicated a saturable uptake (within 10 minutes) in the presence of GSH in this cell type (see Appendix, Figure C2.S1D). However, [^{75}Se]-selenite transport [3.5 μM < K_d] did not attain saturation within 60 min (see Appendix, Figure C2.S1C). One of the important findings of the present study is that both forms of selenium accumulation were ~20 times higher in hepatocytes compared to enterocytes at equimolar concentrations tested at any specific exposure period. In the subsequent experiments, the effect of L-cysteine, another reducing agent, on [^{75}Se]-selenite uptake was investigated. Since L-15 media is supplemented with amino acids, transport experiments were conducted in Hanks' media as well as in L-15 media to elucidate the effect of L-cysteine on [^{75}Se]-selenite transport. The control experiment showed higher uptake of [^{75}Se]-selenite in L-15 media compared to Hanks' media. However, in the presence of equimolar concentrations of L-cysteine, uptake was significantly ($p \leq 0.001$) higher than selenite alone (Figure 2.3A and 2.3B). In the presence of equimolar concentration of L-cysteine, total cellular accumulation was comparable to each other irrespective of transport media composition. It is important to note here that selenium uptake was ~10-fold higher in the presence of L-cysteine compared to ~5-fold in the presence of equimolar concentration of GSH in hepatocytes suspended in Hanks' media. In contrast, uptake was ~18 fold higher in the presence of L-cysteine compared to ~9 fold at equimolar concentration of GSH in the enterocytes (Figure 2.3C and 2.3D). In order to address whether it was the reducing equivalent or sulfhydryl group (GSH or L-cysteine) that facilitates reduced selenium uptake, the effect of equimolar concentration of NADPH to that of GSH and L-cysteine was compared under identical conditions. There was no effect of NADPH on [^{75}Se]-selenite transport in hepatocytes (see Appendix, Figure C2.S2). This observation reinforces the role of interacting free thiol (-SH) group in efficient selenite reduction and subsequent transport of reduced selenium species.

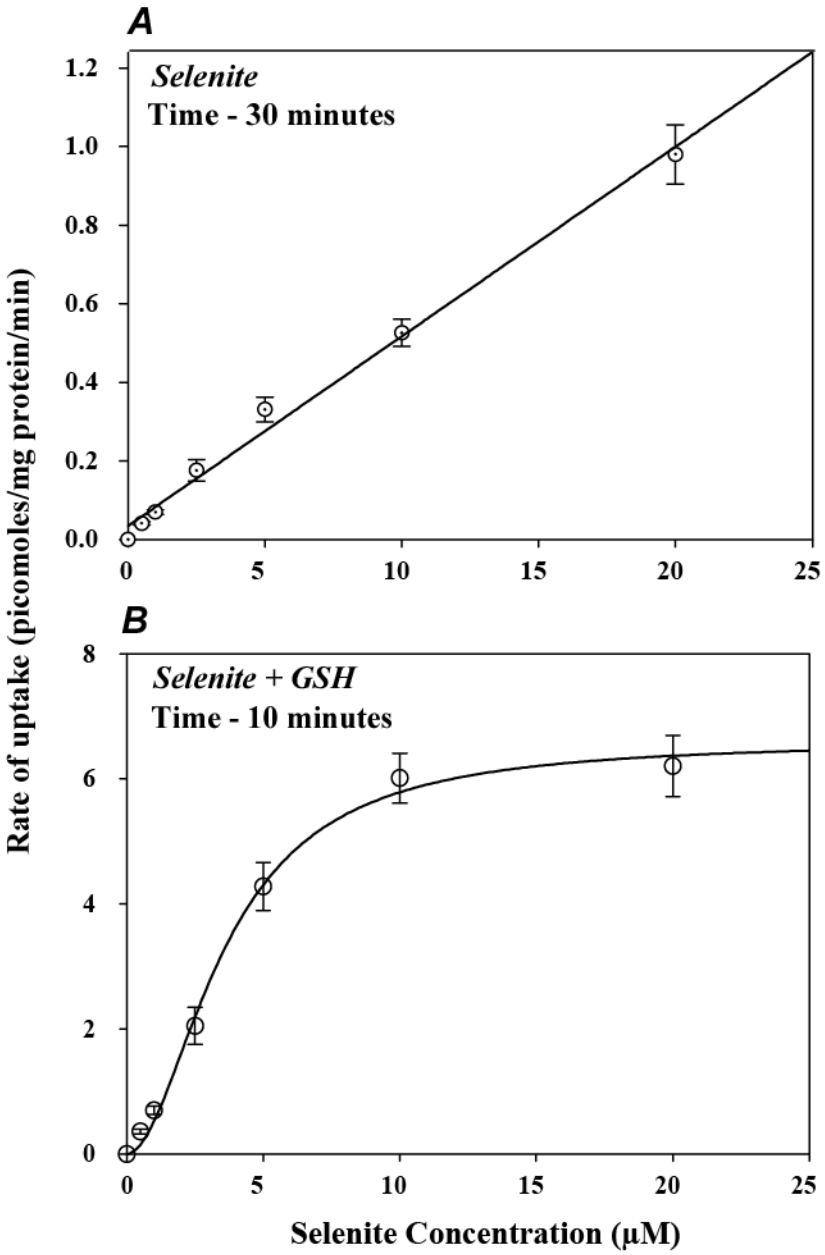

Figure 2.2: Kinetic characterization of selenium transport in enterocytes. Figure 2.2A and 2.2B show the kinetics of selenium transport in isolated enterocytes in the absence or presence of GSH, respectively. The values are mean ± S.E.M. (n=5), where n represents the number of independent measurements using cells from as many fish. The transport rate is expressed as picomoles/mg protein/min. In the presence of GSH (30µM), the uptake showed a high-affinity Hill kinetics (K_d = 3.612±0.283 µM).

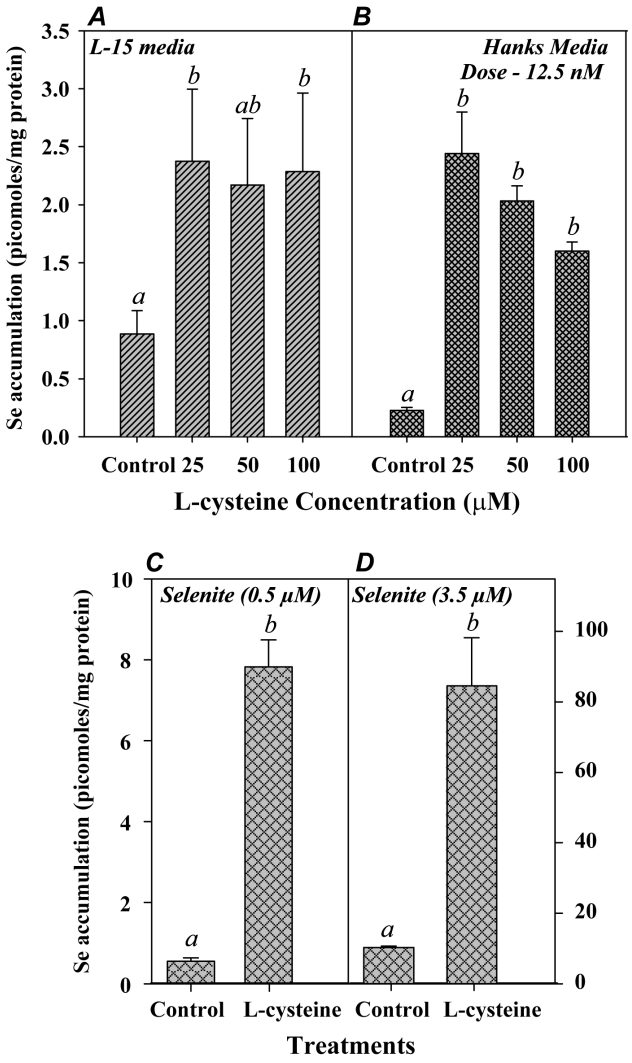

Figure 2.3: L-cysteine augments cellular selenite uptake. Accumulation of selenium in hepatocytes in L-15 media (Figure 2.3A) and Hanks' media (Figure 2.3B), either in the presence or absence of L-cysteine (One way ANOVA, n=5). Prior to the uptake experiment, 12.5 nM of [^{75}Se]-selenite and L-cysteine were mixed and incubated for 10 minutes at 15ºC. The transport experiments were initiated at the end of 10 minutes and were carried out for the next 30 minutes. The effect of equimolar L-cysteine (t-test, n=4) on selenium uptake in enterocytes is presented in Figure 2.3C and 2.3D. Data are presented as mean ± S.E.M., and n represents the number of independent measurements using cells from as many fish. Mean values with different letters are statistically significant ($p < 0.05$).

2.3.2 Energy independence of selenium transport

Orthovanadate did not inhibit uptake of [^{75}Se]-selenite or reduced form(s) of selenium in both cell types (see Appendix, Figure C2.S3B, C2.S3C and C2.S3D). DCCD was equally ineffective at blocking selenium transport in hepatocytes (see Appendix, Figure C2.S3A).

2.3.3 Involvement of anionic transport systems in selenium uptake

Data in Figure 2.4A (hepatocytes) summarize the effects of the anionic transporter blocker, DIDS, on selenium transport. DIDS inhibited accumulation of [^{75}Se]-selenite as well as reduced form(s) of selenium. Percentage inhibition calculation at equimolar concentration of DIDS suggests that this inhibitory effect was of higher magnitude in enterocytes (Figure 2.4C and 2.4D). It has been proposed earlier that both sulphate and sulphite may be transported *via* similar transport pathway in rat liver mitochondria (Crompton et al., 1974). However, sulphite was chosen over sulphate, because of its much closer structural resemblance with selenite. These experiments demonstrated a marked decrease of [^{75}Se]-selenite accumulation by sulphite (Figure 2.4B). Kinetic characterization (ligand binding, two site competition) suggested a competitive interaction with [^{75}Se]-selenite at two transport sites.

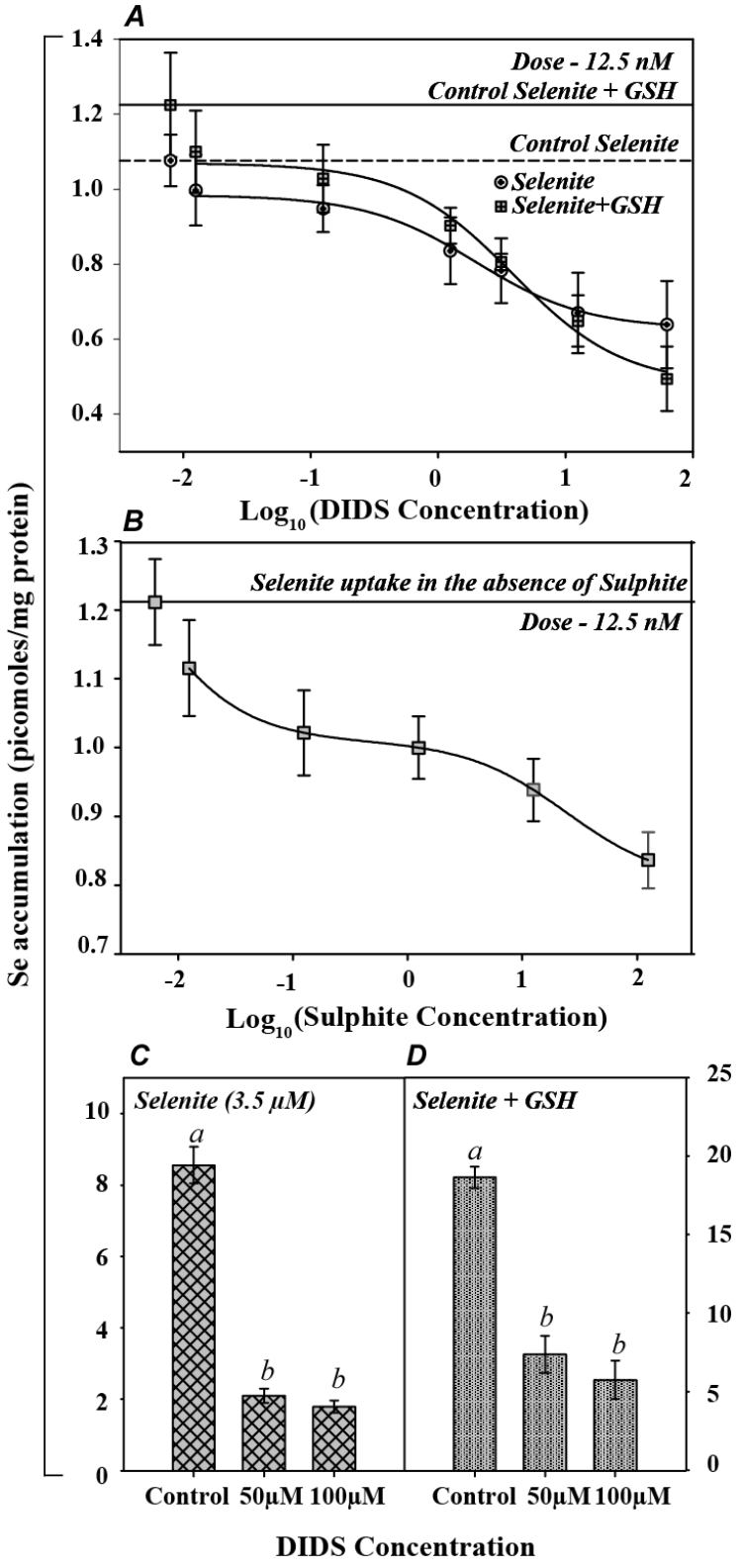
A
Dose - 12.5 nM
Control Selenite + GSH
Control Selenite
Selenite
Selenite+GSH
Log10(DIDS Concentration)
B
Selenite uptake in the absence of Sulphite
Dose - 12.5 nM
Log10(Sulphite Concentration)
Se accumulation (picomoles/mg protein)
C
Selenite (3.5 µM)
D
Selenite + GSH
a
b
b
a
b
b
Control 50µM 100µM Control 50µM 100µM
DIDS Concentration

Figure 2.4: Inhibition of cellular selenium uptake by DIDS and sulphite. Figure 2.4A shows the inhibitory effect of DIDS on selenium transport, in the absence and presence of 30 μM GSH (n=5-8). Inhibition data were fitted with the ligand binding, one site competition model (without GSH, $R^2 = 0.9875$ and with GSH, $R^2 = 0.9917$).

$$\left[f = min + \ (max - min)/\left(1 + 10^{(x - logEC_{50})}\right)\right]$$

Sulphite also inhibited selenite transport (Figure 2.4B, n=5) in the hepatocytes. Best fitting of the inhibition data were obtained with the ligand binding, two-site competition model ($R^2 = 1.000$).

$$\left[f = \min + (max - min) * \left[\left\{\frac{F1}{\left(1 + 10^{(x - logEC_{50[1]})}\right)}\right\} + \left\{\frac{(1 - F1)}{\left(1 + 10^{(x - logEC_{50[2]})}\right)}\right\}\right]\right]$$

Thus, it appears that there may be two apparent interaction sites with sulphite for selenite uptake. In enterocytes, the inhibitory effect of DIDS was much more pronounced (ratiometric evaluation at comparable doses of DIDS), either in the absence (Figure 2.4C) or presence (Figure 2.4D) of 30 μM GSH (n=5-6). Selenite exposure concentration was 12.5 nM for the hepatocytes and 3.5μM for the enterocytes. Data are presented as mean ± S.E.M., and n represents the number of independent measurements using cells from as many fish. Mean values with different letters are statistically significant (One Way ANOVA, $p < 0.05$).

2.3.4 Differential effects of pH on selenium transport

No inhibition of [^{75}Se]-selenite uptake was recorded up to 5 mM pyruvate (sodium salt) in either cell type (see Appendix, Figure C2.S4A). Similar to the observation with pyruvate, 5 mM propionic acid did not inhibit [^{75}Se]-selenite uptake in hepatocytes (See Appendix, Figure C2.S4B) in pH adjusted media (pH – 7.63). However, an important finding rose out of this experiment. Addition of propionic acid reduced the pH of L-15 media (contains phenol red), which was easily discernible by observing the obvious changes in the color. In this pH unadjusted media, selenite transport was significantly ($p \leq 0.001$) higher compared to the control. This observation led us to deduce that pH might play an important role in selenite transport. Indeed, subsequent experiments at different pH proved that selenium uptake is pH dependent. With increasing pH, there was a decrease in [^{75}Se]-selenite uptake in both cell types (Figure 2.5A and 2.5C). Notably, this resembled the functions of many solute transporters including SLC-16 family of proton-dependent monocarboxylate transporters MCT 1-4 (Halestrap and Price, 1999). However, a completely opposite effect of pH was observed on the reduced form(s) of selenium uptake in both cell types (Figure 2.5B and 2.5D).

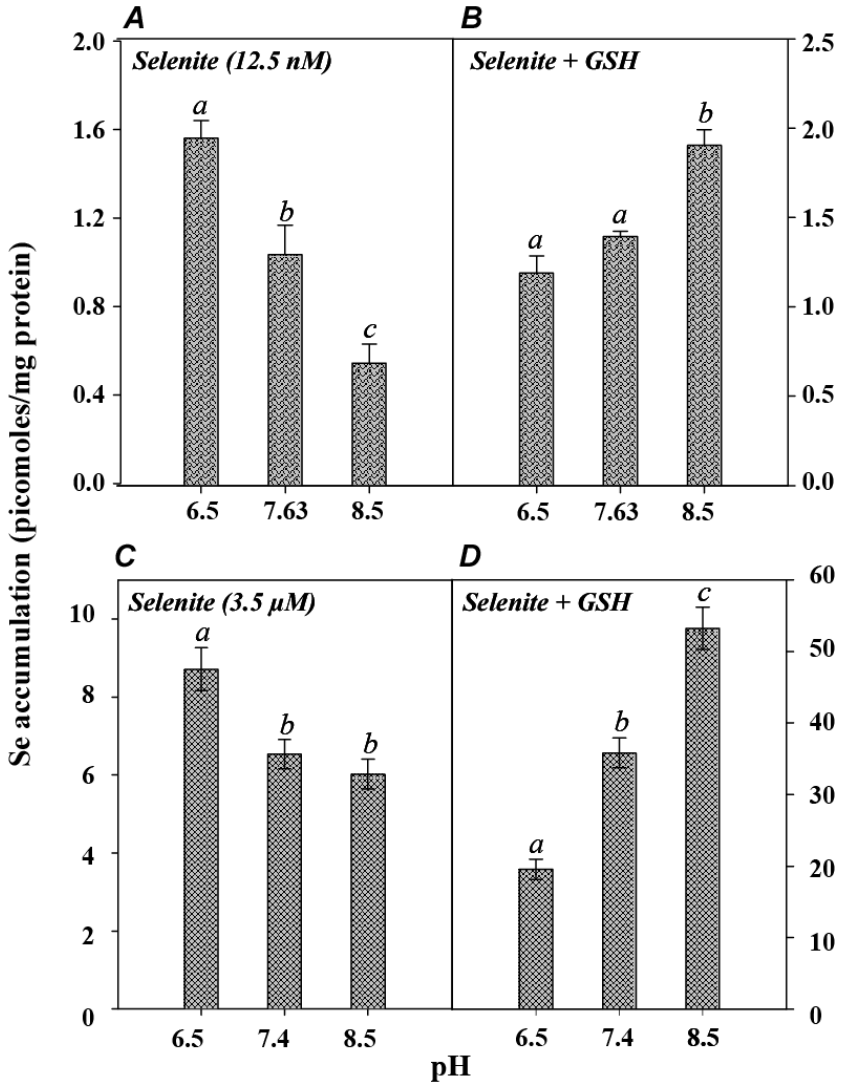

Figure 2.5: Extracellular pH is an important determinant of cellular selenium transport. With increasing pH, there was a reduction in selenite transport, both in hepatocytes (Figure 2.5A) and enterocytes (Figure 2.5C). However, the uptake (10 minutes) of reduced form(s) of selenium showed an opposite response, both in hepatocytes (Figure 2.5B) and enterocytes (Figure 2.5D). Data are presented as mean ± S.E.M. (n=5), where n represents the number of independent measurements using cells from as many fish. Mean values with different letters are statistically significant (One Way ANOVA, $p < 0.05$).

2.3.5 Extracellular component of selenium-mercury interaction

Data in Figures 2.6E and 2.6F illustrate the inhibitory effects of Hg^{2+} on selenite transport (both at low and high dosage) in enterocytes either in the absence or presence of GSH. However, the effect of Hg^{2+} was more complex in hepatocytes. Pre-exposure to mercury inhibited [^{75}Se]-selenite accumulation irrespective of media composition (Figure 2.6A and 2.6C). This inhibitory effect was higher than DIDS alone, which indicates the possible existence of DIDS-insensitive component of the uptake process. Interestingly, significant stimulation of the reduced form(s) of selenium uptake was recorded in the presence of Hg^{2+} (Figure 2.6B and 2.6D). The next experiments were aimed at understanding the individual role of complex formation of [^{75}Se]-selenite with Hg^{2+} as well as the direct transporters inhibition by Hg^{2+}. This series of experiments was conducted in Hanks' media to rule out any possible complex formation of mercury with organic ligands present in L-15 media. To delineate the role of complex formation and thus limiting the substrate availability, [^{75}Se]-selenite (12.5 nM) and mercury (10 μM) was incubated together prior to the uptake study with unexposed hepatocytes. Significant inhibition of [^{75}Se]-selenite transport was observed (Figure 2.6B), indicating the potential role of complex formation. Although, the element of a direct inhibitory effect of Hg^{2+} on the transporter(s) functions cannot be ruled out since the molar concentration of Hg^{2+} was much higher than that of [^{75}Se]-selenite. Nevertheless, when the hepatocytes were pre-exposed to Hg^{2+} and washed with an excess of media prior to the transport experiments, the inhibitory effect was persistent (Figure 2.6B). This clearly demonstrated the interaction of Hg^{2+} with transporter(s). Maximum inhibitory effect was observed in unwashed hepatocytes pre-exposed to Hg^{2+}, but was statistically non-significant compared to the two other treatments. In the presence of GSH, the stimulatory effect of Hg^{2+} remained persistent except when Hg^{2+} was pre-incubated with [^{75}Se]-selenite-GSH mixture and in the presence of DIDS, where the cellular accumulation was similar to that of the control. Among the inhibitors of aquaporins tested, phloretin could not inhibit any forms of selenium transport in enterocytes (Figure 2.7B and 2.7C). However, both phloretin and acetazolamide elicited modest but significant ($p \leq 0.05$) inhibitory effect on [^{75}Se]-selenite transport in hepatocytes (Figure 2.7A).

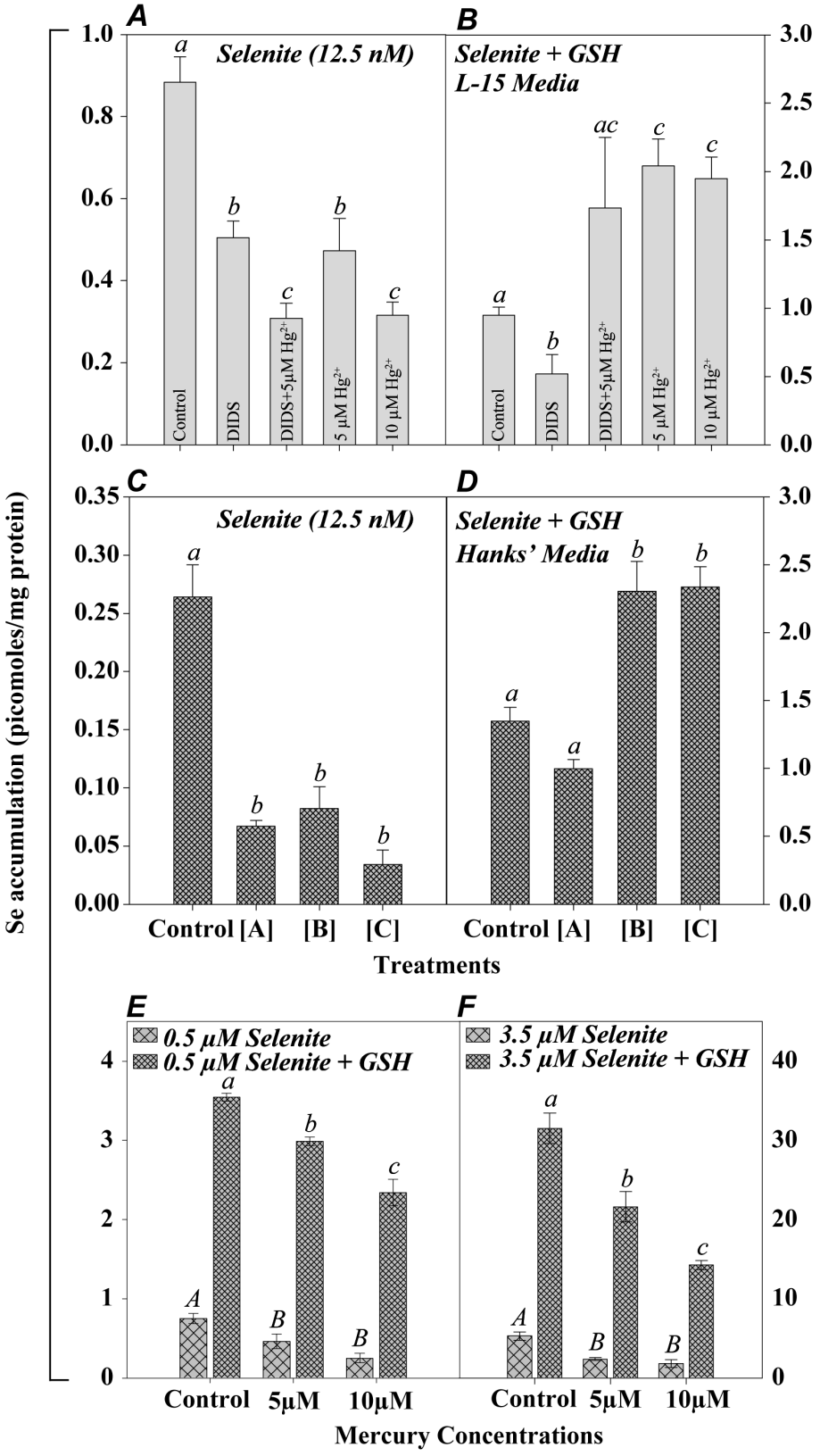
A
Selenite (12.5 nM)
B
Selenite + GSH
L-15 Media
C
Selenite (12.5 nM)
D
Selenite + GSH
Hanks' Media
Control
DIDS
DIDS+5μM Hg2+
5 μM Hg2+
10 μM Hg2+
Se accumulation (picomoles/mg protein)
Control [A] [B] [C] Control [A] [B] [C]
Treatments
E
0.5 μM Selenite
0.5 μM Selenite + GSH
F
3.5 μM Selenite
3.5 μM Selenite + GSH
Control 5μM 10μM Control 5μM 10μM
Mercury Concentrations

Figure 2.6: Conspicuous effects of mercury on the cellular selenite transport in hepatocytes (Figure 2.6A-D) and enterocytes (Figure 2.6E-F). In Figure 2.6C, treatment [A] represents data when 12.5 nM of [^{75}Se]-selenite was incubated with 10μM Hg^{2+} for 20 minutes prior to the uptake experiment with unexposed cells; treatment [B] represents data when 10μM Hg^{2+} pre-exposed (for 20 minutes) cells were thoroughly washed prior to [^{75}Se]-selenite uptake experiments; and treatment [C] represents data for the uptake of 12.5 nM [^{75}Se]-selenite in 10μM Hg^{2+} pre-exposed cells that were not washed (n=5; notations for the columns are same for Figure 2.6D). When GSH was used in these experiments, Hg^{2+} was added 2 minutes after mixing of [^{75}Se]-selenite and 30 μM GSH (final concentration), and transport experiments were initiated on 10th minute after initial mixing. Subsequently, the flux experiments were carried out for another 10 minutes. Data are presented as mean ± S.E.M., and n represents the number of independent measurements using cells from as many fish. Mean values with different letters are statistically significant (One Way ANOVA, $p < 0.05$).

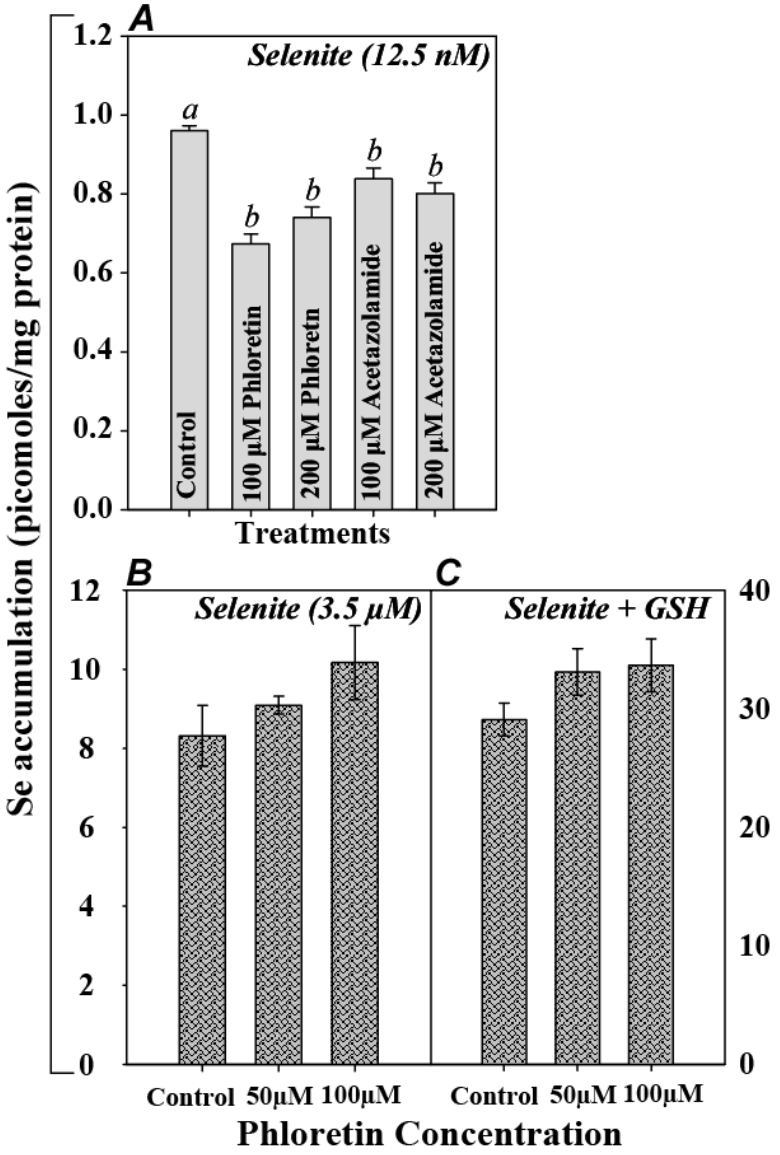

Figure 2.7: The effects of phloretin and acetazolamide on selenium uptake. Aquaporin blockers, phloretin and acetazolamide inhibited [^{75}Se]-selenite transport in hepatocytes (Figure 2.7A). However, no such effect was found in enterocytes, either in the absence (Figure 2.7B) or presence (Figure 2.7C) of 30 µM GSH. Data are presented as mean ± S.E.M. (n=4), where n represents the number of independent measurements using cells from as many fish. Mean values with different letters are statistically significant (One Way ANOVA, $p < 0.05$).

2.4 Discussion

To date, the knowledge of cellular selenium transport systems in fish is particularly limited. Results presented here provide novel information on the kinetic characteristics of physiologically relevant dosage of selenium transport in primary hepatocytes and enterocytes. [^{75}Se]-selenite transport rate was linear in both cell types. This demonstrates the involvement of low-affinity but high capacity transport systems for [^{75}Se]-selenite in both cell types. This is in agreement with the previous findings in rat hepatocytes exhibiting linear selenite uptake rate even up to supra-physiological dosage (Park and Whanger, 1995). Similarly, the observation that selenite transport does not reach saturation in enterocytes is in agreement with the transport of selenite in rat intestine (Wolffram et al., 1985). In the presence of GSH, fitted data suggest a high-affinity (K_d = 3.61±0.28 μM) sigmoidal kinetics in enterocytes, contrary to that of a linear uptake kinetics in hepatocytes. Sigmoidal transport kinetics indicates a positive cooperativity at transport sites in enterocytes. The Hill coefficient derived from the kinetics data is equal to 1.911±0.2, signifying an interaction of substrate with at least two transport sites. In such allostrically regulated transport pathway, binding of substrate to one site increases the binding affinity of the other. However, it should be pointed out that such calculation is based on fitting the experimental data and remains inferential in the absence of direct evidence of multiple carrier systems. In line with the present observation, Anundi et al. (1984) also reported that incubation of selenite with GSH increases total selenium accumulation in the isolated rat enterocytes.

It was also found that L-cysteine, like GSH, also stimulated selenium uptake, but with greater magnitude. Scharrer et al. (1992) previously reported similar observation in rat intestine. Such apparent differences in the uptake in the presence of different thiols seem to be attributable to either differential reducing potential of the thiol moiety of the reducing agents or differences in transport properties of the intermediates upon reaction with selenite. Examining the reaction of selenite with GSH and L-cysteine can partially explain such dramatic increase in the uptake. Under physiological pH, reaction of selenite with GSH can form selenotrisulfide (GSSeSG), selenopersulfide (GSSeH), hydrogen selenide (HSe^- in solution) and colloidal elemental selenium (Se) (Ganther, 1971). It is assumed that a similar reaction scheme is possible for L-cysteine with free thiol (–SH) group. At physiological pH, selenotrisulfide derivatives of GSH

and L-cysteine are very unstable compared to that of persulfide derivatives, which can also be formed in reaction with GSH and colloidal elemental Se (Ganther, 1971). Given the unknown nature of transport properties of selenopersulfide derivatives, it may be assumed that transport pathway may likely be similar with GSH and L-cysteine based on structural similarity. It is important to note that the kinetics of GSH transport in isolated rat hepatocytes indicates low-affinity sigmoidal influx system with a high K_m value of 2.36 ± 0.26 mM (Sze et al., 1993). However, the possibility of testing such a high K_m value for selenopersulfide in isolated cell systems is difficult because of the inherent high reactivity of this compound as well as its toxicity. In the present experimental system with hepatocytes, the molar ratio of GSH to selenite was more than 6-1000 times and raises the possibility that HSe^- was the major form available for uptake. However, in the enterocytes this ratio varied from 1.5 – 60, which might alter the speciation of selenium in the reaction mixtures. Nevertheless, experimental evidence from the present study strongly suggests the presence of a high-affinity transport system for reduced form(s) of selenium in enterocytes that is markedly different from hepatocytes (both non-polar system). Relative contribution of different chemical forms of selenium upon reaction with selenite to L-cysteine and GSH remains an important yet unresolved issue, nevertheless, HSe^- is probably not the sole participatory species involved in the uptake process.

Selenium transport was energy independent irrespective of the chemical forms under investigation. Empirical evidences with human lymphocytes (Porter et al., 1979) and hamster intestine (McConnell and Cho, 1965) demonstrated this previously. Under the assumption of anion-exchanger mediated selenite transport, energy-dependency of transport violates the fundamental property of this transporter. Rather, such facilitative transport system is dependent on concentration gradients to mediate net bidirectional release or uptake of substrates. However, recent investigation in transformed keratinocytes model indicates that selenite transport is an energy-dependent process (Ganyc and Self, 2008). In this context, it would be interesting to explore why transformed cells like HaCat (human keratinocytes) require energy for selenium transport and what energetic implications it might have on this type of cells when selenite is used as a chemotherapeutic agent.

The finding that DIDS, an inhibitor of anion-exchanger, can block both forms of selenium transport is in agreement with a previous observation (Ganyc and Self, 2008). However, the highest dose of DIDS used in the present experiments could not completely block uptake in both cells types. A study with erythrocytes indicated that about 90% of anion-exchanger protein was bound to DIDS within 20 minutes of incubation (final concentration 10 μM) (Ship et al., 1977). In the present experiment, a much higher concentration of DIDS (200μM) was used with equivalent incubation time, thus increasing the possibility of blocking majority of the anionic-transport activity. If the anion-exchanger was the only membrane protein involved in [^{75}Se]-selenite transport, a much stronger inhibitory effect would have been observed at this dose. However, the observed results were quite different. It is therefore conceivable that a component of selenium uptake may be DIDS insensitive and indicates a strong possibility for the existence of DIDS insensitive selenium (both oxidized and reduced forms) transport pathway(s) (discussed below).

Inhibition of [^{75}Se]-selenite transport by analogous oxyanion, sulphite, links the possible involvement of the transport pathway of the latter. Sulphate has also been found to effectively block selenite transport in human erythrocytes (Galanter et al., 1993). Thus, the involvement of SLC26 members of anionic exchanger in selenite transport cannot be ruled out, since most of the members of this transporter family have been implicated in sulphate and sulphite transport (Labotka et al., 1989). In view of the previous report suggesting Na^+ independency of selenite transport (Wolffram et al., 1986), possible involvement of Na^+-dependent sulphate transport pathway is negligible. Rather, evaluating the role proton sensitive SLC26A1 in hepatocytes and SLC26A3 in enterocytes would be of considerable interest, based on their sensitivity to pH, respective tissue specific expression and differential transport properties (Mount and Romero, 2004). This may explain why the apparent variation in [^{75}Se]-selenite transport characteristics between these two types of cells were observed in this study.

Extracellular pH is an important determinant of selenite speciation. Selenite is in its deprotonated form SeO_3^{2-} at pH 7.63, as evident from the Pourbaix diagram for micro molar concentration (Olin et al., 2005). In contrast, it is in 'biselenite' ($HSeO_3^-$) form at pH 6.5. Such speciation is highly dependent on redox potential of the system and the presence or absence of

interacting organic and inorganic ligands. While examining the effect of pH on selenium transport, two antithetical observations were documented in the absence or presence of GSH. Stimulation of [^{75}Se]-selenite uptake at low pH resembles closely with the characteristics of anion-exchanger family SLC26 involved in sulphate transport (Galanter et al., 1993). Chloride-dependent HCO_3^- anion exchangers (SLC4 family of transporters) may also be considered as important candidates at low pH, based on their sensitivity to DIDS, pH and structural likeliness of $HSeO_3^-$ with HCO_3^- (Romero et al., 2004). It is also noteworthy that pH-dependency is also one of the fundamental properties exhibited by the monocarboxylates transporters [pH sensitive SLC16 family of transporters, MCT1 – 4 (Halestrap and Meredith, 2004)], implicated in selenite transport in yeast (McDermott et al., 2010). In the present experimental system, neither pyruvate nor propionic acid inhibited selenite transport. However, re-examining the involvement of pH-sensitive SLC16 family of transporters might be of particular interest based on their spectrum of substrate choice and variable inhibitory effects elicited by structurally similar compounds. Absence of data on concomitant measurement of intracellular pH or membrane potential precluded the possibility of determining the electrical activity of the transport process. The opposite effect of pH on the transport of reduced form(s) of selenium in both cell types is elusive without valid information on speciation. Thus, comparing the uptake properties with homologous compounds is extremely difficult and would be purely speculative. To the best of my knowledge, this is first report suggesting the differential role of pH in the transport of selenite and its reduced form(s) in different cell types in any fish species.

Much of the scientific interest in selenium-mercury interaction is focused on the intracellular aspects. However, extracellular selenium-mercury interactions have not received much attention. This interaction can occur either by complex formation of selenium with inorganic mercury before being transported into the cell or interaction of mercury with selenium transporters. It has shown here for the first time the inhibitory effect of Hg^{2+} on [^{75}Se]-selenite transport in these cell types. Multiple possibilities exist in this context. Persistence of inhibitory effect after thoroughly washing the cells suggests inhibition at transporter level. Given the possible presence of Hg^{2+} sensitive amino acid residue in the pore-forming domain in the candidate transporter, interaction of Hg^{2+} with cysteine residue can effectively block [^{75}Se]-selenite transport based on the notable similarity of ionic radii (4Å) between Hg^{2+} with that of

SeO_3^{2-}, thus preventing access to the pore. Previous investigation with human lymphocytes suggests that sulfhydryl group modifying agents (NEM, PCMB and iodoacetamide) can block selenite transport (Porter et al., 1979). In this context, it is also important to note that cysteine-residue (Hg^{2+} interaction moiety) in the conserved STAS domain of sulphate transporter plays a pivotal role for its functionality in *A. thaliana* (Rouached et al., 2005). Another possibility may be the limited availability of free selenite for transport during co-exposure of selenite with Hg^{2+} due to the formation of $HgSeO_3$ complex with very low solubility (Zareh et al., 1995). Considering the inhibitory effect of Hg^{2+} on selenite transport, the induction of uptake of reduced form(s) of selenium in the presence of Hg^{2+} was unanticipated, and remains to be clarified. To the best of my knowledge, this is the first report where mercury has been found to augment the transporter activity instead of its characteristic random inhibitory effect on multiple transporters.

Since a pronounced inhibitory effect of Hg^{2+} on cellular [^{75}Se]-selenite accumulation was recorded, the possible involvement of aquaporin in [^{75}Se]-selenite transport was hypothesized, given that Hg^{2+} is a classic inhibitor of aquaporins. The capacity of aquaporin to transport other related metalloids such as arsenite, antimonite and silicon is in line with such possibility (Haddoub et al., 2009). However, the hypothesis on the possible role of aquaporin in selenite transport constrains from the absence of specific inhibitors of aquaporins. Like mercury, acetazolamide and phloretin can also block anionic transporter functionality (Pritchard and Renfro, 1983). In addition, propionic acid at higher concentration can also inhibit aquaporin by inducing intracellular acidification (Tournaire-Roux et al., 2003). Thus, it is difficult to either accept or rule out the possible role of aquaporin in selenite transport. Conversely, other candidate transporters (SLC4, SLC16 and SLC26) show isoform specific and varying degree of inhibition by DIDS, phloretin and acetazolamide (Halestrap and Meredith, 2004; Mount and Romero, 2004; Pritchard and Renfro, 1983; Romero et al., 2004). Thus, using pharmacological approaches alone probably is not enough to ascertain the specific roles of these transporters in selenite transport, if indeed there.

2.5 Conclusion and future perspectives

Collectively, the present study constitutes a major advance in our understanding of how selenite and its reduced form(s) are transported across the cell membranes of enterocytes and hepatocytes in fish. It has been demonstrated that hepatocytes and enterocytes exhibit different properties in selenite transport either in the presence or absence of thiols. The present study also demonstrated that the presence or absence of thiols determines the differential effects of extracellular pH. The apparent existence of selenium species-specific multiple transport mechanisms and their dependence on the proton electrochemical gradient will provide much impetus for future nutritional and toxicological research. Inhibition of selenite transport in enterocytes by inorganic mercury can be of considerable interest in relation to selenium homeostasis in fish living in mercury-contaminated environments. Similar to many other investigations, the lack of understanding of physiological speciation of reduced form(s) of selenite in systemic circulation limited the scope to test the role any possible transport pathway(s) involved in the uptake of structurally similar compounds. A holistic approach to resolve such problem relies on understanding the physiological speciation of selenium using techniques such as synchrotron based X-ray spectroscopy. This will be greatly helpful in addressing the specific problems related to the identification of substrate(s). Once the substrates are being identified, heterologous expression of target transporters can be used to decipher their transport properties.

CHAPTER 3: Characterization of the hepatic pathways involved in selenium (both inorganic and organic) metabolism using isolated hepatocytes [2]

3.1 Introduction

Selenium (Se) is a vital constituent of many protein molecules with diverse physiological functions. Fish have 32-34 seleno-proteins relative to 23-25 in terrestrial vertebrates (Lobanov et al., 2008), and the physiological functions of some of these seleno-proteins are yet to be characterized. Se is known to be toxic to fish at a marginally elevated level beyond the threshold concentration required for normal physiological functioning. In the aquatic environment, seleno-compounds are present either as inorganic (e.g., selenite, selenate) or organic (e.g., selenomethionine, selenocysteine) forms. However, the degree of Se toxicity to aquatic animals differs within and among the organic and inorganic species. For example, selenite (SeO_3^{2-}) is known to be much more toxic to fish compared to selenate (SeO_4^{2-}) and seleno-DL-methionine (Hamilton and Buhl, 1990). The diversity of Se speciation in the aquatic environment, along with its essentiality and chemical species-specific toxicity in biota, makes it a unique element of study from a toxicological perspective. In mammalian systems, the differences in toxicity among different seleno-compounds have been attributed to the differences in their metabolism, resulting in the direct and/or metabolites-mediated generation of reactive oxygen species (ROS), and thereby causing oxidative stress (Spallholz, 1994). This phenomenon though has yet to be investigated in piscine systems despite the fact that metabolic processes are largely conserved between mammals and fish.

To date, the metabolism of Se in fish is poorly understood. Although the metabolism of seleno-amino acids in zebrafish (*Danio rario*) has been described in KEGG (Kyoto Enclycopedia of Genes and Genomes) metabolic pathway database, the functional characterization of such genome based pathway at the metabolite level has not been conducted. In mammalian systems, it

---

[2] This chapter of the thesis has been published in the journal, Metallomics 2: 710-717 (2010) under joint authorship with Derek Peak and Som Niyogi (University of Saskatchewan). doi: 10.1039/C0MT00008F

has been suggested that the metabolism of selenite in the presence of glutathione (GSH) leads to the generation of superoxide anion ($O_2^{\cdot-}$), which is the primary cause of selenite cytotoxicity (Yan and Spallholz, 1992). Seko *et al.* (1989) explained this probable reaction mechanism with the intermediate metabolites of selenite (Figure 3.1). In accordance to these findings, my previous study has also demonstrated a dose dependent increase in the ROS production and subsequent loss of cellular thiol status in cultured rainbow trout (*Oncorhynchus mykiss*) hepatocytes exposed to selenite (Misra and Niyogi, 2009). In contrast, the metabolism of selenomethionine appears to be much more complex with many more intermediates than that of selenite. Based on the KEGG pathway resources, a schematic diagram of selenomethionine metabolism in zebrafish is presented in Figure 3.2A. In this pathway, selenomethionine is metabolized into methylselenol (CH_3SeH) *via trans*-sulfuration pathway. One of the intermediary metabolites of selenomethionine is selenocysteine, which is an important constituent of seleno-proteins. This pathway is thought to be prevalent under the normal nutritional regime. Whereas, at toxic level of selenomethionine, the existence of an enzyme-mediated cellular detoxification pathway has been proposed in mammalian systems, where the enzyme, L-methionine-γ-lyase, metabolizes selenomethionine into CH_3SeH, α-ketobutyrate and ammonia (Okuno et al., 2001). In addition, the GSH-mediated redox cycling of CH_3SeH has been suggested to produce $O_2^{\cdot-}$ (Figure 3.2B, based on Chaudiere *et al.*, 1992). However, the presence of L-methionine-γ-lyase – activity has yet to be confirmed in fish.

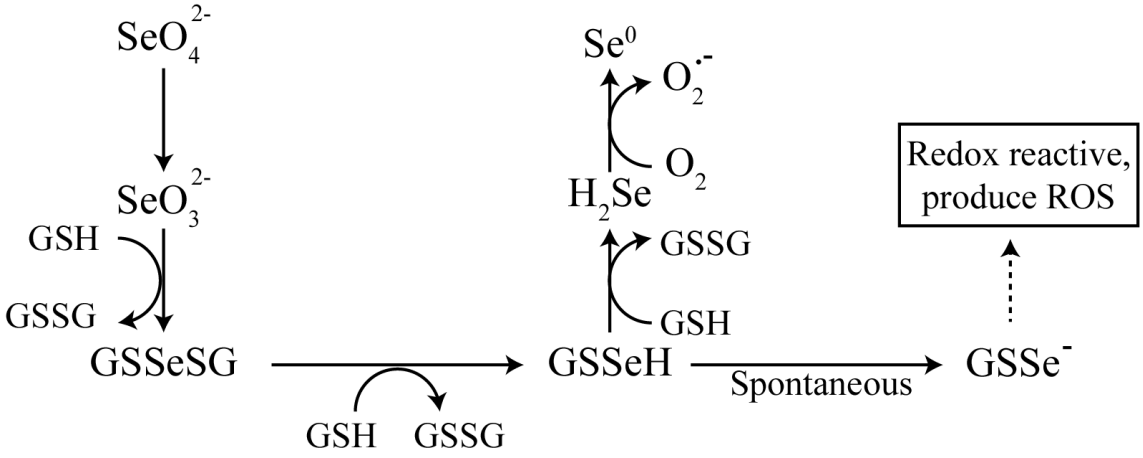

Figure 3.1: Schematic pathway of superoxide anion ($O_2^{\cdot -}$) production from the reaction of selenite (SeO_3^{2-}) with glutathione (GSH) (Modified from Yan and Spallholz, 1992). This reaction mechanism with probable intermediates was proposed by Seko et al. (1989). However, it was Painter (1941) who proposed first that excess GSH reacts with selenite resulting into formation of elemental Se. GSH reacts with selenite to produce selenotrisulfide (GSSeSG). Selenotrisulfide is very labile and is reduced to redox reactive selenopersulfide ($GSSe^{-}$) molecule either by the action of glutathione reductase in the presence of NADPH or in the presence of excess GSH. The conversion of hydrogen selenide (H_2Se) into elemental selenium produces $O_2^{\cdot -}$, leading to selenite induced oxidative stress.

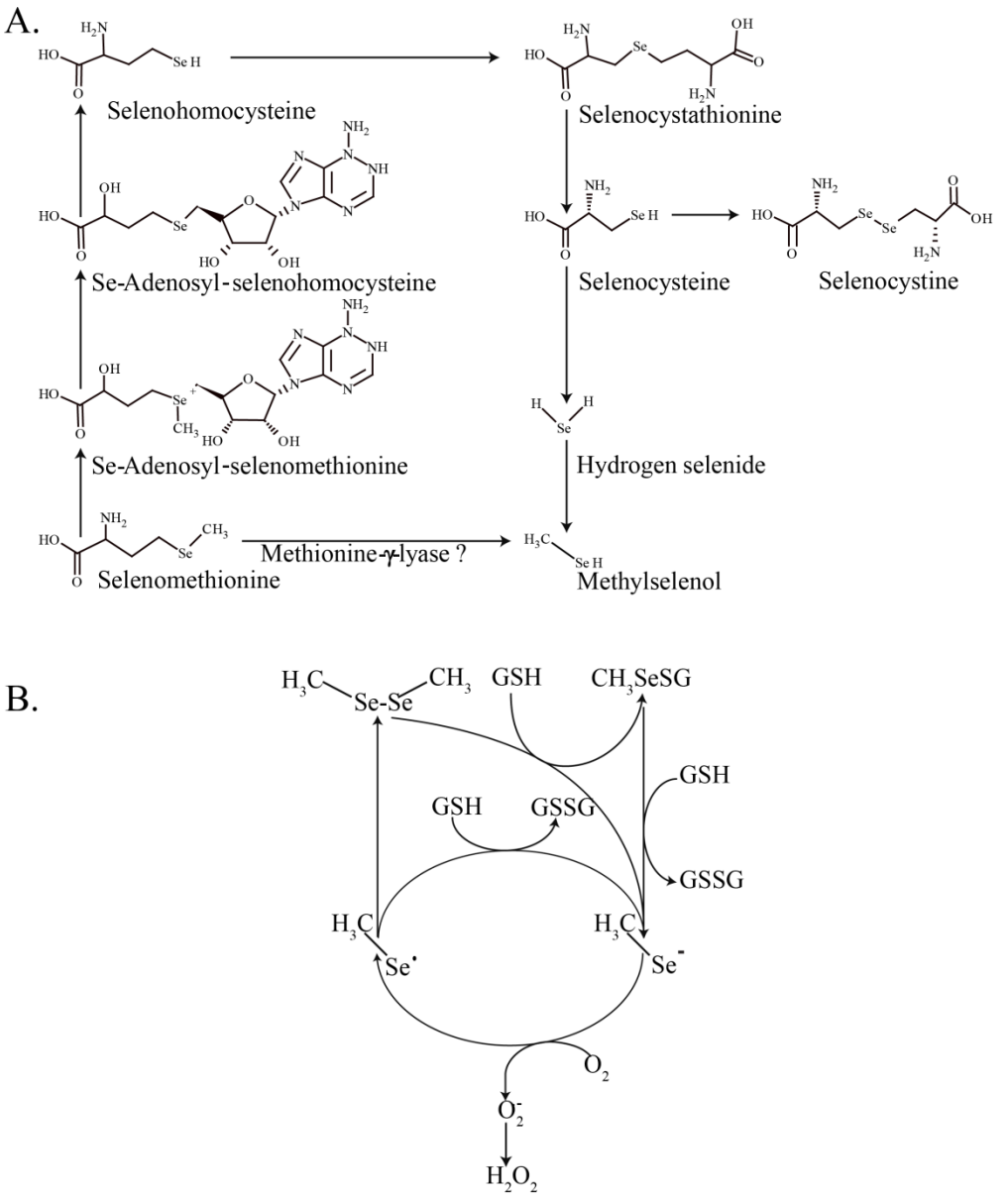

Figure 3.2: Selenomethionine metabolism in zebrafish (*Danio rerio*) as described in the orthology-based KEGG metabolic pathway (Figure 3.2A). The enzymes of the *trans*-sulfuration pathway (conversion of selenomethionine into CH_3Se *via* selenocysteine) are present in zebrafish. However, there is no evidence of direct catalysis of selenomethionine into CH_3SeH. Note that redox cycling of CH_3SeH ($CH_3Se^{\cdot}$ and/or CH_3Se^{-} form) in the presence of GSH (Figure 3.2B) is the only known pathway of $O_2^{\cdot -}$ generation during selenomethionine metabolism (Chaudiere et al., 1992).

One of the major challenges in unravelling the metabolic pathway of Se is the lack of sensitive analytical techniques capable of detecting the intermediate metabolites in biological samples. Most of the current techniques are limited by extensive sample pre-treatment, which can potentially change the oxidation state of metabolites, especially the inorganic intermediates. In this regard, the use of synchrotron-based intense X-ray absorption near edge structure (XANES) spectroscopy can be particularly useful in sensitive intracellular elemental speciation analysis. From the perspective of toxicological research, XANES spectroscopy is a much less explored yet quite promising state-of-the-art tool for investigating metabolic fingerprint of toxic metals/metalloids in complex biological matrices without any major sample pre-treatment steps or artifacts (Gunter et al., 2002). Using this technique, a few recent studies have documented Se speciation in biological samples (Pickering et al., 2000; Vickerman et al., 2004), although this approach has rarely been applied to *in vitro* studies. Since Se contamination in the aquatic environment is a complex and emerging issue, investigating the metabolic fate of this element is critical for understanding its toxicity in aquatic organisms. Keeping this in mind, the metabolism of selenate, selenite and L-selenomethionine is investigated in isolated rainbow trout hepatocytes in primary culture using XANE spectroscopy and biochemical analysis. Cultured hepatocytes were chosen as a model experimental system for this study because liver is the primary site of Se metabolism in fish. It is also important to note here that selenate and selenite are the primary inorganic forms of Se in the aquatic ecosystems (Hamilton and Buhl, 1990), whereas selenomethionine is known to be the most predominant organic selenium species found in the natural prey species of fish (Andrahennadi et al., 2007).

3.2 Experimental

3.2.1 Chemicals

High purity Se standards [elemental selenium (≥99%), sodium selenite (98%), sodium selenate (98%), L-selenomethionine (≥98%), Se-(Methyl)-selenocysteine hydrochloride (≥95%), selenocystine (≥98%), methylseleninic acid (95%) and dimethyl selenide (99%)] were obtained from Sigma-Aldrich, Mississauga, Canada. Sodium selenide was purchased from Alfa Aeser,

USA. CM-H_2DCFDA was purchased from Invitrogen, Burlington, Canada. All other chemicals, unless otherwise mentioned, were purchased from Sigma-Aldrich, St Louis, USA.

3.2.2 Animal

Rainbow trout (*O. mykiss*) weighing 200–300 g were obtained from Lucky Lake Fish Farm, Saskatchewan. Fish were maintained in 1000 l flow-through aquaria receiving dechlorinated Saskatoon City water at a rate of 2 l/min under constant aeration. A photoperiod of 16 h light : 8 h dark and a water temperature of 15 ± 1°C were maintained throughout the experimental period. The fish were fed once daily with Martin's commercial diet (Martin Mills Inc., Elmira, Canada) at a ration of 2% of body weight. All fish were acclimated for at least 2 weeks prior to their use in the experiments. The experimental protocol was in accordance with the Canadian Council for Animal Care Guidelines and was approved by the animal research ethics board at the University of Saskatchewan.

3.2.3 Hepatocytes isolation and culture

Trout hepatocytes were isolated using a two-step collagenase perfusion as outlined elsewhere with minor modifications (Misra and Niyogi, 2009). The fish were euthanized with an overdose of MS-222 (0.5 g/L) in dechlorinated water. The hepatic portal vein was cannulated with PE-50 tubing and perfused with ice-cold modified Hanks' Media (in mM: NaCl 136.9, KCl 5.4, $MgSO_4.7H_2O$ 0.8, $Na_2HPO_4.7H_2O$ 0.33, KH_2PO_4 0.44, HEPES 5.0, Na-HEPES 5.0, pH 7.63). When the liver was completely blanched, the perfusion line was switched to the medium containing 0.2 mg/ml collagenase in Hanks' Media, and the perfusion was continued until the liver was fully digested. The digested liver was carefully scraped with a razor blade on a Petri plate, and the dissociated cells were filtered through 260 and 73 µm mesh size strainers, respectively. The cells were then washed 3 times in Hanks' Media at 700 rpm at 12°C. This was followed by a single washing with the same media containing BSA (1%) and $CaCl_2$ (1.5 mM). The cells were then incubated for 30 minutes in L-15 media (pH 7.63) containing antimicrobial and antimicotic solution (Invitrogen, Burlington, Canada) at 15°C. The settled down cells were

collected by aspirating out the media on the top and resuspended in 20 ml of L-15 media. Cell viability was determined by the trypan blue exclusion test, and the suspensions showing more than 90% cell viability were used for experiments. The cells were plated in 6-well Primaria plates (BD Falcon, Mississauga, Canada) at a density of 0.3×10^6 cells/cm^2 and incubated at 15° C for at least 24 h to form monolayer prior to their use in the experiment.

3.2.4 Sample Preparation for XANES spectroscopy

Aqueous organic and inorganic Se standards were prepared inside an anaerobic chamber in a N_2 atmosphere. Standards were prepared using 18 MΩ H_2O (Barnstead NanoPure) that had been boiled for 15 minutes with continuous N_2 sparging prior to transfer into the anaerobic chamber. All aqueous standards were initially 10-12 mM, but were diluted with 20% glycerol prior to their placement into liquid sample holders to eliminate diffraction in the samples. Sample holders were then frozen in liquid N_2 and stored in a -80°C prior to synchrotron analysis. Hepatocytes were exposed separately to 100 μM of selenite, selenate and L-selenomethionine for 6 and 24h at 15°C in an attempt to understand whether there are any temporal variations in the metabolite profile. This dose was selected based on my preliminary investigation that exhibited no major changes in cell viability following 24h exposure to 100 μM concentration of each compound, except selenite which caused approximately 20% decrease in cell viability relative to control (See Figure 4.1). Moreover, my previous study has shown that rainbow trout hepatocytes exposed to 100 μM sodium selenite for 24h exhibited significant induction of oxidative stress parameters (e.g., superoxide dismutase, glutathione peroxidase and catalase activity, and reduced glutathione level) relative to the control (Misra and Niyogi, 2009), thereby suggesting metabolically active state of the cells at the dose used in this study. After the exposure to different seleno-compounds, the media was removed and cells were harvested using non-enzymatic cell dissociation solution. The detached cells were washed 3 times at 700 rpm at 4°C to enhance the removal of any adsorbed parent compounds. The washed cells were freeze-dried in liquid N_2 and the sample was introduced into the specific sample holder. Equal thickness of the prepared samples was approximated. The sample holder was then wrapped with Kapton tape

and stored at -80°C prior to analysis. No glycerol was added to cell samples due to concerns about detection limits.

3.2.5 Se XANES Data Collection

Se K-Edge XANES were obtained at the Canadian Light Source (CLS) in Saskatoon, SK, Canada at the hard X-ray for Microanalysis (HXMA) beamline. For all samples, data were collected at 2.9 GeV in fluorescence mode using either a single channel Vortex detector for the aqueous standards or a 30 element Ge detector (Canberra, Meriden, USA) for the hepatocytes samples. To minimize beam-catalyzed changes in Se, all data were collected at 40 Kelvin using a liquid He cryostat. The beamline was calibrated to the Se K-Edge by setting the first derivative of an elemental Se standard to 12658 eV. This elemental Se reference remained behind the sample chamber for all data collection so that calibration could be continuously monitored and corrected if necessary. Data were collected from -100 to +50 eV relative to the Se K-Edge using 0.2 eV steps, and multiple scans were averaged to obtain suitable signal to noise ratio for further analysis.

3.2.6 Se XANES Data Analysis

Data deduction and analysis were performed using WINXAS 3.1 software. Scans were averaged with energy adjustments performed automatically *via* the internal reference channel, background corrected by subtracting a linear baseline from 12.56 to 12.63 keV, and normalized to an edge step of 1.0 over a range of 12.62 to 12.7 keV. Linear Combination XANES fits were performed on normalized spectra over the 12.56 to 12.70 keV region using 2 passes, the first with both % contribution and E_0 values allowed to vary, and a second run where E_0 shift was fixed to zero.

3.2.7 Measurement of L-methionine-γ-lyase activity

L-methionine-γ-lyase catalyzes selenomethionine into methylselenol, α-ketobutyrate and ammonia. The enzyme activity was measured in UV transparent 96-well plate (Greiner BioOne, Mississauga, Canada) using the surrogate substrate L-selenomethionine, and by measuring the corresponding α-ketobutyrate generation (Okuno et al., 2001). The assay cocktail contained 20mM potassium phosphate buffer (pH-8.0), 10mM L-selenomethionine and 0.01mM pyridoxal-5′-phosphate. The reaction was started by adding 50µl of S9 fraction of hepatocytes lysate homogenized in 10mM potassium phosphate buffer (pH-7.4) into the assay cocktail. After 15 min of incubation at 15°C, the reaction was stopped using TCA to a final concentration of 10%. For each measurement, a corresponding blank (TCA was added first, followed by substrate at the end) was used to account for the endogenous α-ketobutyrate. The TCA treated sample was centrifuged at 20,000*g* for 20 min and the supernatant was used for α-ketobutyrate measurement (Soda, 1968). Since 3-methylbenzthiazolinone-2-hydrazone (MBTH) derivatives of different keto-acids fall within a narrow range of absorption maxima, the absorption maxima of MBTH derivate of pure α-ketobutyrate was determined under the experimental condition and found to be 316nm. This wavelength was employed for the subsequent measurements in samples, which were carried out using the generated standard curve (R^2 value: 0.998). The Bradford protein assay kit was employed to measure protein content in samples using bovine serum albumin (BSA) as the standard (Bradford, 1976).

3.2.8 GSH measurement

Since GSH is implicated in redox cycling of CH_3SeH (a metabolite of selenomethionine) in mammalian systems, it is postulated that a similar mechanism might be involved in fish hepatocytes, which would influence the GSH concentration in the S9 fraction of hepatocytes lysate following incubation with L-selenomethionine, as described above. GSH was measured following the method described by Hissin and Hilf (1976). The protein precipitated S9 fraction of hepatocytes lysate was used for GSH measurement, adapted herein with 96-well black

microplate (Eppendorf, Mississauga, Canada). Using this technique, it was possible to detect GSH levels as low as 1μg/ml using the adopted assay. Since high concentration of L-selenomethionine was used as substrate for the L-methionine-γ-lyase activity measurement, possible interference of L-selenomethionine on the GSH measurement was evaluated. However, no differences between L-selenomethionine-spiked and non-spiked samples were recorded.

3.2.9 Intracellular ROS measurement

It has been shown previously that CH_3SeH is able to produce ROS in cell-free system (Spallholz et al., 2001). It is therefore hypothesized that if selenomethionine can be enzymatically catalyzed into CH_3SeH, one might observe an increase in intracellular ROS generation in trout hepatocytes following L-selenomethionine exposure. Instead of measuring ROS in the cell lysate upon reaction with L-selenomethionine, live cell imaging of ROS was performed. Intracellular ROS generation was measured using the fluorescent dye, CM-H_2DCFDA. These experiments were conducted only with hepatocytes culture showing >90% viability and within 24-36 h of isolation. Hepatocytes were cultured in poly-D-lysine coated glass bottom (Refractive Index – 1.5) 2×9 μ-well chamber (Ibidi, München, Germany). Briefly, cells were loaded with 10 μM CM-H_2DCFDA dissolved in dimethylformamide (DFO, final concentration <1% in L-15 media) at 15°C for 30 min. ROS generation follwoing L-selenomethionine exposures [0 (control), 100 and 1000 μM] was measured using Carl Zeiss LSM 410 confocal microscope with a 40X, 0.9 numerical aperture oil immersion objective. Changes in the intracellular ROS were measured at room temperature (~21°C) for 30 min (5 min interval) using the 488 nm excitation Argon laser beam and emission was collected using 505-530 nm band pass filter. Cells were not exposed to any UV-light sources prior to image acquisition since immediate burst of ROS generation was detected in the UV-exposed cells. All other confocal and laser parameters were kept identical across the different treatments.

3.3 Results and Discussion

Figure 3.3 shows Se K-Edge XANES spectra of several relevant aqueous selenium standard compounds as well as an elemental selenium solid standard. The main peak is due to the 1s → 4p transition and is systematically shifted to higher energies as Se changes from reduced to oxidized species. However, there are differences in the shape and position of this peak within the organo-selenium standards that are the result of differences in chemical bonding environment of Se rather than oxidation. This has been reported previously (Pickering et al., 1995; Ryser et al., 2005) and it is known that Se XANES is sensitive to changes from aqueous to powder sample environment for organo-selenium compounds. Differences in spectral peak positions and line shapes have been shown to be significant enough to allow for the quantitative analysis of Se speciation in similar experimental systems (Andrahennadi et al., 2007). The XANES spectra in Figure 3.3 appear consistent with those of similar aqueous compounds available in the literature (Andrahennadi et al., 2007; Pickering et al., 1995; Ryser et al., 2005), and there is no evidence of any sample oxidation that could affect the use of these standards in quantitative analysis.

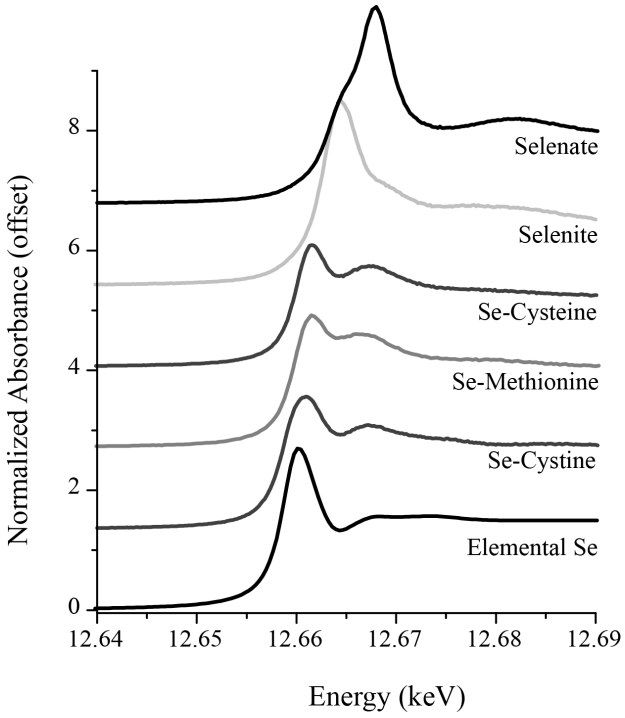

Figure 3.3: Se K-Edge XANES spectra of various inorganic and organic selenium reference compounds.

Figure 3.4 shows Se K-Edge XANES spectra of rainbow trout hepatocytes exposed to selenite and selenate for 6h along with two of the standards (selenate and elemental Se). It is obvious from the shift to lower energies that both selenate and selenite were rapidly reduced by the hepatocytes. It is also evident from the shape of the 6h sample spectra that the elemental Se is the predominant metabolite of selenite and selenate. The 24h sample spectra were essentially identical to the 6h sample spectra. Since hydrogen selenide is known to be an important intermediate metabolite of Se metabolism (See Figure 3.1 and 3.2A), an attempt was made to fit the sample spectra with sodium selenide (in solution) which was used as a surrogate standard for hydrogen selenide since the latter is not commercially available. However, the data from hepatocytes exposed to selenite and selenate did not provide a good fit with sodium selenide, probably because of the fact that hydrogen selenide was not present in sufficiently high enough concentration in the samples. The present observation is in good agreement with the proposed pathway described by Seko *et al*. (1989) (See Figure 3.1). In this pathway, selenite is reduced to elemental selenium in the presence of excess GSH. Hepatocytes are known to have relatively higher GSH levels compared to various other cell types – a condition that likely facilitated the conversion of most of the intracellular selenite and selenate into elemental Se by 6 h. This leads to suggest that this rapid conversion of selenite and selenate into elemental Se is important in understanding the differences in cytotoxicity between selenite and selenate. In line with this, greater cytotoxicity of selenite over selenate was observed when hepatocytes were exposed to equimolar (100 μM) concentration of each compound for 24 h. This occurs possibly due to the relatively faster hepatocellular uptake of selenite over selenate; otherwise one would have observed similar or greater cytotoxicity of selenate compared to selenite, given that both compounds are metabolized by the same cellular pathway (See Figure 3.1). Overall, the present findings are in agreement with the results of Sarret *et al*. (2005), who also reported 100% conversion of selenite into elemental Se within 48 h of exposure to metal resistant bacteria, *Ralstonia metallidurans*.

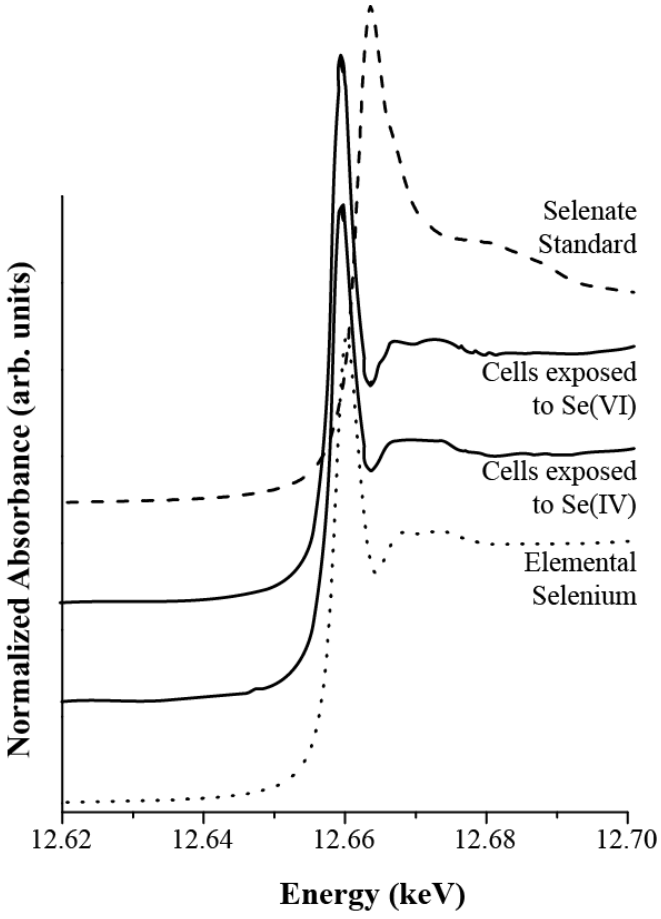

Figure 3.4: Se K-Edge XANES spectra for rainbow trout hepatocytes exposed to 100 μM of sodium selenite and sodium selenate for 6 h.

Figure 3.5A shows the differences in the spectra obtained from trout hepatocytes cultures exposed to L-selenomethionine for 6 and 24 h. In contrast to the hepatocytes exposed to inorganic Se, there is clear time dependent change in the position of the main (dotted line) peak which shifted to the lower energy after 24 h. This can readily be explained, as detailed in Figure 3.5B and 3.5C, by fitting the sample spectra as a mixture of selenomethionine and selenocystine. At 6 h, the sample appears to be a mixture of selenomethionine (63%) and selenocystine (37%), whereas the data at 24 h is described well with the combination of selenocystine (80%) and selenomethionine (20%). It is important to note that the potential contribution of selenomethionine due to entrained growth media is expected to be less than 5% of the observed signal, and therefore selenomethionine spectra recorded in the present study was not an artifact of the sample preparation. Higher concentration of intracellular selenomethionine at 6 h observed in our study is in agreement with the observation of Beilsten and Whanger (1987), who reported 90% of intracellular ^{75}Se remained as selenomethionine in Chang liver cells. It should also be noted that fits were attempted with combinations of selenocysteine, selenocystine, selenomethionine, sodium selenide and elemental selenium, and in all cases the simple 2 component model in Figure 3.5B and 3.5C produced the best fit. A similar fit of the 24 hour sample spectra can be obtained with either selenomethionine or selenocysteine as the minor component, however neither standard successfully reproduces the higher energy portion of the sample data very well. This could be due to two possibilities: either there are other components for which there are no available standards that more successfully reproduces the 12.68-12.7 keV region, or there are multiple co-occurring species of similar Se coordination but none of them are high enough in concentration to substantially improve the fit. It is known that a large variety of organic selenium compounds exist as metabolic intermediates of the form R-Se-S-R; it is plausible that these would be modeled successfully near the Se Edge with selenocystine but less successfully at higher energies. Selenocysteine is one of the major intermediate in the *trans*-sulfuration pathway of selenomethionine metabolism. However, experimental results suggest selenocystine as the major metabolite after 24 h exposure in the present study. It is not possible to determine from the present experiment whether this selenocystine is free or protein-incorporated. Under normal physiological condition, the reducing state of the intracellular environment might favour the presence of selenocysteine. However, selenocysteine is reported to

be very unstable and readily oxidized into the corresponding diselenide, selenocystine (Beld et al., 2007). The concurrent experiment shows that 100 μM L-selenomethionine exposure dose induced ROS generation in trout hepatocytes (Figure 3.7). Therefore, it is suggested that increased ROS concentration have likely contributed to the oxidation of free selenocysteine to selenocystine.

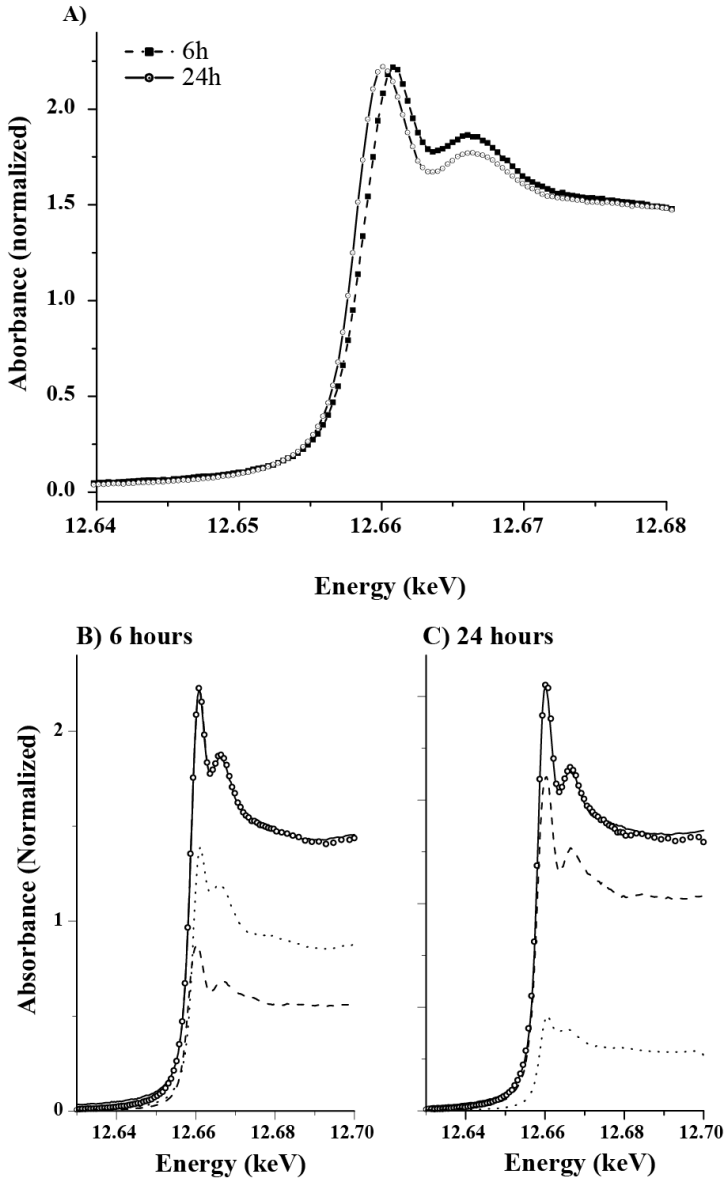

Figure 3.5: Differences in the Se K-edge XANES spectral profiles of rainbow trout hepatocytes exposed to 100 µM of L-selenomethionine for 6 h and 24 h (3.5A). A shift in the main peak towards lower energy is indicative of reduction of Se over time. The figure exhibits linear combination fitting results for 6h (3.5B) and 24h (3.5C) L-selenomethionine samples. In both Figure 3.5B and 3.5C the dotted line represents L-selenomethionine standard, dashed line represents selenocystine standard, open circle represents experimental data, and solid line represents fit results.

As outlined previously, two different pathways of selenomethionine metabolism in vertebrates have been proposed to date. Under normal nutritional regime, selenomethionine is metabolized into selenocysteine *via trans*-sulfuration pathway. However, rapid transformation of selenomethionine into methylselenol by L-methionine-γ-lyase enzyme has been observed in mouse (Okuno et al., 2001) and bacteria (Inoue et al., 1995) at a higher or potentially toxic level. There is no direct evidence supporting the presence of L-methionine-γ-lyase enzyme in piscine systems. According to KEGG metabolic pathway, there is also no orthologue of L-methionine-γ-lyase gene in zebrafish. Palace et al. (2004) suggested the presence of L-methionine-γ-lyase – like enzyme activity in rainbow trout embryo based on the ability of embryo extract to produce $O_2^{\cdot-}$ in the presence of GSH, which was implicated to the redox cycling of CH_3SeH. In the present study, the activity of this enzyme is recorded and found to be much higher (3.52 ± 0.96 nmol/min/mg protein, mean ± SD, n=12) than that reported in mouse liver (0.35± 0.29 nmol/min/mg protein). However, the present data are quite comparable to the activity (2.8± 0.29 nmol/min/mg protein) reported in the crude extract of bacteria, *Brevibacteruim linen*. Since there is no prior evidence of the presence of such an enzyme in fish, it is described herein as L-methionine-γ-lyase – like activity. Interestingly, no CH_3SeH was detected in selenomethionine-exposed samples through XANES spectroscopy. The plausible explanations for the above observation are either the CH_3SeH level in the samples was below the detection limit of the current analytical technique or spontaneous oxidation of methylselenol resulted into the formation of volatile dimethyl-diselenol (Gabel-Jensen et al., 2010). It is important to note here that CH_3SeH, the L-methionine-γ-lyase catalyzed product of selenomethionine, may be present as $CH_3Se^{\cdot}$ radical and/or CH_3Se^{-} anion depending on the homolytic or heterolytic cleavage. The redox cycling between both forms in the presence of excess intracellular GSH will lead to $O_2^{\cdot-}$ generation (Figure 3.2B). However, the spontaneous generation of dimethyl-diselenol from $CH_3Se^{\cdot}$ will be more favourable if the GSH level is depleted. In either case, it is likely that CH_3SeH is one of the important metabolites of selenomethionine in trout hepatocytes.

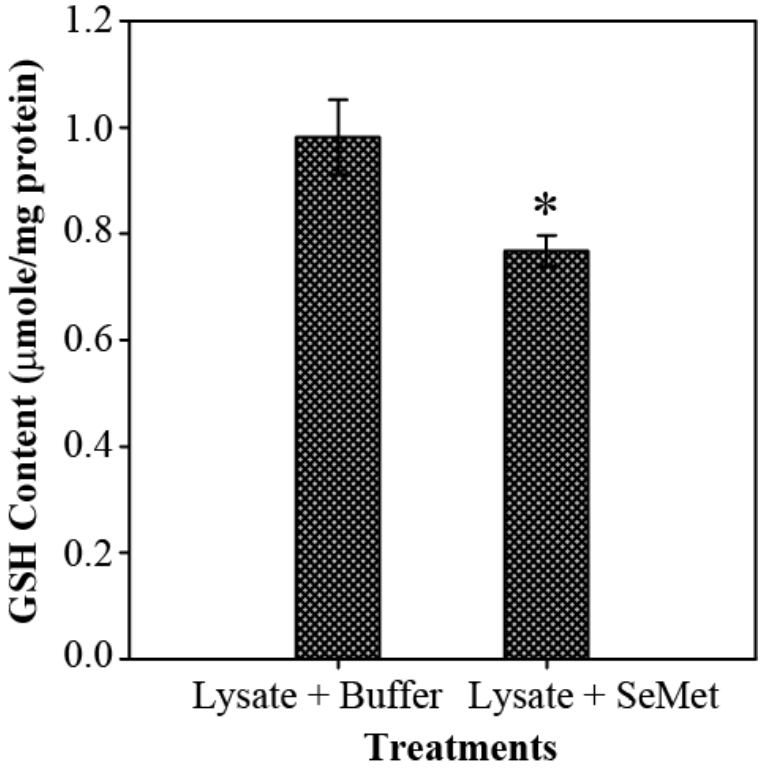

Figure 3.6: Reduction in GSH content following the reaction of L-selenomethionine with the S9 fraction of rainbow trout hepatocytes. Bar with asterisk shows significant decrease in the GSH content of reaction mixture (Mann-Whitney rank sum test, $p \leq 0.05$, $n = 10$). Data are presented as mean ± S.E.M.

Since L-methionine-γ-lyase – like activity was detected in trout hepatocytes, the role of cellular GSH in the redox cycling of CH_3SeH was also investigated. It was postulated that if GSH mediated redox cycling of CH_3SeH occurred in the present experimental system, the GSH content would decrease in the assay mixture used to measure L-methionine-γ-lyase - like activity. Interestingly, a significant ($p \leq 0.05$) decrease in the GSH content was recorded of the assay mixture after 15 min of reaction time (Figure 3.6). The current observation further corroborates previous observation that GSH is involved in the redox cycling of selenomethionine metabolites (Spallholz et al., 2001). Based on the proposed pathway of redox cycling of CH_3SeH, the conversion of CH_3Se^- into $CH_3Se^{\cdot}$ leads to the generation of $O_2^{\cdot -}$ (See Figure 3.2B). Since O_2 is the substrate for this reaction, ROS production was evaluated in the trout hepatocytes instead of the cell lysate to ensure that this mechanism persists under intracellular O_2 tension. This experiment demonstrated that ROS generation in hepatocytes increased moderately following 30 min exposure to 100 μM L-selenomethionine compared to that in control, however this effect was more rapid and pronounced at 1000 μM exposure dose (Figure 3.7). These observations provide an important insight into the role of L-methionine-γ-lyase –like activity in the metabolism of selenomethionine and subsequent ROS generation. In the *trans*-sulfuration pathway, selenomethionine can be converted into CH_3SeH *via* selenocysteine, a process that requires multiple steps. This process is suggested to be mediated by selenocysteine-γ-lyase, which has a high K_m value (0.83 mM) for seleno-L-cysteine (Esaki et al., 1982). Therefore, it is likely that only a small quantity of selenocysteine can be metabolized by this pathway when substrate concentration is low - as might have been the case with 100 μM L-selenomethionine exposure doses. Based on the XANES spectroscopy and ROS data, it can be suggested that the generation of CH_3SeH *via trans*-sulfuration pathway was limited since selenocystine was the predominant metabolite instead of selenocysteine. Thus, low selenocysteine concentration was probably the rate-limiting step for CH_3SeH generation in *trans*-sulfuration pathway. Taken together, these observations indicate a slow process of CH_3SeH generation by *trans*-sulfuration pathway even at high or toxic concentration of selenomethionine. Moreover, if the *trans*-sulfuration pathway would have been the only pathway of selenomethionine metabolism in trout hepatocytes, one would not have observed such a rapid increase of ROS generation and

reduction of GSH content. Thus, the present study provides an indirect evidence of the critical role of L-methionine-γ-lyase – like activity in selenomethionine metabolism in trout hepatocytes.

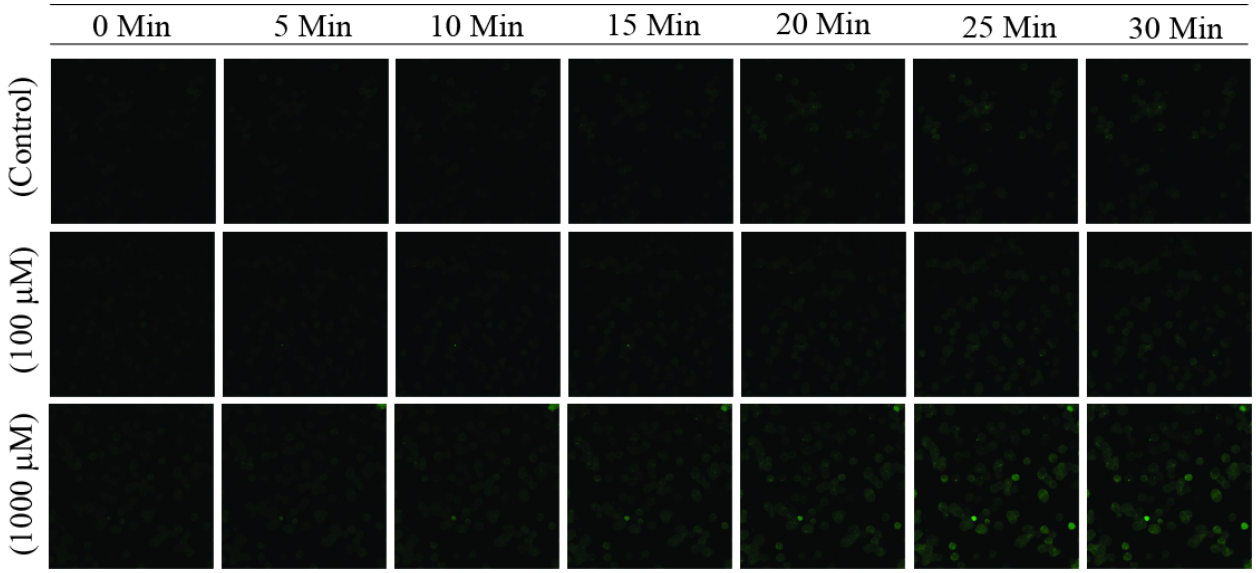

Figure 3.7: Time-dependent changes in ROS generation in rainbow trout hepatocytes exposed to 0 (control), 100 and 1000 µM of L-selenomethionine for a period of 30 min.

3.4 Conclusion

The present study suggests that inorganic and organic selenium are metabolized *via* different metabolic pathways in rainbow trout hepatocytes. It has been shown that elemental Se is the major metabolite of selenate and selenite. In contrast, it appears that there are probably two different pathways of selenomethionine metabolism. In *trans*-sulfuration pathway, selenocystine is the dominant metabolite of selenomethionine, whereas selenomethionine is directly metabolized into CH_3SeH by L-methionine-γ-lyase mediated catalysis in the other pathway. The latter process likely becomes more prominent during exposure to a higher dose since increasing ROS generation was observed as a result of GSH dependent redox cycling of CH_3SeH, with increasing selenomethionine exposure dose. The present study also demonstrates the usefulness of XANES spectroscopy in analyzing speciation of Se at cellular level, which can be very helpful in understanding the mechanistic aspects of Se cytotoxicity.

CHAPTER 4: Investigation of the role of oxidative stress in mediating selenite toxicity in isolated hepatocytes [3]

4.1 Introduction

Selenium is an essential micronutrient for all the vertebrates including fish. However, it can be toxic to animals at a slightly elevated dose beyond the threshold level (NRC, 1980). In freshwater fish, selenium exposure has been reported to cause reproductive impairment, teratogenic deformities and histopathological alterations of liver, gill and kidney (Hamilton, 2004; Holm et al., 2005; Kennedy et al., 2000; Lemly, 2002; Muscatello et al., 2006; Teh et al., 2004).

The mechanism of selenium toxicity has most often been attributed to its sulphur-like chemical characteristics and its ability to substitute for that element in amino acids during the assembly of proteins (Maier and Knight, 1994). However, all of the toxic effects of selenium cannot be explained by this mechanism. Instead, selenium-induced oxidative damage has been suggested as another potential mechanism of toxicity in recent studies. Spallholz and Hoffman (2002) suggested that the reactive oxygen species (ROS) play a significant role in inducing selenium toxicity in birds exposed to high levels of selenium. Selenium toxicity in mammalian systems has also been attributed to the harmful effects of ROS (Albrecht et al., 1994; Lin and Spallholz, 1993). To date, oxidative damage as a potential mechanism of selenium toxicity in fish, either *in vivo* or *in vitro*, has received very little attention. Palace et al. (2004) reported that the metabolism of selenomethionine in rainbow trout (*Oncorhynchus mykiss*) embryos led to ROS generation. Orun et al. (2005) reported an induction of enzymatic antioxidants [superoxide dismutase (SOD) and glutathione peroxidase (GPx)] at low to intermediate doses followed by a sharp decline at the high dose in trout exposed to waterborne sodium selenite. Miller et al. (2007) recently reported that the concentration of hepatic glutathione (GSH), one of the most important

---

[3] This chapter of the thesis has been published in the journal, Toxicology in Vitro 23: 1249-1258 (2009) under joint authorship with Som Niyogi (University of Saskatchewan). doi:10.1016/j.tiv.2009.07.031. For additional results, please see the appendix.

non-enzymatic antioxidants, decreased in trout exposed to acute levels of waterborne sodium selenite. These findings indicate that oxidative stress can be an important factor in selenium toxicity to fish. Therefore, the current knowledge requires more in-depth investigations to further elucidate the mechanistic underpinnings of selenium-induced oxidative damage in fish.

In mammalian systems, the metabolism of catalytic selenium compounds (e.g., selenite) is known to produce intermediary metabolites that are redox reactive compounds, and are capable of generating free radicals (Spallholz, 1994). GSH, a ubiquitous sulfhydryl-containing molecule in the cells, plays an important role in this process (Arteel and Sies, 2001). GSH reacts with selenite to produce highly reactive selenopersulfide (Ganther, 1971) and thiyl radical (Arteel and Sies, 2001). The former can produce superoxide anion ($O_2^{\cdot -}$) spontaneously in the presence of oxygen. In addition, selenopersulfide anions can also react with GSH to produce hydrogen selenide, and the conversion of hydrogen selenide to elemental selenium produces superoxide anion (Lin and Spallholz, 1993). On the other hand, thiyl radicals can react with GSH to form glutathione disulfide radicals ($GSSG^{\cdot -}$) (Arteel and Sies, 2001). Besides acting as a pro-oxidant during selenium metabolism, GSH is also known to play an important role in the scavenging of ROS. The dual role of GSH, both as an antioxidant and a pro-oxidant, has been exhibited in human hepatoma cells exposed to selenite (Shen et al., 2000). Thus, the involvement of GSH in selenium metabolism may deplete its intracellular storage during selenium exposure, resulting into the loss of cellular thiol redox. Consequently, the scavenging of hydrogen peroxide as well as organic peroxide radicals may also become limited. The accumulating free radicals can oxidize the cellular membranes and macromolecules, resulting into the loss of structural integrity of the cell, and ultimately lead to the cell death (Kelly et al., 1998). The selenium induced cell death can occur due to the induction of either apoptosis or necrosis (Shen et al., 2000; Weiller et al., 2004).

The liver is known to be the major organ of selenium accumulation and metabolism in fish (Sato et al., 1980). Isolated fish hepatocytes (the key functional units of liver) in primary culture are often used as a model *in vitro* system for understanding the mechanisms of toxicity of various types of contaminants in fish. Therefore, the present study was designed to examine the hypothesis that selenium [as selenite, the most toxic inorganic form of selenium (Hamilton,

2004)] causes cytotoxicity in fish by inducing oxidative stress, using isolated hepatocytes of rainbow trout in primary culture as the experimental system. The main objectives of this study were: (i) to determine the dose response relationship of selenite cytotoxicity, (ii) to evaluate the responses of key enzymatic antioxidants [CAT (Catalase), SOD and GPx] in relation to selenite exposure, (iii) to evaluate the selenite induced intracellular ROS production, and (iv) to determine whether selenite exposure impairs cellular thiol status [as measured by reduced to oxidized glutathione (GSH:GSSG) ratio], causes membrane damage (as measured by lipid peroxidation), and triggers apoptosis (as measured by caspase-3/7 activity) as a probable pathway for cell death.

4.2 Materials and methods

4.2.1 Chemicals

Cell culture tested sodium selenite (Na_2SeO_3, purity ~ 98%), dimethylformamide, reduced and oxidized glutathione (GSH and GSSG), trichloroacetic acid (TCA) and trypan blue solution were obtained from Sigma-Aldrich, USA. ACS grade NaCl, KCl, $MgSO_4$, Na_2HPO_4, KH_2PO_4, HEPES, NaOH, EDTA, $CaCl_2$, and methanol were obtained from VWR International, Canada. Antibiotic and antimicotic solution, 5',6'-chloromethyl-2',7'– dichlorodihydro-fluorescein diacetate (CM-H_2DCFDA) and L-15 media were obtained from Invitrogen, Canada. Tricaine methanesulfonate (MS-222) was obtained from Syndel Laboratories Ltd., Canada.

4.2.2 Experimental animal

Rainbow trout (*Oncorhynchus mykiss*) weighing 200-300g were obtained from Lucky Lake Fish Farm, Saskatchewan. Fish were maintained in 1000L flow-through aquaria receiving dechlorinated Saskatoon City water at a rate of 2L per minute under constant aeration. A photoperiod of 16h light: 8h dark and a water temperature of 15±1°C were maintained throughout the experimental period. The fish were fed once daily with Martin's commercial diet

(Martin Mills Inc., Canada) at a ration of 2% of body weight. The fish were acclimated for at least 2 weeks prior to their use in the experiments.

4.2.3 Hepatocyte isolation

Trout hepatocytes were isolated using a two-step collagenase perfusion technique (Sathiyaa et al., 2001). The fish were euthanized with an overdose of MS-222 (0.5 g/L) in dechlorinated water. The hepatic portal vein was cannulated with PE-50 tubing and perfused with ice-cold modified Hanks' Media (136.9 mM NaCl, 5.4 mM KCl, 0.8 mM $MgSO_4.7H_2O$, 0.33 mM $Na_2HPO_4.7H_2O$, 0.44 mM KH_2PO_4, 5.0 mM HEPES, 5.0 mM Na-HEPES, pH 7.63). The perfusion line was switched to the medium containing 0.2 mg/ml collagenase in Hanks' Media when the liver was completely blanched, and the perfusion was continued until the liver was fully digested. The digested liver was chopped with a razor blade into small pieces on a Petri plate, and the dissociated cells were filtered through 260 and 73 μm mesh size strainers, respectively. The cells were then washed 3 times in Hanks' Media at 700 rpm at 4°C. This was followed by a single washing with the same media containing BSA (1%) and $CaCl_2$ (1.5 mM). The cells were then incubated for 20 minutes in L-15 media (pH 7.63) containing antimicrobial and antimicotic solution on an ice bath. The settled down cells were collected by aspirating out the media on the top and resuspended in 10 ml of L-15 media. Cell viability was determined by the trypan blue exclusion test, and the suspensions showing more than 85% cell viability were used for experiments. The cells were plated in 6-well Primaria plates (BD Falcon, USA) at a density of 0.3×10^6 cells per cm^2 and incubated at 15°C for 24h to form monolayer before their use in the experiment.

4.2.4 Selenite exposure and sampling

At first, the dose-dependent effects of selenite (as sodium selenite) on the viability of trout hepatocytes were examined to determine the acute cytotoxicity dose (LD_{50} of selenite). After 24h of incubation, the culture medium was replaced with the fresh medium containing different doses of selenite (0 - 5000 μM), and the cells were incubated for another 24h at 15°C.

The osmolality of the exposure media was measured using a 5100C vapour pressure osmometer (Wescor Inc., USA), and no change was recorded in any treatment due to the addition of sodium selenite. At the end of the exposure period, cells were collected from the culture plate using a non-enzymatic cell dissociation solution (Sigma-Aldrich, USA). Cell viability was measured immediately by the trypan blue exclusion test. This experiment was performed five times using hepatocytes isolated from an individual fish at each time. The 24h LC_{50} of selenite was determined by Probit analysis (SPSS, version 16) and found to be 587 µM.

To investigate whether selenite exposure causes oxidative stress, the cultured hepatocytes were exposed to 50, 100 and 200 µM of selenite in addition to control (0 µM selenite) for 24h at 15°C. Prior to that, the time-dependent effects of selenite exposure on the viability of hepatocytes were examined. Cells were exposed to the same dose levels mentioned above for three different time periods: 1h, 6h and 24h. At the end of each exposure period, cells were harvested as described previously and cell viability was evaluated by trypan blue exclusion test. As an additional measure of cell viability, lactate dehydrogenase (LDH) activity in the extracellular medium (an indicator of membrane leakage) was measured spectrophotometrically using a LDH assay kit (Sigma-Aldrich, USA) and following manufacturer's specifications.

For the measurement of oxidative stress parameters (except the intracellular ROS) and caspase-3/7 activity, selenite exposed cells were harvested after 24h of exposure, washed carefully with Dulbecco's Phosphate Buffer Saline (2.67 mM KCl, 1.47 mM KH_2PO_4,137.93 mM NaCl, 8.10 mM Na_2HPO_4) for three times, and then lysed with 500 µl of CelLytic™-M reagent (Sigma-Aldrich, USA). A portion of the lysed cells were stored at -80°C for analysis of thiobarbituric acid reactive substances (TBARS). The other portion was centrifuged at 16,000 rpm for 20 min at 4°C to pellet the cellular debris. The supernatant was stored at -80°C for the enzymatic analysis. For the measurement of oxidized and reduced glutathione, cells were treated alike except that an ice-cold 5% TCA solution was used along with CelLytic™-M reagent during the cell lysis and stored at -80°C until analysis. All of the experiments were performed five times using hepatocyte cultures obtained from an individual fish at each time. The data of each replicate analysis in any microplate-based assay were calculated as an average from the

independent measurement obtained from six different cell lysate in a single replicate exposure dose.

4.2.5 Measurement of antioxidant enzyme activities

The activities of three antioxidant enzymes (SOD, CAT and GPx) were measured using 96-well microplates (BD Falcon, USA) and a multi-well plate reader (Varioskan Flash, Thermo Electron Corporation, Finland). The SOD activity was measured using a SOD kit (Fluka, Switzerland) and expressed as % inhibition. The CAT activity was measured using the Amplex® Red catalase assay kit (Molecular Probes, USA). One unit of CAT activity was defined as the amount of enzyme that will decompose 1.0 µM of H_2O_2 into H_2O per minute. The CAT activity was expressed as milli unit (mU) per mg of protein. The GPx activity was determined using a GPx assay kit (Calbiochem, USA) and expressed as nmol per minute per mg protein.

4.2.6 Measurement of reduced and oxidized glutathione

The concentrations of the reduced (GSH) and oxidized (GSSG) glutathione were measured using a fluorometric method (Hissin and Hilf, 1976), modified to a 96-well microplate based assay. In order to confirm the linearity of the reaction rate in the adopted method, commercially purified GSH and GSSG were used to calibrate the standard curve. For GSH measurement, the final reaction mixture volume was 200 µl, which contained 180 µl of phosphate-EDTA buffer (0.1 M sodium phosphate – 0.005 M EDTA, pH 8.0), 10 µl of *o*-Phthalaldehyde (OPT, 100 µg per 100µl methanol) and 10 µl of diluted sample (1:10 in phosphate-EDTA buffer). The reaction mixture was incubated for 15 minutes at room temperature, and the fluorescence was measured at excitation and emission wavelength of 350 nm and 450 nm, respectively. The GSH content was expressed as µg per mg of protein.

GSSG was measured using the same method outlined above, except that the sample was diluted with 10 volumes of 0.1 N NaOH containing 0.04 M of *N*-ethylmaleimide, instead of

phosphate-EDTA buffer, in order to prevent the oxidation of GSH to GSSG. The GSSG content was also expressed as μg per mg of protein.

4.2.7 Lipid peroxidation assay

Lipid peroxidation was determined fluorometrically as the amount of thiobarbituric acid reactive substances (TBARS) in the sample using the OXI-TEK TBARS kit (Alexis Biochemicals, USA). The data were expressed as nmol of TBARS equivalent per mg of protein.

4.2.8 Measurement of caspase-3/7 activity

Caspase-3/7 assay was performed using the Apo-ONE® homogenous kit (Promega, USA). This assay uses the caspase-3/7 substrate rhodamine 110, bis-N-CBZL-aspartyl-L-glutamyl-L-valyl-L-aspartic acid amide (Z-DEVD-R110). The dissociated product, rhodamine 110, fluoresces following cleavage by the enzyme. Equal volume of diluted caspase-3/7 reagent was mixed with the sample in a 96-well microplate and incubated for 45 min at 15°C. Subsequently, the fluorescence was measured at excitation and emission wavelengths of 499 and 521 nm, respectively. The blank control (culture medium without cell) is used as a measure of background fluorescence and subtracted from the experimental values. The enzyme activity was expressed as relative fluorescence unit per mg protein.

4.2.9 Measurement of intracellular reactive oxygen species (ROS)

Intracellular ROS was measured following the modified method of Campanucci et al. (2008). The hepatocytes were loaded with 10 μM of 5',6-chloromethyl-2',7'– dichlorodihydro-fluorescein diacetate (CM-H_2DCFDA) dissolved in anhydrous dimethylformamide for 45 min at 15°C and washed with fresh media three times. Subsequently, the hepatocytes were exposed to 0 (control), 50, 100 and 200 μM of selenite for 2h. An exposure period of 2h was employed instead of 24h, primarily to capture the effects during the early exposure stage and also to

prevent any leakage of the dye from the cells due to potential selenite-induced membrane damage. The esterified form of the dye can easily diffuse into the cell and is deacetylated by intracellular esterases, and reacts with ROS to form the fluorescent product 2',7'-dichlorodihydro-fluorescein. At the end of the exposure period, cells were washed four times with fresh L-15 culture medium to minimize the background fluorescence. The fluorescence intensity was measured using the Argon laser of a confocal microscope (Zeiss Axiovert LSM 510 Meta Confocal System, Carl Zeiss, Germany). Similar microscopic settings for the imaging were maintained throughout to allow conformity of the results. The fluorescence intensity was measured using the LSM 510 software (Carl Zeiss, Germany). The fluorescence intensity was determined by taking the average of at least 20 cells per replicate culture, and expressed as relative fluorescence unit (RFU) per cell. The experiment was performed three times using hepatocyte cultures obtained from an individual fish at each time.

4.2.10 Protein assay

Protein content of the cell lysates was determined by a protein assay kit (Microlowry, Sigma-Aldrich, USA).

4.2.11 Statistical analysis

All Data have been presented as mean ± S.E.M. (n) except the cell viability data, which were expressed as a percentage of the control value. Significant differences among the treatment groups were analyzed by one-way analysis of variance (ANOVA) followed by Tukey's multiple comparison test (SPSS, version 16 for Windows). Mean value was considered significantly different at $p<0.05$. The assumptions of ANOVA, i.e., normality of distribution and homogeneity of variances were examined by K-S test and Levene's test, respectively (both at $\alpha = 0.05$). The log transformed data met the assumptions of ANOVA.

4.3 Results

4.3.1 Dose- and time-dependent cytotoxicity of selenium

There were no noticeable changes in cell viability in the control as well as in 50 μM (approximately 10% of the 24h LD_{50}) of selenite exposure up to 24h (Figure 4.1). Cell viability was also not affected up to 6h in 100 and 200 μM (approximately 20% and 35% of the 24h LD_{50}, respectively) exposure doses relative to the control. However, cell viability decreased by 22% and 40% after 24h of exposure to 100 and 200 μM of selenite, respectively (Figure 4.1). Simultaneously, an increase of 40% and 60% in the extracellular LDH activity was also recorded after 24h of exposure to 100 and 200 μM of selenite, respectively (see Appendix, Figure C4.S1), compared to that in the control. Thus, there was a good agreement in cell viability data obtained by trypan blue exclusion test and LDH leakage into the extracellular media.

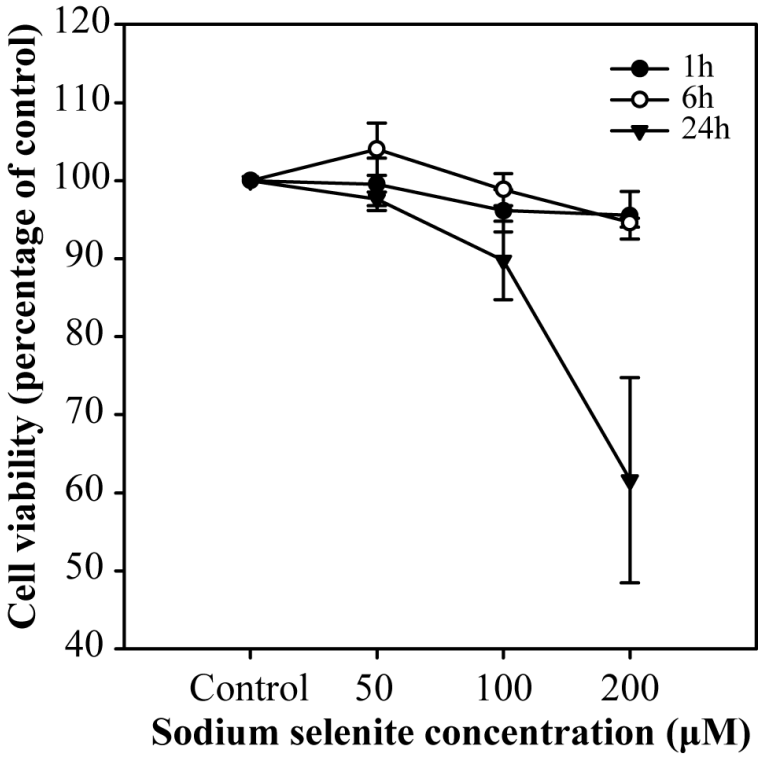

Figure 4.1: Time- and dose-dependent changes in the viability of trout hepatocytes exposed to selenite ranging from 0-200 µM. At the highest exposure dose, the cell viability decreased by 40% compared to the control. Data are mean ± S.E.M. (n=5), where n represents the number of independent measurements using cultured cells from as many fish.

4.3.2 Effects of selenite exposure on the activity of enzymatic antioxidants

A dose-dependent increase in the SOD activity was observed up to 100 μM of selenite exposure (Figure 4.2A). The magnitude of induction of SOD activity was about 40% at 100 μM, however the activity decreased to the control level at 200 μM. A similar pattern of increase at 50 and 100 μM followed by a decrease at 200 μM selenite exposure was recorded in CAT activity (Figure 4.2B). However, unlike SOD, the CAT activity remained significantly elevated at 200 μM relative to the control. In contrast, a significant increase in GPx activity was recorded at 100 and 200 μM of selenite exposure, but not at 50 μM, compared to the control (Figure 4.2C).

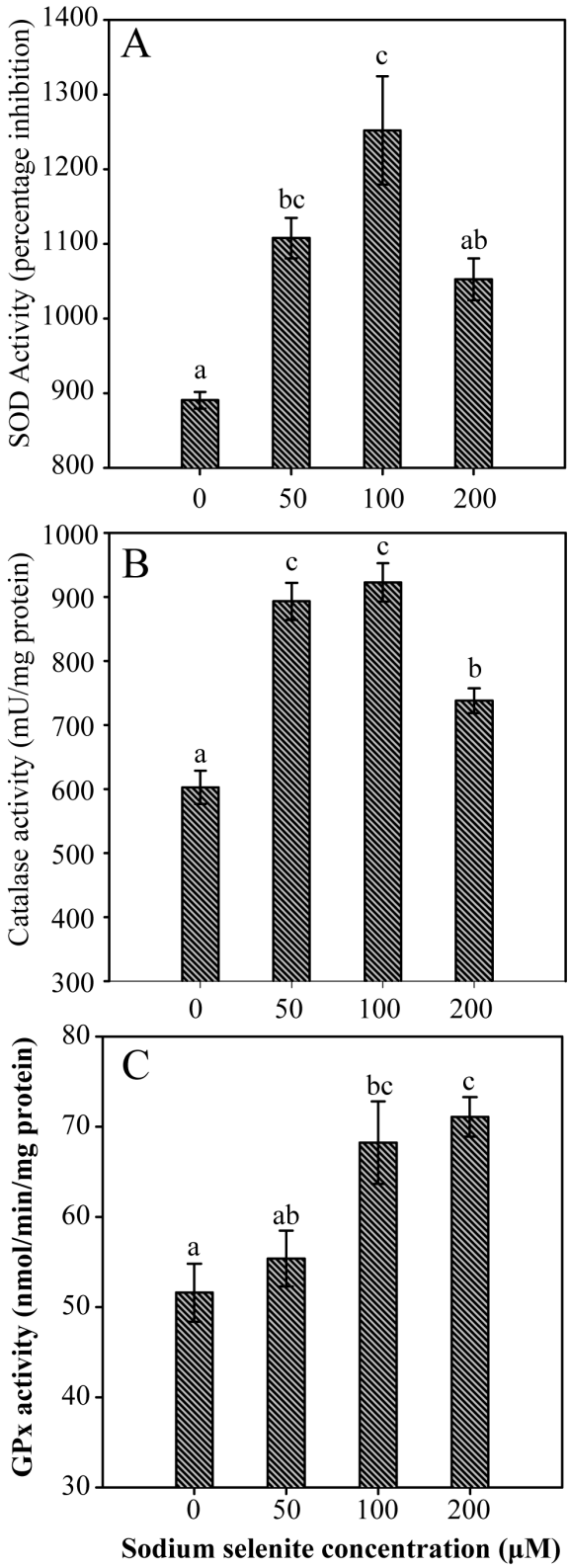
A
SOD Activity (percentage inhibition)
1400
1300
1200
1100
1000
900
800
a
bc
c
ab
0
50
100
200
B
Catalase activity (mU/mg protein)
1000
900
800
700
600
500
400
300
a
c
c
b
0
50
100
200
C
GPx activity (nmol/min/mg protein)
80
70
60
50
40
30
a
ab
bc
c
0
50
100
200
Sodium selenite concentration (µM)

Figure 4.2: Effect of sodium selenite exposure on superoxide dismutase (Figure 4.2A), catalase (Figure 4.2B) and glutathione peroxidase (Figure 4.2C) activities in isolated trout hepatocytes in primary culture. One unit of SOD activity is defined as the amount of enzyme necessary to inhibit the reference rate of superoxide anion production in the assay mixture by 50% (IC_{50}). Data are mean ± S.E.M. (n=5), where n represents the number of independent measurements using cultured cells from as many fish. Mean values with different letters are statistically significant (One Way ANOVA, $p < 0.05$).

4.3.3 Effects of selenite exposure on cellular thiol status

A dose-dependent decrease of the GSH to GSSG ratio was observed in trout hepatocytes exposed to selenite (Figure 4.3). A four-fold decrease in the GSH to GSSG ratio was recorded at 200 μM exposure relative to the control, which indicated a markedly diminished cellular reducing capacity. Interestingly, a significant increase in the cellular GSH level was recorded at 100 μM exposure in comparison to the control. However, cellular GSH level dropped sharply at 200 μM and no difference was recorded relative to that in the control. In contrast, the cellular GSSG level increased almost in a dose-dependent manner following selenite exposure.

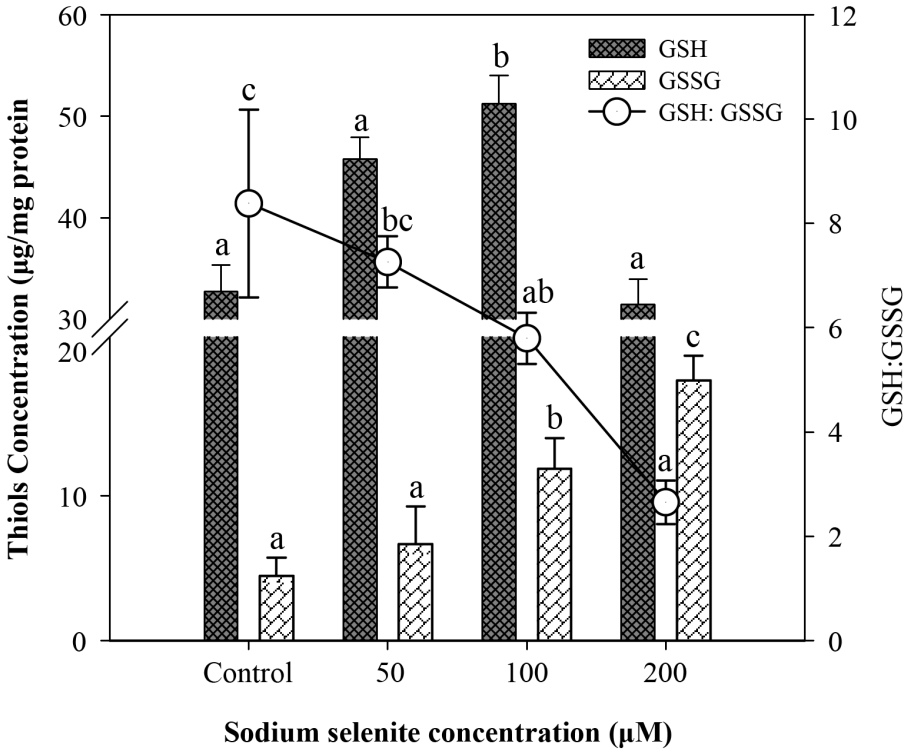

Figure 4.3: Cellular glutathione status (GSH to GSSG ratio) in isolated trout hepatocytes following exposure to 0-200 µM of sodium selenite for 24h. Data are mean ± S.E.M. (n=5), where n represents the number of independent measurements using cultured cells from as many fish. Mean values with different letters are statistically significant (One Way ANOVA, $p < 0.05$).

4.3.4 Effects of selenite exposure on intracellular ROS formation

The confocal images of hepatocytes loaded with CM-H_2DCFDA following exposure to 0 (control), 50, 100 and 200 μM of selenite are presented in Figure 4.4A (i, ii, iii and iv, respectively). Each panel reflects a typical view of green fluorescent cells from respective treatment group, exhibiting a gradual increase in the fluorescence intensity with the increasing exposure dose.

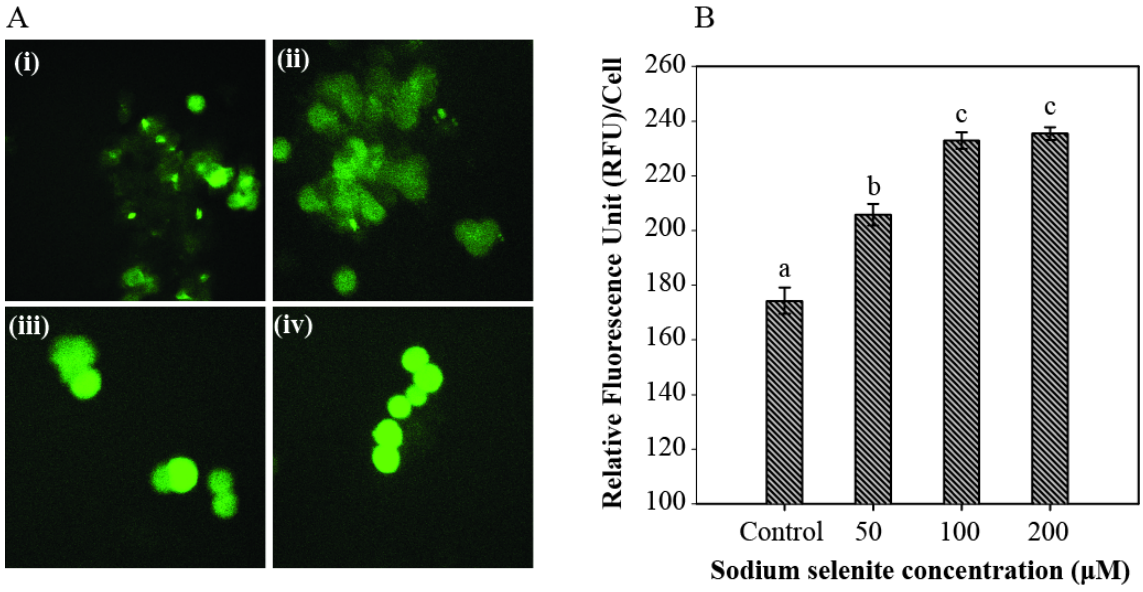

Figure 4.4: Representative confocal fluorescent images (Figure 4.4A) and average relative fluorescent intensity (Figure 4.4B) of isolated trout hepatocytes exposed to 0-200 µM sodium selenite for a period of 2h. The cells were loaded with CM-H_2DCFDA for 45 min, followed by exposure to sodium selenite at 0 [Figure 4.4A (i)], 50 [Figure 4.4A (ii)], 100 [Figure 4.4A (iii)] and 200 µM [Figure 4.4A (iv)] doses. The intensity of fluorescent signals was measured using the LSM 510 software (Carl Zeiss, Germany). The relative fluorescent intensity is expressed in arbitrary units. Data are presented as mean ± S.E.M,of average fluorescence intensity of 15-20 cells from each replicate, and the experiment was repeated 3 times using cultured cells obtained from 3 individual fish. Mean values with different letters are statistically significant (One Way ANOVA, $p < 0.05$).

Using the confocal images the average relative fluorescence intensity (RFU) per cell was determined in different treatment groups (Figure 4.4B). The relative fluorescence intensity increased significantly with increasing selenite dosage, thereby indicating elevated intracellular ROS formation as a consequence of selenite exposure. However, a dose dependent effect was recorded only up to 100 μM of selenite exposure.

4.3.5 Effects of selenite exposure on lipid peroxidation

Lipid peroxidation, measured as TBARS equivalent, in hepatocytes exposed to selenite is presented in Figure 4.5. An increasing trend of lipid peroxidation was recorded with increasing exposure dose, although the effect was statistically significant only at the highest exposure dose (200 μM). The magnitude of increase was more than two fold at 200 μM relative to the control.

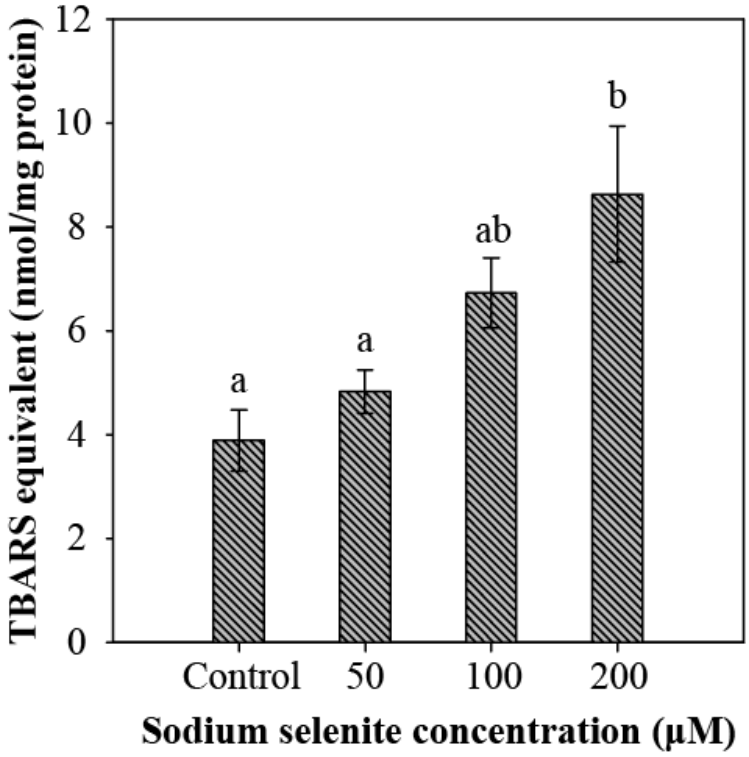

Figure 4.5: Lipid peroxidation, as measured by TBARS, in isolated trout hepatocytes exposed to 0-200 µM of sodium selenite. Data are mean ± S.E.M. (n=5), where n represents the number of independent measurements using cultured cells from as many fish. Mean values with different letters are statistically significant (One Way ANOVA, $p < 0.05$).

4.3.6 Effects of selenite exposure on caspase-3/7 activity

The effect of selenite exposure on caspase-3/7 activity is presented in Figure 4.6. No significant change was observed in caspase-3/7 activity at 50 μM selenite exposure. However, caspase-3/7 activity increased significantly (≥ two fold) at 100 and 200 μM of exposure dose, which was concomitant with the decrease in cell viability at the same treatments (See Figure 4.1).

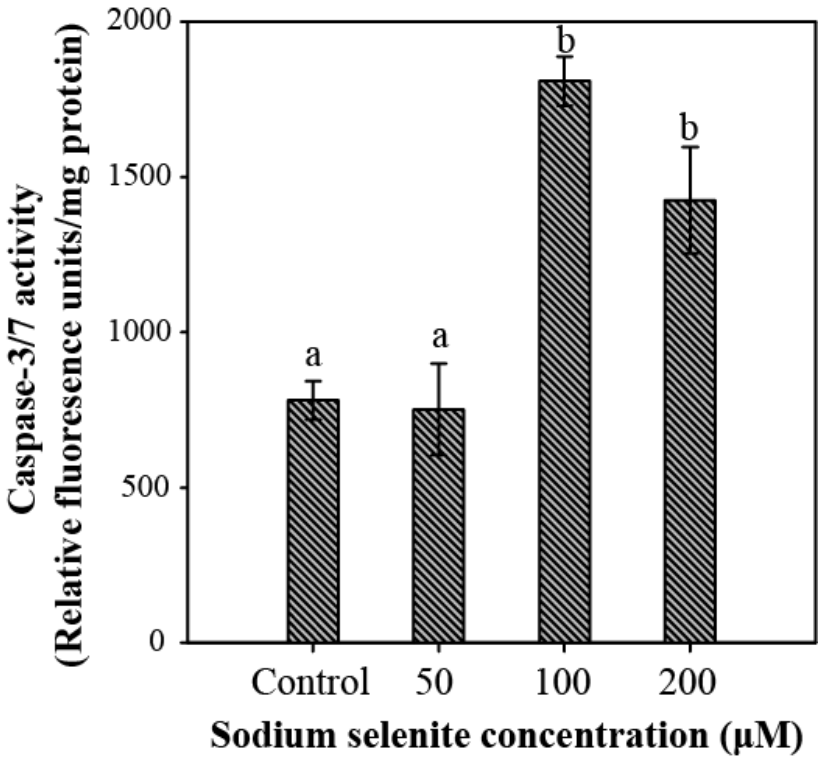

Figure 4.6: Caspase-3/7 activity in isolated trout hepatocytes following 0-200 µM sodium selenite exposure. Data are mean ± S.E.M. (n=5), where n represents the number of independent measurements using cultured cells from as many fish. Mean values with different letters are statistically significant (One Way ANOVA, $p < 0.05$).

4.4 Discussion

4.4.1 Induction of antioxidant enzymes following selenite exposure

The toxic effects of selenium compounds depend on the dose-dependent and selenium-species specific generation of intermediary metabolites capable of producing ROS (Seko et al., 1989; Spallholz, 1994). However, cellular antioxidative defense mechanisms can intercept the ROS both enzymatically and non-enzymatically. The enzymatic interception is carried out by a suite of antioxidant enzymes, primarily SOD, CAT and GPx. SOD converts $O_2^{\cdot -}$ to H_2O_2, which is then catalyzed either by CAT or GPx (Sies, 1986). The induction of SOD at low and intermediate doses observed in the current study might have occurred as a direct response to selenite induced superoxide anion ($O_2^{\cdot -}$) production as reported in mammalian tumour cells (Lin and Spallholz, 1993). The decrease in SOD activity at the high exposure dose can be correlated with the concomitant loss of cellular GSH level. This is because the cellular reduction of selenite to hydrogen selenide, a process that produces $O_2^{\cdot -}$, requires 4-6 molecules of GSH (Seko et al., 1989). Therefore, it is assumed that GSH depletion at the high selenite exposure dose might have contributed to the decrease in $O_2^{\cdot -}$ production, and subsequently the reduction of SOD activity occurred due to the substrate limitation. It is also presumed that when cellular $O_2^{\cdot -}$ generation is predominantly GSH dependent, GSH depletion can affect SOD activity at the substrate level in a greater way than the GPx activity. The dose-dependent response pattern of CAT in trout hepatocytes exposed to selenite was almost identical to that of SOD. The catalytic substrate for CAT is H_2O_2, which is the end product of the reaction catalyzed by SOD. Therefore, the response pattern of cellular CAT activity is expected to reflect the variation in cellular H_2O_2 production, which is partly dependent on the cellular SOD activity.

Unlike SOD and CAT, GPx activity in trout hepatocytes remained significantly elevated at the highest exposure dose. This probably reflects the fact that in addition to H_2O_2, GPx protects against the cytotoxicity of lipid hydroperoxides, which are produced due to the peroxidation of membrane lipids, by converting them into alcohol. It has been proposed that when the production of H_2O_2 is limited by low SOD activity, the termination reaction of hydroperoxide radical cycle slows down leading to the accumulation of hydroxyl radicals

(Michiels et al., 1994). This ultimately results into the increase in membrane lipid peroxidation. In the present study, a significant increase in the lipid peroxidation was also recorded at the highest exposure dose, which corresponded with the decrease in cellular SOD activity. Thus, it is postulated that the elevated GPx activity at the highest exposure dose was a response to the generation of excess lipid hydroperoxide radicals. Interestingly, Orun et al. (2005) reported an increase in hepatic SOD activity in rainbow trout exposed to low (10 μM) and medium (20 μM) concentrations of waterborne sodium selenite, however the activity dropped to the control (0 μM selenite) level at the high exposure concentration (30 μM). Moreover, they also observed an increase in hepatic GPx activity at the medium and high selenite exposure concentrations, but not at the low exposure level. Thus, my *in vitro* findings are quite similar to the *in vivo* observations in fish.

4.4.2 Loss of intracellular glutathione redox following selenite exposure

High metabolic turnover rate of liver makes it susceptible to oxidative damage mediated by free radicals. Therefore, a balance between the production and scavenging of free radicals is essential for its normal functioning (Cai et al., 1995). Cellular GSH plays a critical role in the scavenging of free radicals and thus protect important cellular macromolecules and organelles from oxidative damage. As discussed previously, GSH is also closely involved in selenium metabolism and bioactivity. The findings from previous studies examining the effects of selenite exposure on intracellular GSH level are controversial, and it appears that changes in intracellular GSH are dependent on the dose and duration of selenite exposure as well as the difference in types of cells or species. For example, Kuchan et al. (1990) and Kuchan and Milner (1991) reported that selenite treatment (3.2 to 12.6 μM) elevated GSH levels in canine mammary tumor cells, whereas other studies showed that similar dosage of selenite reduced intracellular GSH in other tumor cells (Caffrey and Frenkel, 1992; Kitahara et al., 1993; 2000; Shen et al., 1999). *In vivo* examination in fish also exhibited a 25% reduction in hepatic GSH level during acute exposure to waterborne selenite (Miller et al., 2007). Recently, Gad and Abd El-Twab (2009) examined the changes in intracellular GSH level in quail (*Coturnix coturnix*) hepatocytes exposed to selenite. They observed that GSH level increased by 1.5-2 fold at 100 and 200 μM

during early exposure periods (2-4h), followed by a sharp decrease at later stages (6-8h). Similarly, a 50% increase of the intracellular GSH content is observed at 100 μM of selenite exposure followed by a sharp decline at 200 μM. It is possible that the metabolic turnover of intracellular GSH was upregulated in trout hepatocytes during selenite exposure, since GSH is known to have a dual role in selenite metabolism both as a pro-oxidant (facilitating selenite-induced ROS formation) and an antioxidant (protecting against selenite-induced oxidative stress). However, it appears that the metabolic turnover rate of GSH was overwhelmed at the high selenite dose due to the increased utilization of intracellular GSH, as reflected by a dose-dependent increase of intracellular GSSG content. This is evident because selenite is reduced to H_2Se with the help of 4-6 molecules of GSH, thereby producing GSSG (Lin and Spallholz, 1993). In addition, the catalysis of H_2O_2 and lipid hydroperoxides by GPx requires GSH. The gradual increase of intracellular GSSG in association with modest or no change of intracellular GSH resulted in the dose-dependent decrease of GSH to GSSG ratio in trout hepatocytes during selenite exposure. Similar decrease in intracellular GSH to GSSG ratio was also observed in human hepatoma cells (Shen et al., 1999) and isolated rabbit hepatocytes (Kiersztan et al., 2007) exposed to selenite. The decrease in GSH to GSSG ratio indicates the development of an increasingly pro-oxidative intracellular milieu from the normal reducing state, and thereby making vital intracellular macromolecules vulnerable to oxidative damage.

4.4.3 Selenite induced intracellular ROS generation and membrane damage

In order to confirm the involvement of ROS in cytotoxicity of selenite, the intracellular ROS level was measured in trout hepatocytes. Shen et al. (1999) demonstrated a dose-dependent increase in intracellular ROS formation in human $HepG_2$ cells exposed to selenite. In the present study, a dose-dependent increase in the intracellular ROS level is observed up to 100 μM selenite exposure with no further increase at the 200 μM. It is likely that the depleted intracellular GSH level at 200 μM selenite exposure might have been a limiting factor for selenite-induced ROS production.

The peroxidation of membrane lipids occurs when the cellular antioxidant capacity is overwhelmed by oxidative stress. In the present study, a significant increase in lipid peroxidation

was observed at 200 μM, while the SOD and CAT activities and intracellular GSH level were all declining. The GPx activity, although remained increased, was probably not adequate to intercept the accumulating hydroperoxides. The cumulative effect of all of these factors might have resulted in the marked increase of membrane lipid peroxidation in trout hepatocytes. The increased LDH leakage into the extracellular media at 100 and 200 μM of exposure doses also indicated the occurrence of selenite-induced membrane damage in the present study. Consistent with the current observation, elevated membrane lipid peroxidation was also recorded in rat hepatocytes (Kitahara et al., 1993) and mice $HepG_2$ cells (Weiller et al., 2004), when exposed to similar doses of selenite.

4.4.4 Selenite induced apoptosis

The intracellular ROS generation is known to be an important apoptotic signal in the cells (Buttke and Sandstrom, 1994). Moreover, it has been demonstrated that selenium-induced oxidative stress mediates the induction of apoptosis in human hepatoma $HepG_2$ cells (Celik et al., 2004; Shen et al., 1999). On the other hand, selenite exposure was also reported to induce necrotic cell death in mice $HepG_2$ cells exposed to selenite (25-200 μM) (Weiller et al., 2004). It is likely that the mechanism of selenite-induced cell death (apoptosis or necrosis) depends to the exposure dose as well as cell types.

Caspase-3 and caspase-7 have been identified as the key executioner caspases, and are considered to be the most important caspases downstream of the apoptotic pathway (Hengartner, 2000). In the present study, the significant increase of caspase-3/7 activity at 100 and 200 μM exposures was also associated with 20-40% decrease in cell viability. A concomitant increase in intracellular ROS formation is recorded at the same selenite dose during the very early stage (2h) of exposure. Based on these findings, it can be suggested that selenite-induced oxidative stress is capable of triggering caspase-mediated apoptotic cell death in trout hepatocytes.

4.5 Conclusion

In summary, the current results support my hypothesis that selenite causes cytotoxicity in trout hepatocytes by inducing oxidative damage. It is demonstrated that selenite exposure triggers intracellular ROS generation in trout hepatocytes at an early stage. The present findings also indicated that the cellular antioxidative defense, both enzymatic and non-enzymatic, becomes activated during low to moderate level of selenite exposure. However, the defensive response is compromised at the high exposure dose possibly due to the depletion of intracellular GSH, thereby resulting in the loss of cellular reducing capacity. It appears that the development of such a condition ultimately leads to the membrane damage and cell death *via* caspase-mediated apoptosis.

CHAPTER 5: Investigation of the role of oxidative stress in mediating selenomethionine toxicity in isolated hepatocytes [4]

5.1 Introduction

Selenium is an essential micronutrient for vertebrates, including fish (Hodson and Hilton, 1983). It is an essential component of many selenoproteins that function as enzymes (e.g., glutathione peroxidase, thioredoxin reductase) or transport proteins (e.g., selenoprotein P) or play important role in muscle physiology (e.g., selenoprotein W) (Thisse et al., 2003). Fish can utilize selenium more efficiently as evident from higher deployment of selenocysteine during selenoprotein synthesis in fish relative to mammals (Kryukov and Gladyshev, 2000). The higher efficiency in harnessing selenium by fish is also obvious from a markedly greater number of selenoproteins in fish (32-34) than terrestrial mammals (23-25) (Lobanov et al., 2007). Although fish can acquire selenium both from the water and diet, diet is considered to be the predominant pathway of selenium acquisition (Janz, 2011). Selenomethionine is the primary component of selenium in fish diets (Maher et al., 2010), and it is known to have a higher bioaccumulative and trophic transfer potential relative to other organic and inorganic forms of selenium (Besser et al., 1993; Fan et al., 2002).

Selenium has a low margin between essentiality and toxicity, and when selenium concentration in the body exceeds the threshold level, toxic effects occur. In mammals, selenomethionine is absorbed and metabolized similar to methionine, where it is incorporated into proteins as selenomethionine. Recently, the existence of similar mechanisms of selenomethionine absorption has been reported in fish intestine (Bakke et al., 2010). Once ingested from the diet, the majority of absorbed selenium is effluxed from the intestine into the hepatic portal system, with or without first pass metabolism by enterocytes, and taken up in the liver by hepatocytes. This is consistent with the observation that dietary selenomethionine

---

[4] This chapter of the thesis has been communicated for publication under joint authorship with Som Niyogi (University of Saskatchewan).

supplementation results in the maximum selenium accumulation in the liver compared to other organs in fish (Lorentzen et al., 1994). Liver is the primary site for metabolism of selenium, and is probably one of the key target organs for selenium toxicity. Recent studies have shown that dietary exposure to selenomethionine can affect the physiological functions in fish such as swimming performance, energy metabolism (Thomas and Janz, 2011) and steroidogenesis in fish (Wiseman et al., 2011). However, current knowledge on the mechanistic underpinnings of selenomethionine toxicity in fish, particularly at the cellular level, is very limited.

Previous studies have demonstrated that selenite, a common inorganic form of selenium, exerts its cytotoxicity in fish by inducing oxidative stress (Miller and Hontela, 2011; Misra et al., 2010). It is important to note here that selenite and selenomethionine are metabolized through different cellular pathways. Selenite reacts with glutathione (GSH) and produces hydrogen selenide, which then reacts with oxygen to produce reactive oxygen species (ROS) (Misra et al., 2010; Seko et al., 1989). To date, only few studies have investigated the cellular mechanisms of selenomethionine metabolism in fish. It has been suggested that selenomethionine is metabolized into methylselenol, either *via* the *trans*-sulfuration pathway or directly by the enzyme methioninase, and the subsequent redox cycling of methylselenol leads to the generation of ROS (Misra et al., 2010; Palace et al., 2004). Palace et al. (2004) reported that the redox cycling of methylselenol in the presence of GSH produces superoxide radical, which likely accounts for the oxidative lesions in fish embryos. Misra et al. (2010) detected methioninase activity in fish hepatocytes, and also demonstrated a rapid dose-dependent increase in intracellular ROS generation following exposure to selenomethionine. These findings suggest that oxidative damage may be a potential mechanism of selenomethionine toxicity in fish, although further investigations are required to validate this hypothesis.

In the present study, the role of oxidative stress in cytotoxicity of selenomethionine was examined using rainbow trout (*Oncorhynchus mykiss*) hepatocytes in primary culture as the model experimental system. The main goal was to understand how dose-dependent exposure to selenomethionine influences the cellular oxidative status and its consequences to cellular viability. The specific objectives of this study were: (i) to determine the dose-response relationship for selenomethionine cytotoxicity, (ii) to evaluate how exposure to selenomethionine

affects the responses of key cellular enzymatic antioxidants, and the cellular thiol redox balance, and (iii) to determine whether selenomethionine exposure impairs structural integrity of cells including membrane and DNA integrity, disrupts intracellular calcium homeostasis and triggers apoptosis as a pathway for cell death.

5.2 Materials and Methods

5.2.1 Chemicals

Six-well and 96-well BD Falcon Primaria™ culture plates were purchased from VWR International, Canada. High purity (99%) selenomethionine was purchased from Acros Organics, Canada. Reduced and oxidized glutathione (GSH and GSSG, respectively), dimethylformamide, Na-HEPES and trypan blue solution were obtained from Sigma-Aldrich, USA. Analytical grade NaCl, KCl, $MgSO_4$, Na_2HPO_4, KH_2PO_4, HEPES, NaOH, EDTA, $CaCl_2$, and methanol were obtained from VWR International, Canada. L-15 media (powder form with L-glutamine) and calcium dye (Fluo-4 AM based kit) were obtained from Invitrogen, Canada. Tricaine methanesulfonate (MS-222) was obtained from Syndel Laboratories Ltd., Canada.

5.2.2 Fish

Rainbow trout (*O. mykiss*) weighing 200–300 g were obtained from the Saskatchewan Government Fish Farm, Qu'Appelle, Saskatchewan. Fish were maintained in 1000 l flow-through aquaria receiving dechlorinated Saskatoon City water at a rate of 2 l/min under constant aeration at the Aquatic Toxicity Research Facility (ATRF) of the University of Saskatchewan. A photoperiod of 16 h light: 8 h dark and a water temperature of 15 ± 1°C were maintained throughout the experimental period. The fish were fed once daily with Martin's commercial diet (Martin Mills Inc., Elmira, Canada) at a 2% body weight ration. All fish were acclimated for at least 2 weeks prior to their use in the experiments. The experimental protocol was in accordance with the Canadian Council for Animal Care Guidelines and approved by the animal research ethics board at the University of Saskatchewan.

5.2.3 Isolation and culture of hepatocytes and selenomethionine exposure regime

Hepatocytes were isolated and cultured following the method described elsewhere (Misra et al., 2010). Following isolation, cells were cultured at 15°C for 24 h prior to their use in any experiments outlined below. Only the primary cultures showing ≥ 90% cell viability were used for subsequent experiments. First, cells were exposed to an increasing concentration of Se-Met for 24 h to determine the dose level that affects the cell viability, as measured by trypan blue exclusion test using the Countess Automated Cell Counter (Invitrogen, Canada). Based on these results and morphological changes (cell population showing discernible changes in structural integrity), a dose regime [0(control), 250, 500 and 1000µM] was selected to study the biochemical changes associated with selenomethionine exposure. To examine the onset and progression of toxic effects, all of the experimental parameters were evaluated at three different exposure periods (0, 4 and 24 h) unless stated otherwise (See below for details). In this series of experiments, cells were cultured in selenomethionine spiked L-15 media (except control) for the intended exposure periods in 6-well culture plates. At the end of the exposure, cells were washed gently with phosphate buffered saline (pH adjusted to 7.63) and collected using non-enzymatic cell dissociation solution (Millipore, Canada), and the cell viability was measured as outlined above. In a parallel experimental series, cells were plated in 96-well BD primaria™ plates at a density of 50,00 cells per well, with each well containing 200µl of L-15 media, and exposed to identical selenomethionine concentrations and time periods as described above. At the end of the exposure, 100µl of media was collected from each well to measure the lactate dehydrogenase (LDH) leakage into the media using the LDH assay kit (Promega, Canada). LDH data were expressed as relative fluorescent unit (RFU)/50,000 cells.

5.2.4 Antioxidant enzyme assays

The activities of superoxide dismutase (SOD), glutathione peroxidase (GPx) and catalase (CAT) were measured using the 96-well microplate based assays. Once the viability of the suspended cells (in cell dissociation solution) exposed to selenomethionine was measured, cells were pelleted at 500*g* for 4 min at 4°C and subsequently lysed with CelLytic™-M reagent

(Sigma-Aldrich, USA) following the manufacturer's instructions. A portion of the lysed cells was stored at -80°C for the measurement of thiobarbituric acid reactive substances (TBARS) without centrifugation (See below). The rest of the cell lysates were centrifuged at 14,000*g* for 20 min at 4°C to pellet the cellular debris. The supernatant was collected and stored at -80°C for the analysis of all enzymes activities and measurement of GSH and GSSG. The SOD and GPx activities were measured using the commercial kit obtained from Assay Design (USA). The activity of SOD was measured as units/mg protein, where one unit of enzyme activity refers to 50% inhibition of the changes in absorbance. The GPx activity was measured as nmole/min/mg protein. The CAT activity was measured using the Amplex® Red catalase assay kit (Molecular Probes, USA). One unit of CAT activity was defined as the amount of enzyme that will decompose 1.0 μM of H_2O_2 into H_2O per minute and measured as milliunit (mU)/mg of protein. The protein content of the cell lysates were measured by the Bradford method (Bradford, 1976) using BSA as the standard. Varioskan Flash multimode plate reader (Thermo Electron Corporation, Finland) was used for all the photometric and fluorescence measurements in these assays. All the antioxidant enzyme activities in the experimental treatments are expressed as the percentage of control at time '*zero*'.

5.2.5 Quantification of reduced and oxidized thiols

The concentration of the reduced (GSH) and oxidized (GSSG) glutathione in the cell lysates were measured using a fluorometric method (Hissin and Hilf, 1976), modified to a 96-well microplate based assay (Misra and Niyogi, 2009). The GSH and GSSG content was expressed as μg/mg of protein.

5.2.6 Confocal imaging of intracellular calcium

Intracellular calcium was measured using the Fluo 4 NW assay kit (Molecular probes, Eugene, OR). Hepatocytes were cultured in poly-D-lysine coated glass bottom (Refractive Index – 1.5) 18 well chambers (Ibidi, München, Germany). Changes in the cell calcium response were measured using the Carl Zeiss LSM 510 confocal microscope with a 63X, 0.9 numerical aperture

water immersion objective. Briefly, cells were loaded with the assay buffer containing the dye and probenecid (2.5 mM) for 1 h at 15°C. Subsequently, the assay buffer was carefully replaced with L-15 media containing the appropriate concentrations of selenomethionine. Time-dependent changes in the intracellular calcium were measured at room temperature (~ 20°C) for 30 min (at 30 s interval) using the 488 excitation Argon laser beam, and emission was collected using 505-530 band pass filter. All other confocal and laser parameters were kept identical across the experimental treatments.

5.2.7 Measurement of lipid peroxidation

Lipid peroxidation was measured fluorometrically as the amount of thiobarbituric acid reactive substances (TBARS) in the samples (cell lysate without centrifugation) using the OXI-TEK TBARS kit (Alexis Biochemicals, USA). The data were expressed as nmol of TBARS equivalent/ mg of protein.

5.2.8 Caspase 3/7 activity

Caspase-3/7 assay was performed using the EnzChek® Caspase-3 Assay Kit (Invitrogen, Canada). This assay utilizes the caspase-3/7 substrate rhodamine 110, bis-N-CBZL-aspartyl-L-glutamyl-L-valyl-L-aspartic acid amide (Z-DEVD-R110). The dissociated product, rhodamine 110, fluoresces following cleavage by the enzymes. Equal volume of diluted caspase-3/7 reagent was mixed with the samples in a 96-well microplate and incubated for 30 min at 15°C in the dark. Subsequently, the fluorescence was measured at excitation and emission wavelengths of 496 and 520 nm, respectively. The enzyme activity was expressed as relative fluorescence unit/mg of protein.

5.2.9 Agarose gel electrophoresis

Total genomic DNA was isolated from the cells following 24 h exposure to selenomethionine, using a commercially available kit (Qiagen, Canada). Following the extraction, equal amount of DNA was loaded into 1% agarose gel in 0.5 X TBE buffer containing ethidium bromide. The DNA samples were run in the gel for 30 min at 170V.

5.2.10 Scanning electron microscopy

For the scanning electron microscopy (SEM), cells were cultured in poly-D-lysine (Sigma, Canada) coated 10mm glass coverslips (Electron Microscopy Sciences, USA) placed in 6-well plate for 24 h. This culture protocol was used to minimize mechanical damage, and thereby to reduce any artefacts during the processing of samples. At the end of the 24 h exposure period, the coverslips were carefully removed from the wells and fixed in 2.5% glutaraldehyde in 0.1 M sodium-cacodylate buffer (SCB), pH 7.40 for 2 h at 4°C. Subsequently, the coverslips were rinsed with the SCB buffer for 4 times over a period of 30 min at 4°C. The cells were then fixed in 1% osmium tetroxide for 1 h at 4°C. This was followed by washing of the cells with the SCB buffer for 4 times and the cells were kept at 4°C overnight. Then, the cells were dehydrated first with graded series of ethanol (30 – 90%), with the final 2 washing steps in 100% acetone for 10 min each. The samples were dried with a critical point dryer (Polaron E3000 Series II) and sputter coated with gold (Edwards S150B). The images were captured using Philips 505 scanning electron microscope.

5.2.11 Data Analysis

All data are presented as mean ± standard error of mean (S.E.M.). Sample size 'n' indicates that experiments were repeated using cells isolated from 'n' number of fish. Significant differences among the treatment groups were analyzed by one-way analysis of variance (ANOVA) (SigmaPlot®, version 11, Systat Software, Inc., USA). The assumptions of ANOVA (normality of distribution and homogeneity of variances) were examined using Shapiro-Wilk and

Levene's tests, respectively. When the data did not meet one of the assumptions of ANOVA, the data were analyzed using ANOVA on ranks followed by Tukey's multiple comparison tests. A p-value of ≤ 0.05 was considered to be significant while comparing different treatments. All the graphs were created using OriginPro® (OriginLab Corporation, USA).

5.3 Results

5.3.1 Cytotoxicity of selenomethionine

Data in Figure 5.1A depict the changes in the cell viability upon selenomethionine exposure (0 – 1000μM) for 4 and 24 h. No significant change ($p \geq 0.05$) in cell viability was recorded among the experimental treatments at any exposure period except at 24 h of 1000μM selenomethionine exposure. Even at such a high exposure dose, the decrease in cell viability was modest (~15% relative to the control). The LDH leakage data (Figure 5.1B) correlated well with the cell viability data, since a significant increase ($p \leq 0.05$) compared to the control (4 h) was only observed in cells exposed to 1000μM selenomethionine for 24 h.

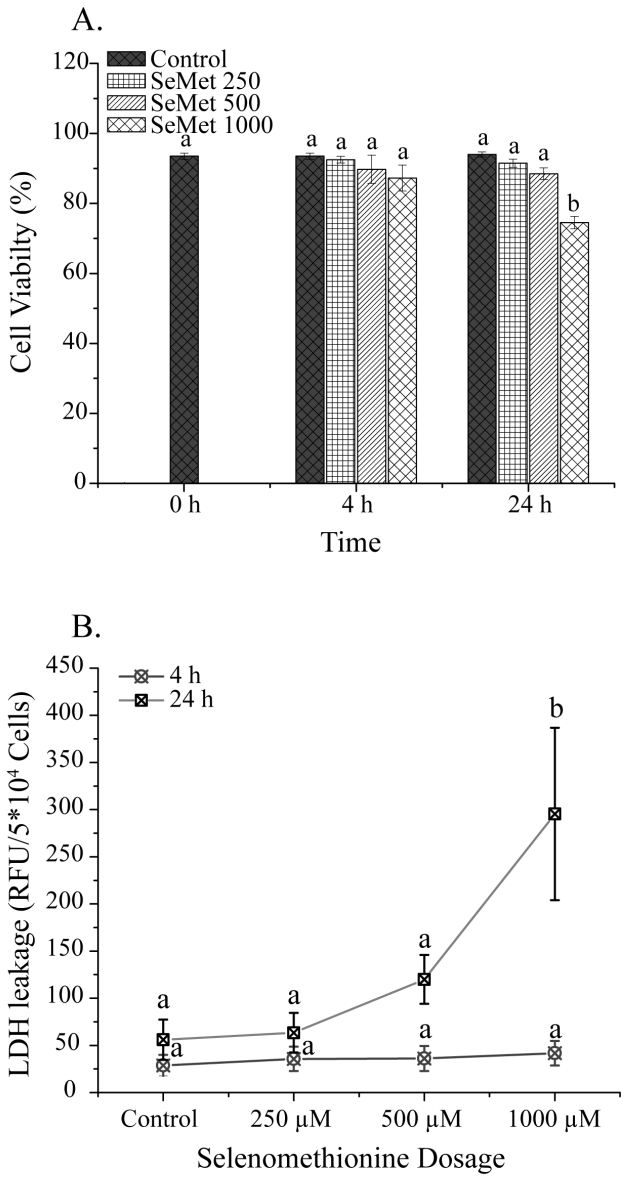

Figure 5.1: Cell viability (Figure 5.1A) and LDH leakage into the exposure media (Figure 5.1B) from hepatocytes exposed to selenomethionine (0 – 1000µM) for 4 and 24 h. The control value in Figure 5.1A indicates the initial cell viability before exposing the hepatocytes to selenomethionine. Significant changes in cell viability ($p \leq 0.05$) and LDH leakage ($p \leq 0.01$) were recorded only at the highest exposure dose after 24 h. The data are presented as the mean ± S.E.M. of 4 – 5 independent observations, where each observation represents cells isolated from an individual fish. Mean values with different letters are statistically significant (One Way ANOVA by ranks).

5.3.2 Response of the antioxidant enzymes

The induction of all three antioxidant enzymes (SOD, GPx and CAT) was recorded in cells exposed to selenomethionine (Figure 5.2A-5.2C). A significant ($p \leq 0.001$) increase of the SOD activity was observed relative to that in the control in cells exposed to 500 and 1000μM at 24 h, but not at 4 h. In contrast, a significant ($p \leq 0.01$) increase of the GPx activity was recorded in cells exposed to 1000μM selenomethionine at both 4 and 24 h. The CAT activity was also significantly ($p \leq 0.05$) higher in cells exposed to 1000μM, but only at 24 h. Interestingly though, the magnitude of induction of CAT was more robust than GPx in cells exposed to 1000μM of selenomethionine for 24 h. No significant changes occurred in the activities of any of the three antioxidant enzymes examined, either at 4 or 24 h, at the lowest selenomethionine exposure dose (250 μM).

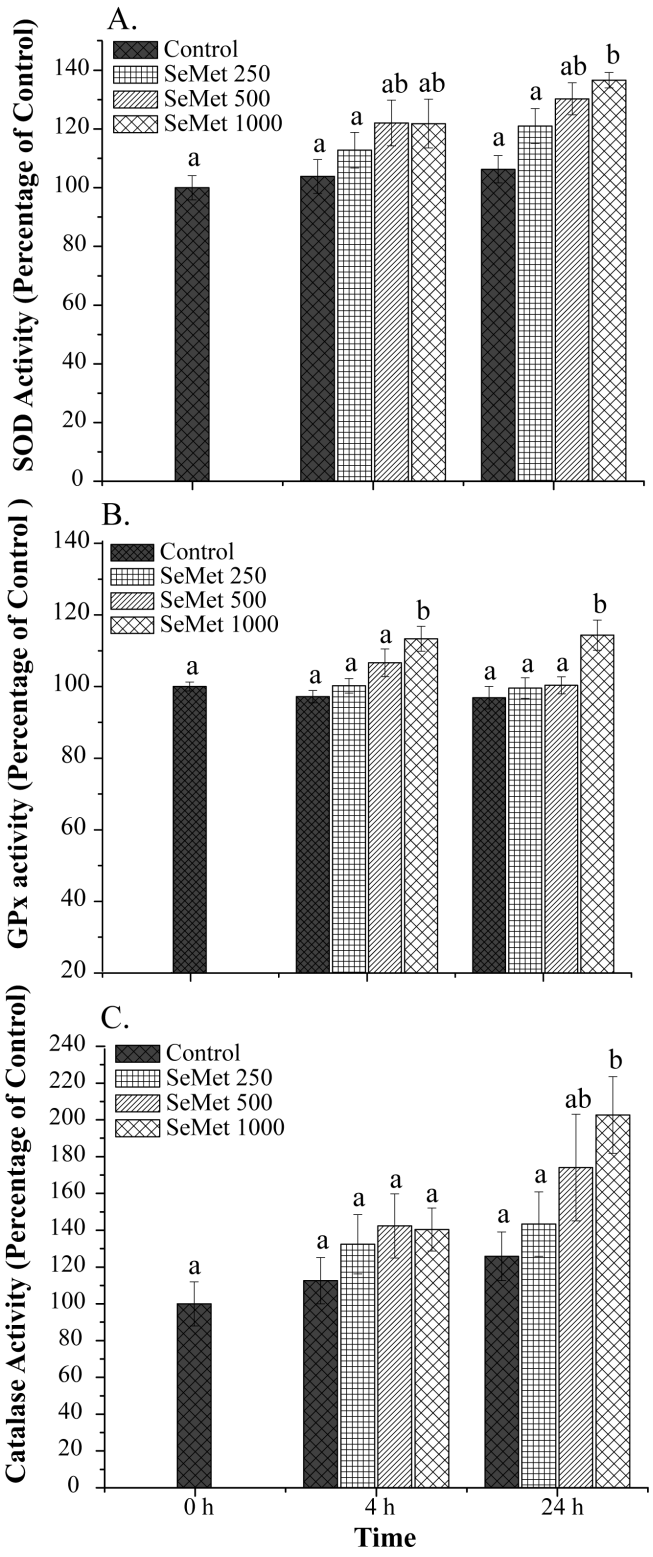
A.
Control
SeMet 250
SeMet 500
SeMet 1000
SOD Activity (Percentage of Control)
B.
GPx activity (Percentage of Control)
C.
Catalase Activity (Percentage of Control)
0 h
4 h
24 h
Time

Figure 5.2: Activities of antioxidant enzymes (Figure 5.2A – SOD, Figure 5.2B – GPx, Figure 5.2C – CAT) in hepatocytes upon exposure to selenomethionine (0 – 1000μM) for 4 and 24 h. Compared to the control, SOD activity ($p \leq 0.001$) increased significantly in the cell lysates obtained from hepatocytes exposed to 500 and 1000μM selenomethionine for 24 h. A significant increase ($p \leq 0.01$) in the GPx activity was observed only at 1000μM exposure dose at 4 and 24 h. In contrast, CAT activity was only significantly ($p \leq 0.05$) different from the control when hepatocytes were exposed to 1000μM selenomethionine for 24 h. The data are presented as the mean ± S.E.M. of 4 – 5 independent observations, where each observation represents cells isolated from an individual fish. Mean values with different letters are statistically significant (One Way ANOVA by ranks).

5.3.3 Alteration of the cellular thiol redox

Data in Figure 5.3 demonstrate the changes in thiol redox (measured as GSH to GSSG ratio) in selenomethionine exposed cells at different time periods. No significant changes in the thiol redox were recorded in the control cells over 24 h. However, a significant decrease ($p \leq 0.001$) in GSH to GSSG ratio was recorded with increasing doses of selenomethionine exposure (Figure 5.3). The decrement was more dramatic at 24 h relative to that at 4 h, particularly at 500 and 1000μM exposure doses (~ 2.5 fold decrease compared to the control). A decreasing thiol redox indicated a shift of intracellular milieu towards an oxidizing state with diminishing reducing thiol equivalents.

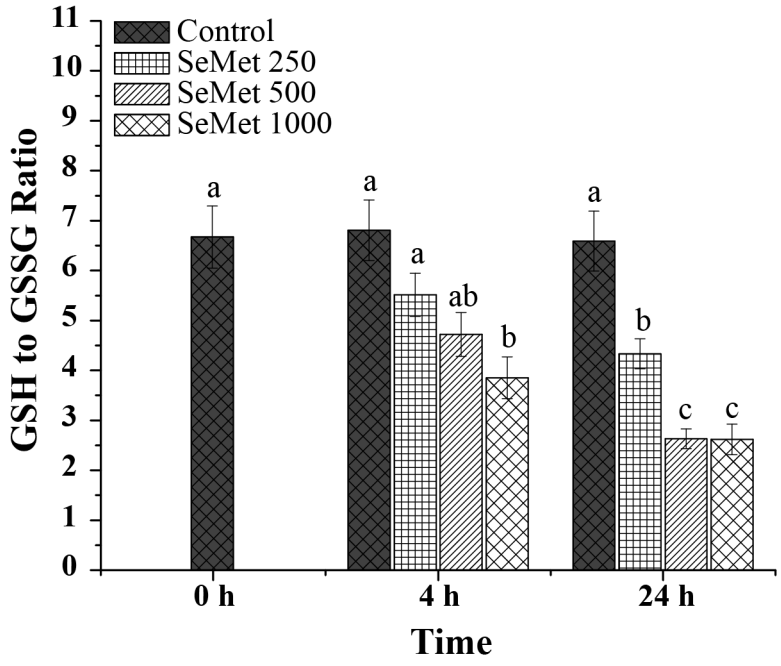

Figure 5.3: Changes in the cellular thiol redox status, expressed as a ratio of reduced (GSH) to oxidized (GSSG) glutathione, in hepatocytes upon exposure to selenomethionine. Exposure to 1000µM selenomethionine for either 4 h or 24 h, and 500µM selenomethionine for 4 h resulted in a significant ($p \leq 0.001$) decrease in thiol redox compared to that in the control. Such marked decrease in redox status is conducive for the potential induction of oxidative stress in these cell types. The data are presented as the mean ± S.E.M. of 4 – 5 independent observations, where each observation represents cells isolated from an individual fish. Mean values with different letters are statistically significant (One Way ANOVA by ranks).

5.3.4 Perturbation of intracellular calcium homeostasis

My previous investigation suggests that selenomethionine at an exposure dose of 1000μM causes a rapid increase in ROS generation in rainbow trout hepatocytes (Misra et al., 2010). Since ROS generation can trigger an increase in intracellular Ca^{2+} level (Nicotera et al., 1988), it is hypothesized that similar effects might occur in the current experimental system. To investigate the changes in the intracellular Ca^{2+}, the hepatocytes were exposed with an increasing dosage of selenomethionine (0 – 1000μM) over a period of 0-30 min. A rapid elevation of intracellular Ca^{2+} was observed at 1000μM of selenomethionine exposure dose, however no such effects were recorded either at 250 or 500 μM exposure dose (Figure 5.4).

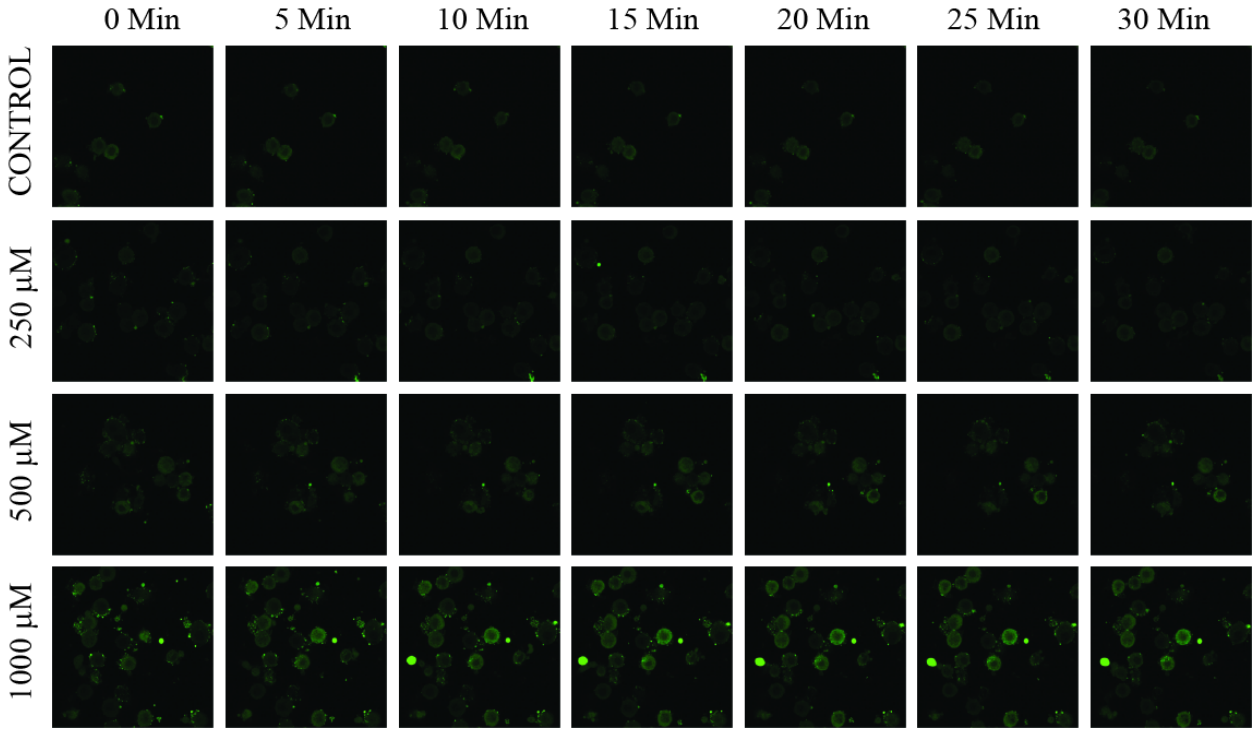

Figure 5.4: Confocal images of hepatocytes showing time-dependent changes in $[Ca^{2+}]_i$ following short-term (30 min) exposure to 0 – 1000µM selenomethionine. Time '0' indicates the initiation of time series image capture that took about 5 min (sample processing) from the initiation of exposure. A rapid increase in the $[Ca^{2+}]_i$ was recorded over time in hepatocytes exposed to 1000µM selenomethionine. The images shown here are the representative of 2 independent experiments, where each experiment was conducted using cells isolated from an individual fish.

5.3.5 Loss of membrane integrity

Membrane lipid peroxidation was quantified to assess the structural integrity of membrane in trout hepatocytes. No alteration in cellular lipid peroxidation occurred in the control during the experimental period. However, a dose-dependent increase in cellular lipid peroxidation was recorded following exposure to selenomethionine, both at 4 and 24 h (Figure 5.5). Compared to the control, TBARS values were 4-5 fold higher ($p \leq 0.001$) when hepatocytes were exposed to 500 and 1000μM selenomethionine for 24 h.

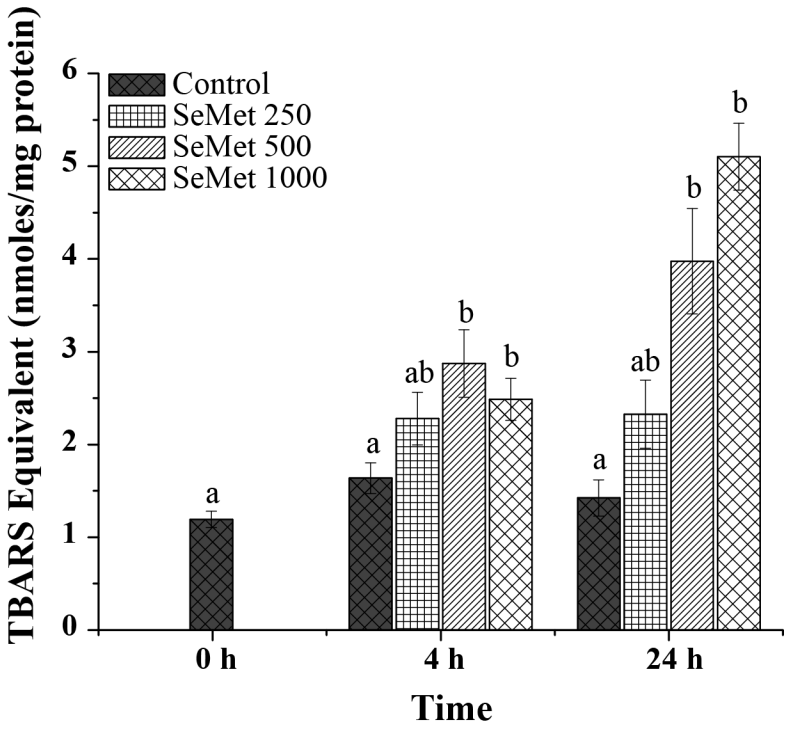

Figure 5.5: Lipid peroxidation (measured as TBARS equivalent) in hepatocytes upon exposure to selenomethionine. There was significantly higher ($p \leq 0.001$) lipid peroxidation at 500μM and 1000μM selenomethionine exposure dosage at 4 h and 24 h, when compared to the control at 0 h. The data are presented as the mean ± S.E.M. of 4 – 5 independent observations, where each observation represents cells isolated from an individual fish. Mean values with different letters are statistically significant (One Way ANOVA by ranks).

5.3.6 Caspase 3/7 activity

The activity of caspase 3/7 (both have the similar substrate with peptide sequence Asp-Glu-Val-Asp) was measured to investigate whether the selenomethionine exposure induces the caspase-dependent pathway of apoptotic cell death. A significant increase ($p \leq 0.001$) of the caspase3/7 activity was observed only at the highest exposure dose of selenomethionine (1000μM) over 24 h (Figure 5.6). This indicated that a high dose of selenomethionine could trigger the onset of enzymatic pathway of apoptosis.

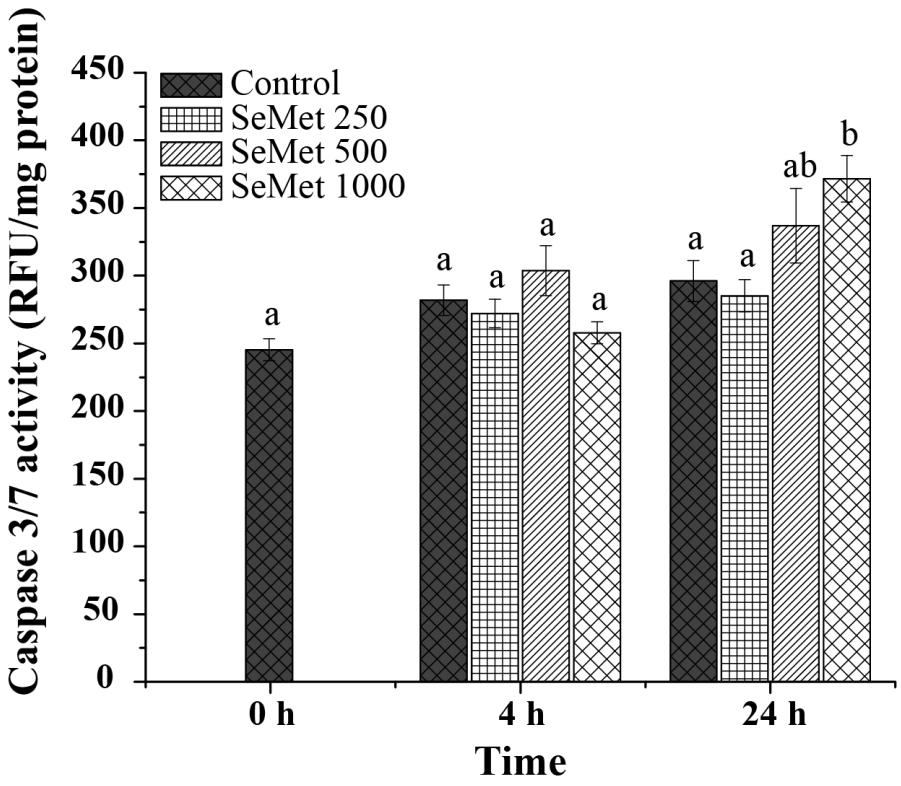

Figure 5.6: Caspase 3/7 activity was measured as a marker of caspase-dependent apoptotic pathway induced by selenomethionine exposure. Following 24 h exposure of selenomethionine to hepatocytes, a significant increase ($p \leq 0.001$) in caspase 3/7 activity was detected, when compared with that in the control. The data are presented as the mean ± S.E.M. of 5 independent observations, where each observation represents cells isolated from an individual fish. Mean values with different letters are statistically significant (One Way ANOVA by ranks).

5.3.7 DNA damage

Data in Figure 5.7 show the integrity of genomic DNA in trout hepatocytes exposed to different doses of selenomethionine. From the smearing pattern of DNA, it appears that there was nicking of DNA extracted from the cells exposed to 1000μM of selenomethionine, although the effect was marginal and may not be significant.

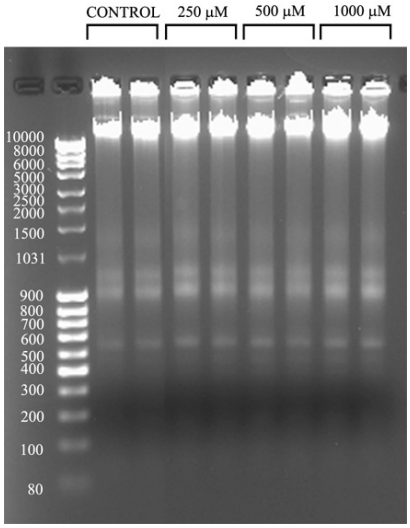

Figure 5.7: Ethidium bromide stained gel was used to demonstrate the effect of selenomethionine exposure for 24 h on the integrity of genomic DNA in hepatocytes. The left most panel shows the molecular weight markers that correspond to their molecular weight (kb). Apparent smearing pattern at the highest exposure dose (1000µM) indicates probable DNA damage. However, without a clear smearing pattern, this was not considered to be significant. Two lanes for each dose are the representative of genomic DNA isolated from 2 independent experiments, where each experiment was conducted using cells isolated from an individual fish.

5.3.8 Alteration of cellular morphology

One of the common features of isolated hepatocytes in culture is that certain numbers of cells show altered cellular morphology (mainly bleb formation in the plasma membrane) even in the absence of toxicant exposure (Braunbeck and Storch, 1992). In the present study, similar effects were observed in the control cell population. However, following exposure to selenomethionine for 24 h, the number of cells showing bleb formation increased across the treatments (Figure 5.8), and this effect was particularly evident at 500 and 1000µM exposure doses. Such morphological change is often associated with the apoptotic cell death.

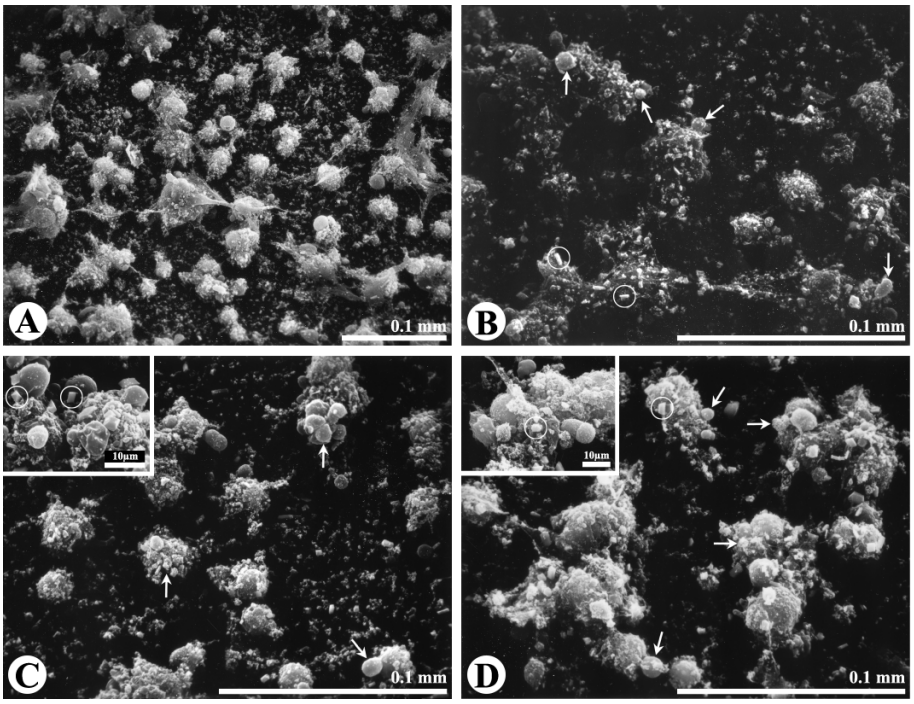

Figure 5.8: Scanning Electron Microscope (SEM) images of trout hepatocytes exposed to different doses of selenomethionine (A – Control, B – 250µM, C – 500µM and D – 1000µM) for 24 hrs. Arrows indicate bleb formation in the plasma membrane of exposed hepatocytes, representing typical morphological changes associated with apoptosis. Insets in Figures 5.8C and 5.8D show protruding blebs in higher magnification. Some unknown crystal structures were observed in the selenomethionine treatment groups (indicated in white open circles). The images shown here are the representative of 2 independent experiments, where each experiment was conducted using cells isolated from an individual fish.

5.4 Discussion

5.4.1 Cytotoxicity of selenomethionine

The present study was designed to determine the dose- and time-dependent cytotoxicity of selenomethionine in isolated hepatocytes of rainbow trout, and also to examine whether its toxicity is mediated by oxidative stress. Results from the cell viability and LDH leakage experiments suggest that rainbow trout hepatocytes are quite resistant to selenomethionine relative to the inorganic forms of selenium such as selenite. Twenty percent reduction in the cell viability has been found in trout hepatocytes exposed to 100 µM of selenite for 24 h (Misra and Niyogi, 2009), whereas a 10-fold higher selenomethionine exposure dose resulted in only about 15% decrease in cell viability in the present study. This is consistent with the recent investigation by Miller and Hontela (2011), who reported that the EC_{50} [measured as the effects on adrenocorticotropic hormone (ACTH) stimulated cortisol secretion] of selenomethionine in isolated adrenocortical cells of rainbow trout (*O. mykiss*) and brown trout (*Salvelinus fontinalis*) is >20-fold higher relative to that of selenite. Similarly, Hoefig et al. (2010) reported that mammalian hepatic cells are also much less sensitive to selenomethionine relative to selenite and selenate. In comparison to the trout hepatocytes, murine hepatocytes have been shown to be much more sensitive to selenomethionine (24 h EC_{50} = 30µM). Also, human lymphocytes in primary culture have been shown to elicit toxic effects when exposed to ≥ 23.5µM selenomethionine for 9 days (Wu et al., 2009). The comparison of these results suggests that primary cells of piscine origin are generally less susceptible to selenomethionine toxicity relative to those of mammalian origin, although differences in exposure time and conditions may also partially account for the differences in selenomethionine sensitivity among these studies. Similarly, the transformed piscine epithelioid cells were also found to be less sensitive to selenite and selenate compared to the mammalian epithelioid cells (Babich et al., 1989). To explain such discrepancies in selenium toxicity between mammals and fish, it has been argued that reduced reliance on selenium during evolution has made it less essential in mammals than fish (Lobanov et al., 2008). It is also evident from the fact that the nutritional requirement of selenium in human (0.92 µg/kg body weight/day, considering the body weight of an average human being is 60 kg)

(Pain, 2000) is much lower than that in fish (5-25 µg/kg body weight/day) (Janz, 2011). In comparison to primary cells, some cancer cells elicit extraordinary resistance to selenomethionine toxicity. In human carcinoma cell HepG2, selenomethionine has been reported to be non-toxic even up to an exposure dose as high as 10 mM (Weiller et al., 2004). The differences in toxic effects between the normal and malignant cells should be an important factor while considering selenomethionine as a therapeutic agent for treatment against cancer, in order to minimize unsolicited toxic effects to normal somatic cells.

5.4.2 Selenomethionine induced oxidative stress

Findings from my previous work suggest that the short term exposure to selenomethionine results in rapid generation of ROS in trout hepatocytes (Misra et al., 2010). Thus, the responses of key cellular enzymatic antioxidants (SOD, GPx and CAT) were explored in order to understand the efficiency of ROS scavenging in these cells. An increasing trend in SOD activity was observed with increasing selenomethionine exposure dose; however significant changes occurred only when the hepatocytes were exposed to 500 and 1000µM selenomethionine for 24 h. This is consistent with my previous observation that ROS generation was associated only with a high selenomethionine exposure dose (1000µM) (Misra et al., 2010). Palace et al. (2004) previously suggested that selenomethionine exposure leads to the generation of superoxide anion ($O_2^{\cdot -}$) in rainbow trout embryos. Since, it is the substrate of SOD, an increase in its activity observed in this study was probably a response to the increased intracellular $O_2^{\cdot -}$ production. However, the catalysis of $O_2^{\cdot -}$ by SOD does not terminate the redox reactions as the end product of this reaction is H_2O_2, which can subsequently be catalyzed by either by GPx or CAT. Since, GPx has a much lower K_m value than CAT (Izawa et al., 1996), preferential catalysis of H_2O_2 by GPx might be expected when H_2O_2 concentration is low. Interestingly, the induction of both GPx and CAT were observed in cells exposed to 1000µM of selenomethionine for 24 h, and the magnitude of induction of CAT was actually much greater relative that of GPx. It is presumed that it occurred because of a significant increase in intracellular H_2O_2 production at 1000µM exposure dose. Overall, it appears that

selenomethionine exposure at higher dosage leads to the induction of cellular enzymatic antioxidants.

The GSH to GSSG ratio serves an important indicator of the redox state of intracellular milieu (Deleve and Kaplowitz, 1990). During sustained oxidative stress, a considerable pool of intracellular GSH is oxidized to GSSG, resulting in GSH to GSSG ratio to fall below the normal level. This manifests negative implications on cell physiology by altering several key biochemical pathways that depend on a reducing intracellular environment. In general, GSH plays a major role in the detoxification of many organic compounds by enzymatic conjugation. However, GSH plays a unique role in selenium toxicity depending on the oxidation state and chemical speciation of selenium. For instance, GSH reacts with selenite and forms elemental selenium *via* several intermediates (Misra et al., 2010). This leads to enhanced oxidation of GSH, resulting in diminished thiol redox. In the present study, it was found that thiol redox was compromised in a dose dependent manner over time following exposure to selenomethionine. It is hereby presumed that multiple biochemical pathways might be involved that could lead to such changes. Selenomethionine is known to be oxidized to methionine selenoxide (SeMetO) by flavin containing monooxygenase 3 (FMO3) - a microsomal enzyme, in mammals (Krause and Elfarra, 2009) and fish (Lavado et al., 2011). However, SeMetO can be converted back into selenomethionine by the oxidation of GSH, resulting into GSSG formation. The existence of FMO enzymes has recently been reported in trout liver (Rodríguez-Fuentes et al., 2008), and therefore this pathway might have contributed to elevated GSSG. It is important to note that microsomal origin of this enzyme suggests endoplasmic reticular localization of this enzyme. Hence, such oxidation of selenomethionine may be organelle specific – indicating a possible compartmentalized effect. Apart from this, it is reported earlier that selenomethionine can be enzymatically oxidized into methylselenol, and the redox cycling of methylselenol can lead to elevated GSSG level at the expense of GSH (Misra et al., 2010; Palace et al., 2004). Also a non-enzymatic pathway may be important in the overall decrease in thiol redox since it has been reported earlier that H_2O_2 can catalyze direct conversion of selenomethionine into SeMetO (Gammelgaard et al., 2003). Therefore, subsequent reduction of SeMetO by GSH may lead to increased accumulation of GSSG. It is important to mention here that cysteine and ascorbic acid can also participate in such reduction of SeMetO. A schematic diagram (Figure 5.9) has been

presented to illustrate the probable pathways involved in diminishing cellular thiol redox during selenomethionine exposure.

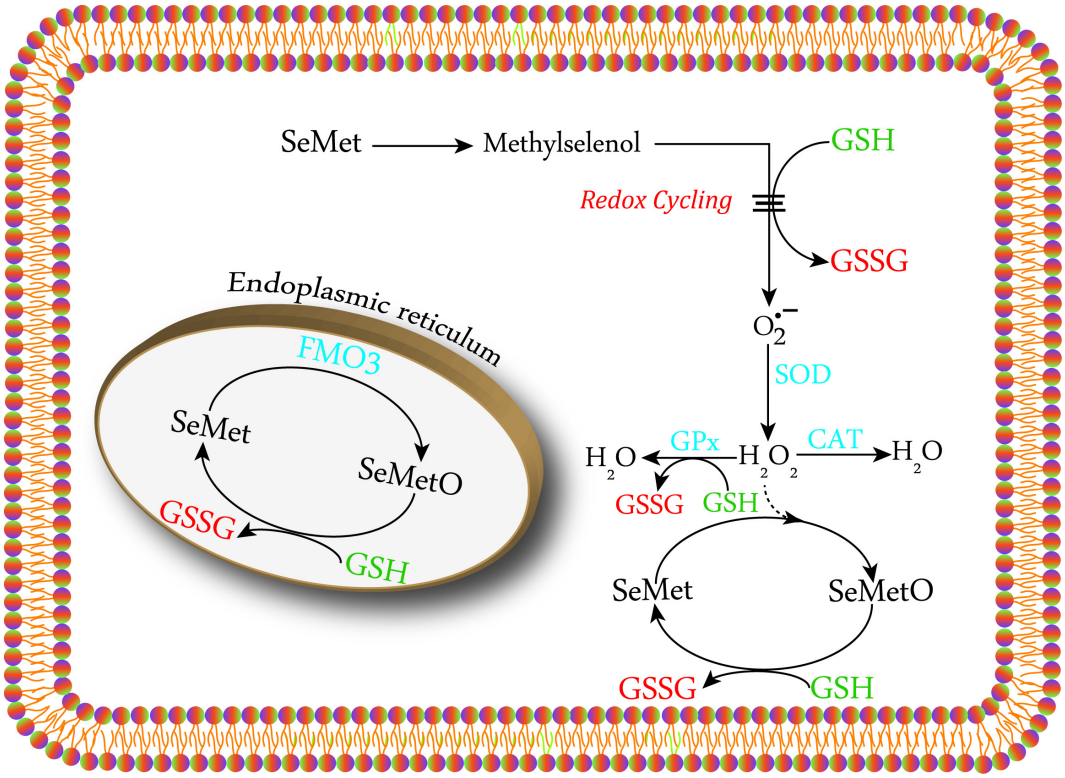

Figure 5.9: Schematic diagram showing the metabolism of selenomethionine and subsequent redox cycling with GSH. The redox cycling of methylselenol, a metabolite of selenomethionine, with GSH produces reactive oxygen species (ROS). The redox cycling of selenomethionine in the endoplasmic reticulum is mediated by FMO 3 enzyme (Krause and Elfarra, 2009; Lavado et al., 2011). Since endoplasmic reticulum (ER) is one of the major storage sites of $[Ca^{2+}]_i$, it is possible that the ER membrane damage, induced by increased intracellular ROS generation, may lead to the release of stored Ca^{2+} into the cytosol, resulting into elevated $[Ca^{2+}]_i$. Also, selenomethionine can react with H_2O_2 to form SeMetO, leading to localized (cellular micro-domain) redox cycling with GSH (Gammelgaard et al., 2003).

5.4.3 Manifestation of toxic effects

With a progressive shift of intracellular environment from reducing to oxidizing state, the macromolecular structures (proteins, lipids and DNA) become susceptible to oxidative damage by free radicals. The peroxidation of membrane lipids (both the plasma membrane and organelles membranes) often results in leaky membrane, leading to perturbation of intracellular ionic homeostasis. In this regard, the loss of intracellular calcium ($[Ca^{2+}]_i$) homeostasis is one of the major changes that determines the ultimate fate of the cells. Increased lipid peroxidation in the present experimental system was an indication of membrane damage, possibly due to the selenomethionine-induced increase in intracellular ROS generation (Misra et al., 2010). In addition, an associated increase in $[Ca^{2+}]_i$ level was observed at the highest selenomethionine exposure dose, which was probably a consequence of ROS-induced membrane damage. Previous observation with rat hepatocytes supports such hypothesis that oxidative stress can lead to a progressive increase in $[Ca^{2+}]_i$ in a dose-dependent manner (Nicotera et al., 1988), although the magnitude of increase in $[Ca^{2+}]_i$ depends on the extent of the oxidative damage. Elevated intracellular $[Ca^{2+}]_i$ is known to activate some phospholipases that also induce membrane damage (Dong *et al.*, 2006). It is important to note here though that apart from the oxidative damage, the modulation of signal transduction pathways associated with the regulation of $[Ca^{2+}]_i$ may also be involved in SeMet-induced increase in $[Ca^{2+}]_i$ (Dong *et al.*, 2006).

Because of the lack of any significant smearing pattern of DNA, any possible selenomethionine-induced damage of genomic DNA cannot be suggested in the present study. This is consistent with previous observation suggesting selenomethionine has a limited ability to induce DNA damage relative to selenite (Letavayová et al., 2006). In the previous experiment, selenite has been found to cause extensive DNA damage in trout hepatocytes at a much lower selenium exposure dose, compared to this study (see Appendix, Figure C4S3). However, an increased caspase 3/7 activity at the highest selenomethionine exposure dose suggests initiation of the apoptotic pathway of cell death. It is suggested here that two different mechanisms might be involved in this process: (i) the progression of apoptotic signalling cascades directly triggered

by elevated ROS generation, resulting in the activation of caspase 3/7 (Zhuang et al., 2001), and (ii) increased $[Ca^{2+}]_i$ leading to the initiation of apoptotic signalling (Rong and Distelhorst, 2008). Morphological features of cells as revealed by scanning electron microscopy also support the proposition of apoptotic cell death in the present study. Elevation of cytosolic calcium and apoptotic/aponecrotic cell death have also been observed in human erythrocytes (Sopjani et al., 2008) as well as in trout hepatocytes (see Appendix, Figures C4S2 and C4S4), following exposure to selenite. At 500 and 1000µM selenomethionine exposure doses, an obvious increase in ruffled plasma membrane represents morphological change typically associated with cells undergoing apoptosis (Van Cruchten and Van Den Broeck, 2002). Such changes in the cellular morphology might have occurred due to the increased $[Ca^{2+}]_i$, since it has been reported earlier that increased $[Ca^{2+}]_i$ is associated with the loss of cytoskeletal structures such as the fragmentation of F-actin fibre, destabilization of microtubules, and detachment of the cytoskeleton from the plasma membrane (Dong et al., 2006).

It has been suggested that during apoptotic cell death cellular content is not released (Elmore, 2007), so it was unexpected to observe increased LDH leakage into the media as a result of the apoptotic cell death. Should apoptosis be the only mechanism of cell death associated with selenomethionine exposure, why an increase in LDH leakage was observed at the highest exposure dose? It is important to note that these two processes are not mutually exclusive and can occur at the same time (Elmore, 2007). In addition, a clear distinction exists between the apoptotic cell death *in vivo* and *in vitro*. Under *in vivo* condition, phagocytes recognize apoptotic cells and subsequently engulf the dying cells (Van Cruchten and Van Den Broeck, 2002). However, the absence of phagocytes under *in vitro* culture condition often leads to necrotic death of those cells committed to apoptosis – a process described as aponecrosis (Formigli et al., 2000).

5.5 Conclusion

In conclusion, it was found that rainbow trout hepatocytes are quite tolerant against selenomethionine toxicity since the toxic effects (loss of cell viability and increased LDH leakage) were evident mostly at 1000µM. It appears that the redox cycling of selenomethionine

and its metabolite (methylselenol), facilitated by GSH, leads to the generation of ROS and subsequently triggers the induction of enzymatic antioxidants for the scavenging of ROS. However, selenomethionine exposure causes a marked dose-dependent decline in cellular thiol redox, and as a result the cells become susceptible to oxidative damage. Consequently, the cells suffer from membrane damage and disruption of $[Ca^{2+}]_i$ balance. Ultimately, when the selenomethionine-induced toxic insults impair the critical cellular structures and physiology beyond repair, the cells die probably *via* aponecrosis. Overall, the present study suggests that oxidative stress plays a major role in mediating the toxicity of selenomethionine in fish hepatocytes.

CHAPTER 6: Examination of *in vivo* accumulation and metabolism of dietary selenomethionine [5]

6.1 Introduction

Selenium is an essential micronutrient for vertebrates including fish. It is specifically incorporated into selenoproteins as selenocysteine, and these proteins are known to play a critical role in many vital physiological functions (e.g., free radical scavenging, thyroid metabolism, muscle function) (Lu and Holmgren, 2009). Fish selenoproteomes are the largest among all organisms including mammals (Lobanov et al., 2007), and therefore fish are an interesting model organism to study selenium homeostasis. Selenium has a narrow margin between essentiality and toxicity, and becomes toxic to fish at a slightly elevated level beyond the optimum intake. Fish require dietary concentrations of 0.1-0.5 μg $Se.g^{-1}$ (dry weight) to maintain their normal growth and physiological functions, however selenium rapidly bioaccumulates and causes toxicity to fish when the dietary concentration reaches ≥3.0 μg $Se.g^{-1}$ (dry weight) (Hamilton, 2004; Lemly, 1997). Due to the increasing anthropogenic contamination of selenium into the aquatic ecosystems, feral fish populations are often exposed to diet that contains elevated and/or toxic level of selenium (Lemly, 1999; Lemly, 2002).

Although fish can accumulate selenium *via* both water and diet, diet is considered to be the primary exposure route of selenium in the natural environment (Janz et al., 2010). Environmental selenium exists in inorganic (e.g., selenite, selenite) and organic (e.g., selenomethionine, selenocysteine) forms, with selenomethionine being the predominant form of selenium in natural fish diet (Andrahennadi et al., 2007; Fan et al., 2002; Maher et al., 2010). Selenomethionine has higher bioavailability and trophic transfer properties compared to other forms of selenium (Besser et al., 1993; Fan et al., 2002), and thus exposure to elevated dietary selenomethionine leads to a rapid increase in selenium body burden in fish (Besser et al., 1993).

---

[5] This chapter of the thesis will be communicated for publication under joint authorship with Chamain Hamilton, Ning Chen (Canadian Light Source), Derek Peak and Som Niyogi (University of Saskatchewan)..

It has been demonstrated that liver and muscle selenium concentrations increase markedly in fish following dietary supplementation of selenomethionine (Lorentzen et al., 1994), however the examination of selenium accumulation in other major tissues may also be useful in understanding selenomethionine handling and toxicity in fish.

The metabolism of selenium differs based on its chemical forms and oxidation states. Therefore, the characterization of selenium speciation in tissues may help to better understand the metabolic fate of selenium in fish exposed to selenomethionine. Using X-ray absorption near edge spectroscopy (XANES), recent field-based investigations have reported that selenium in fish exists mainly as selenomethionine and selenocystine, with selenomethionine being more abundant with increasing selenium exposure level (Phibbs et al., 2011a; Phibbs et al., 2011b). Although tissue-specific selenium speciation was not examined in these studies, the whole-body profile of selenium speciation was more or less consistent with our previous *in vitro* observation that selenomethionine and selenocystine are the predominant selenium species in fish hepatocytes exposed to selenomethionine (Misra et al., 2010). Nevertheless, it is important to note here that tissue-specific differences in selenium metabolism have been observed in rats treated with selenomethionine (Suzuki et al., 2006a), which is likely to produce a distinctive selenium speciation profile in different tissues. With this perspective in view, the present study was designed: (i) to conduct a comprehensive analysis of tissue-specific selenium accumulation in fish chronically exposed to dietary selenomethionine; and (ii) to characterize tissue-specific differences in selenium metabolism and speciation in fish.

6.2 Materials and methods

6.2.1 Chemicals

High purity Se compounds [elemental selenium (≥99%), sodium selenite (98%), sodium selenate (98%), L-selenomethionine (≥98%), Se-(Methyl)-selenocysteine hydrochloride (≥95%), selenocystine (≥98%), and selenium standard and palladium (sample matrix modifier) for atomic

absorption spectrometry] were obtained from Sigma-Aldrich, Mississauga, Canada. All other chemicals were purchased from Sigma-Aldrich, St Louis, USA, unless mentioned otherwise.

6.2.2 Fish

Juvenile rainbow trout (*Oncorhynchus mykiss*) weighing 200–300 g were obtained from the Lucky Lake Fish Farm, Saskatchewan, Canada. Fish were maintained in 1000 l flow-through aquaria receiving dechlorinated Saskatoon City water at a rate of 2 l/min under constant aeration. A photoperiod of 16 h light: 8 h dark and a water temperature of 15 ± 1°C were maintained throughout the experimental period. Fish were fed once daily with the commercial trout chow (Martin Mills Inc., Elmira, Canada) at a ration of 2% body weight. All fish were acclimated for at least 2 weeks prior to their use in the experiments. The experimental protocol was in accordance with the Canadian Council for Animal Care Guidelines and was approved by the animal research ethics board at the University of Saskatchewan.

6.2.3 Diet preparation and feeding trial

The experimental diets were prepared from the same commercial trout chow used to feed the fish during acclimation. The trout chow was ground into fine particles using a blender, and the ground feed was freeze-dried (Labconco Freezone, USA) until all the moisture was removed. A fraction of the dried feed was mixed homogenously with L-selenomethionine to achieve a nominal total selenium concentration of ~ 40 $\mu g.g^{-1}$. This mixture was used to prepare a dough, which was then passed through a hand-pelletizer to make feed pellets. The pellets were freeze-dried until a stable weight was obtained. The control feed was prepared following the same procedure except that no L-selenomethionine was added. The total selenium concentration in the experimental diets was measured using the graphite furnace atomic absorption spectroscopy (GFAAS) (See below for details), and the measured concentrations of selenium in the control and selenomethionine-spiked diets were 00.63±0.02 and 39.03±1.72 $\mu g\ Se.g^{-1}$ (dry weight, n=3 for both), respectively.

A total of 12 fish were equally divided into two 1000 l experimental tanks, with each tank divided into 3 equal chambers containing 2 fish each (i.e., 3 replicates per treatment). A week prior to the beginning of the experiment, fish in both treatments were introduced to the experimental control diet at a daily single ration of 2% of body weight. On day 1 of the experimental feeding trial, fish in one of the experimental tanks were introduced to the L-selenomethionine-spiked diet, and fish in the other tank were continued on the control diet. The experimental feeding was conducted at the same ration for 2-weeks. Any uneaten feed was siphoned out of the tank daily 3 h post-feeding.

6.2.4 Sampling procedure

Fish were not fed 24 h prior to the sampling. For the analysis of selenium speciation in tissues by XANES, the individual fish was first anaesthetized using an overdose of MS-222 (0.5 g/L). The ventral side was cut open, and the blood was collected directly from the heart. The collected blood sample was kept on ice to separate serum and red blood cells (RBC). Subsequent sampling technique was designed to minimize the blood contamination in all of the tissue samples used for XANES spectroscopy analysis (See below for details), in order to reduce any potential confounding contribution of selenium species present in the blood. To achieve this, the hepatic portal vein was cannulated with a PE-50 tubing following collection of the blood, and perfused with ice-cold modified Hank's media using a peristaltic pump. Silicone tubing connected with a 22-gauge needle was used to remove the perfusate from the heart, receiving Hank's media and blood from other parts of the body. The perfusion was continued until the liver and gill were completely blanched, although it was not possible to remove all the blood from kidney using this procedure. Therefore, the kidney tissue was sliced with a razor blade on its surface and washed several times with Hank's media to remove the blood as much as possible. The gonad tissues were collected after carefully removing the surface blood vessels. To collect muscle samples, skin on the upper left dorsal side was removed and tissue samples were surgically removed. All of the tissue samples were sliced into small pieces except the gonad samples, which were already small in size. These samples were freeze-dried in liquid N_2 and transferred into the specific sample holders for XANES analysis. The sample holders were then

wrapped with Kapton tape and stored at -80°C until their analysis. No glycerol was added to the tissue samples due to concerns about the detection limits.

For the analysis of tissue-specific total selenium body burden, fish were anaesthetized and the blood was collected to separate serum and RBC as described previously. Subsequently, all of the other major tissues (gill, liver, kidney, muscle, anterior and posterior intestine, stomach, spleen, gonads and brain) were dissected out and stored at -20°C.

6.2.5 Selenium XANES spectroscopy

Selenium K-Edge XANES data were collected at Hard X-ray for Microanalysis (HXMA) beamline available at the Canadian Light Source (CLS) in Saskatoon, SK, Canada. Due to the limited availability of beam time, the XANES analysis was conducted in different tissues collected only from selenomethionine-exposed fish. For all of the samples, data were collected at 2.9 GeV in fluorescence mode using either a single channel Vortex detector for the aqueous standards or a 30 element Ge detector (Canberra, Meriden, USA) for the tissue samples. The beamline was calibrated to the selenium K-Edge by setting the first derivative of an elemental selenium standard to 12658 eV. This elemental selenium reference remained behind the sample chamber for all of the data collection to ensure that the calibration could be continuously monitored and corrected if necessary. Data were collected from -100 to +50 eV relative to the selenium K-Edge using 0.2 eV steps, and multiple scans were averaged to obtain a suitable signal to noise ratio for further analysis.

6.2.6 Total selenium analysis

The experimental diets and frozen tissue samples were thawed at room temperature, weighed and transferred into borosilicate glass vials with polypropylene screw (Metal free, EPA certified, VWR, Canada). The samples were digested using concentrated nitric acid (15.8 N; in 1:5 tissue weight to acid volume ratio) (Ultrapure, Merck, Canada) overnight at 60°C following the modified method of Ari et al. (1991). The total selenium concentration in the sample digests

was measured after appropriate dilutions using the GFAAS (AAnalyst 800, Perkin Elmer, USA). The quality control and quality assurance of the analytical method were maintained by using a certified selenium standard and the standard addition and recovery procedure. The recovery of selenium in samples ranged between 88.43 to 106.41%. The detection limit of the total selenium analysis protocol used in this study was 1 ppb.

6.2.7 Data analyses

For XANES spectroscopy, data reduction and analysis were performed using the WINXAS 3.1 software. Scans were averaged with energy adjustments performed automatically *via* the internal reference channel, background corrected by subtracting a linear baseline from 12.56 to 12.63 keV, and normalized to an edge step of 1.0 over a range of 12.62 to 12.69 keV. Linear Combination XANES fits were performed on normalized spectra over the 12.56 to 12.69 keV region using 2 passes, the first with both % contribution and E_0 values were allowed to vary, and a second run where E_0 shift was fixed to zero. Significant differences among the tissue selenium accumulation data were analyzed by student's t-test or Mann-Whitney Rank Sum Test, as appropriate (SigmaPlot 11, Systat Software, Inc., USA). All the graphs were created using OrginPro 8.1 (OriginLab Corporation, USA).

6.3 Results

Reduced feed intake was observed during the second week of the exposure in fish treated with selenomethionine-spiked diet (data not shown). There was no mortality among the control fish, however one fish died on the 10^{th} day of the exposure in the selenomethionine treated group.

Figure 6.1 shows selenium K-Edge XANES spectra of several relevant aqueous selenium standard compounds and the solid elemental selenium standard. The main peak is due to the 1s → 4p transition which systematically shifted to higher energies as oxidation state of selenium changes from reduced to oxidized species. However, differences in the shape and position of the main peak within the organo-selenium standards may also occur due to differences in chemical

bonding environment of selenium. This has been reported previously (Pickering et al., 1995; Ryser et al., 2005), and selenium XANES spectral differences in peak positions and line shapes have been shown to be significant enough to allow the quantitative analysis of selenium speciation in similar experimental samples (Andrahennadi et al., 2007; Misra et al., 2010; Phibbs et al., 2011a; Phibbs et al., 2011b). The XANES spectra of the standard organo-selenium compounds (Figure 6.1) appeared to be consistent with those reported in previous studies (Andrahennadi et al., 2007; Pickering et al., 1995; Ryser et al., 2005), and there was no evidence of any sample oxidation that could affect the use of these standard spectra in quantitative analysis.

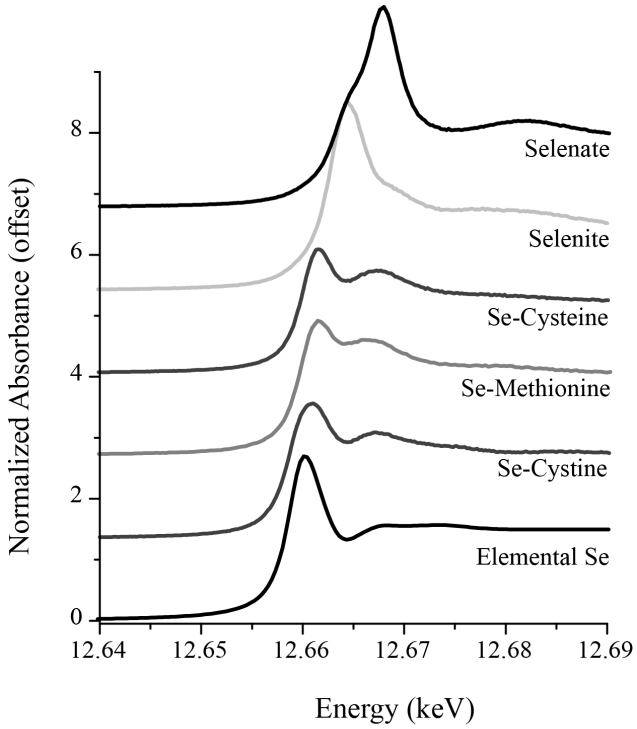

Figure 6.1: Representative X-ray absorption near edge spectroscopy (XANES) spectra of different selenium compounds used as standards in this study.

The results of linear combination fitting of the standard compounds to the selenium XANES spectra obtained from different tissues of selenomethionine-exposed fish are shown in Figure 6.2. For all of the tissue samples except liver, the best fits were obtained by using a combination of selenocystine, selenocysteine, and selenomethionine (Figure 6.2A-E). In contrast, only selenomethionine and selenocystine spectra were needed to achieve the best fit of data obtained from the liver (Figure 6.2A). For the muscle sample (Figure 6.2E), the higher energy portion of the spectrum could only be reconciled by the addition of selenate (albeit a small fraction of 10%) to the standards. It is unclear whether the presence of selenate (+6 oxidation state) is due to the oxidation of some other forms of selenium in the presence of the beam, or whether this is a metabolically relevant species of selenium in the muscle. Interestingly, selenocysteine fraction was about 32-33% of total selenium in the gonads and muscles, whereas it was only about 13-15% in the gill and kidney. Selenomethionine and selenocystine were present in relatively greater amounts (≥30%) in all of the tissues (Figure 6.3). This was particularly prominent in the liver, where selenocysteine was not required to fit the data. The fitting performed for the gonad did not seem to provide a 100% resolution with the available standard spectra; nevertheless the data seemed to fit reasonably well with a few different ratios of the three organic selenium compounds tested. This might imply that either the 3 component fit for the gonad is somewhat over-parameterized, or since all 3 components are present in 20-40%, it has greater error for any one of the components.

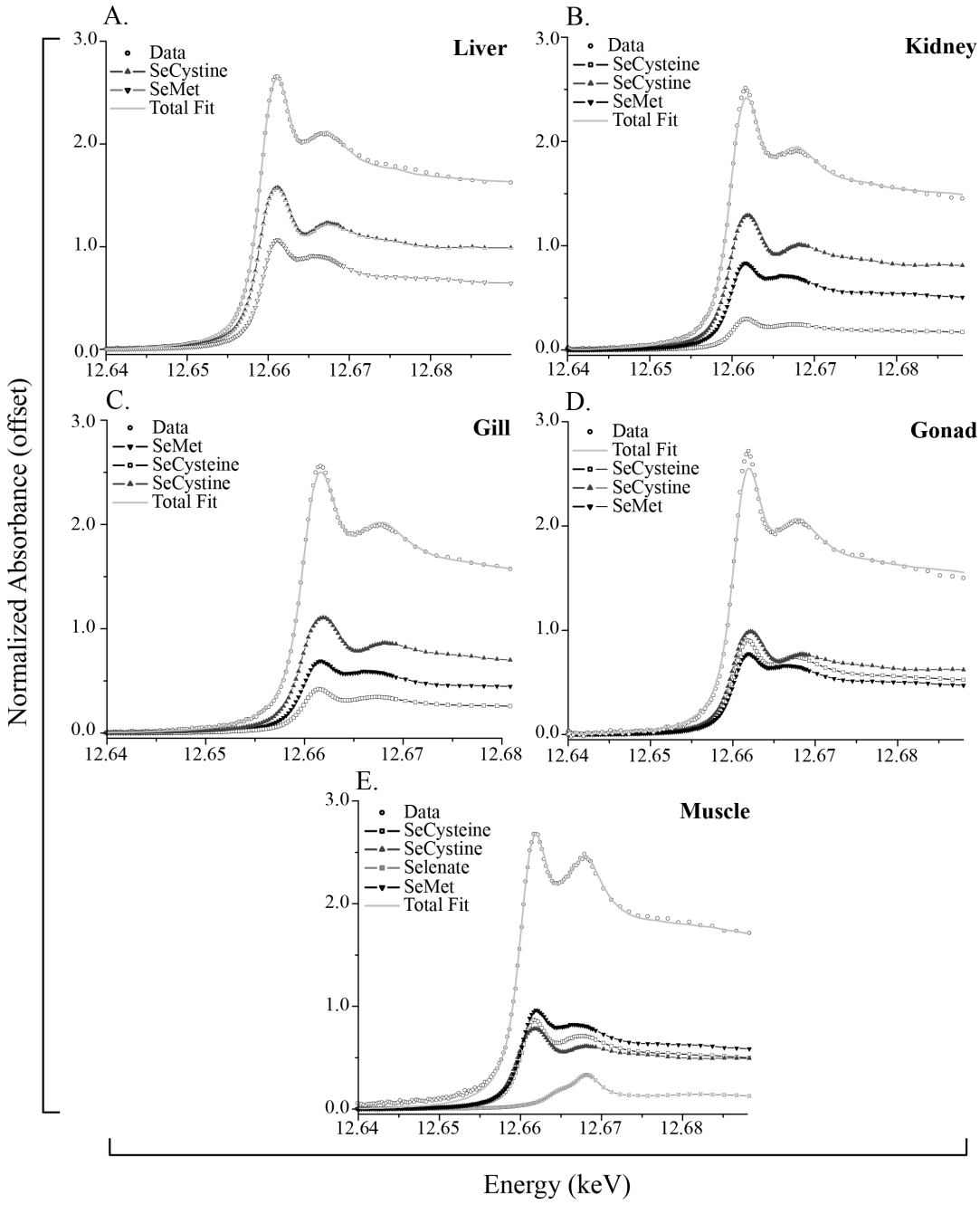

Figure 6.2: X-ray absorption near edge spectroscopy (XANES) spectra showing the raw data and fitted results for liver (Figure 6.2A), kidney (Figure 6.2B), gill (Figure 6.2C), gonad (Figure 6.2D) and muscle tissue (Figure 6.2E), obtained from rainbow trout exposed to dietary L-selenomethionine (40 µg $Se.g^{-1}$ dry weight) for 2 weeks (n=2 for each sample). The combinations of standards that provided the best fitting are included in each data plot.

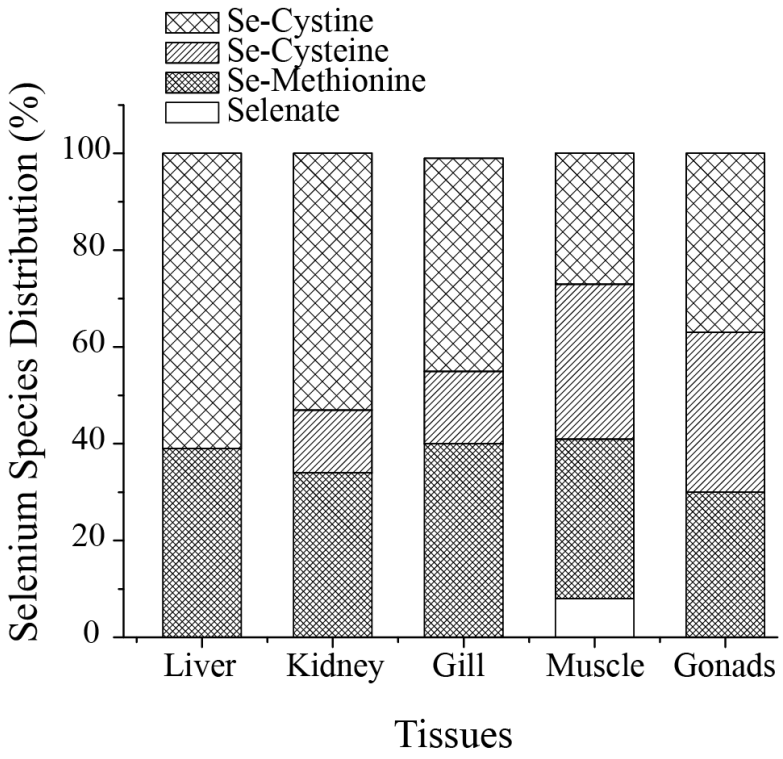

Figure 6.3: Relative fraction of different selenium species as a percentage of total selenium in different tissues of rainbow trout exposed to dietary L-selenomethionine (40 µg $Se.g^{-1}$ dry weight) for 2 weeks.

Figure 6.4 presents the tissue-specific accumulation of total selenium in the control and selenomethionine exposed fish. In the control fish, highest selenium concentration was recorded in the liver. The selenium burden increased significantly in all of the tissues examined in fish treated with dietary selenomethionine. The maximum accumulation was recorded in the gastrointestinal tract (stomach, anterior and posterior intestine), which was followed by the gonad, liver and brain. Interestingly, the tissues with higher total selenium burden tended to have a higher percentage of selenocystine (Figure 6.5).

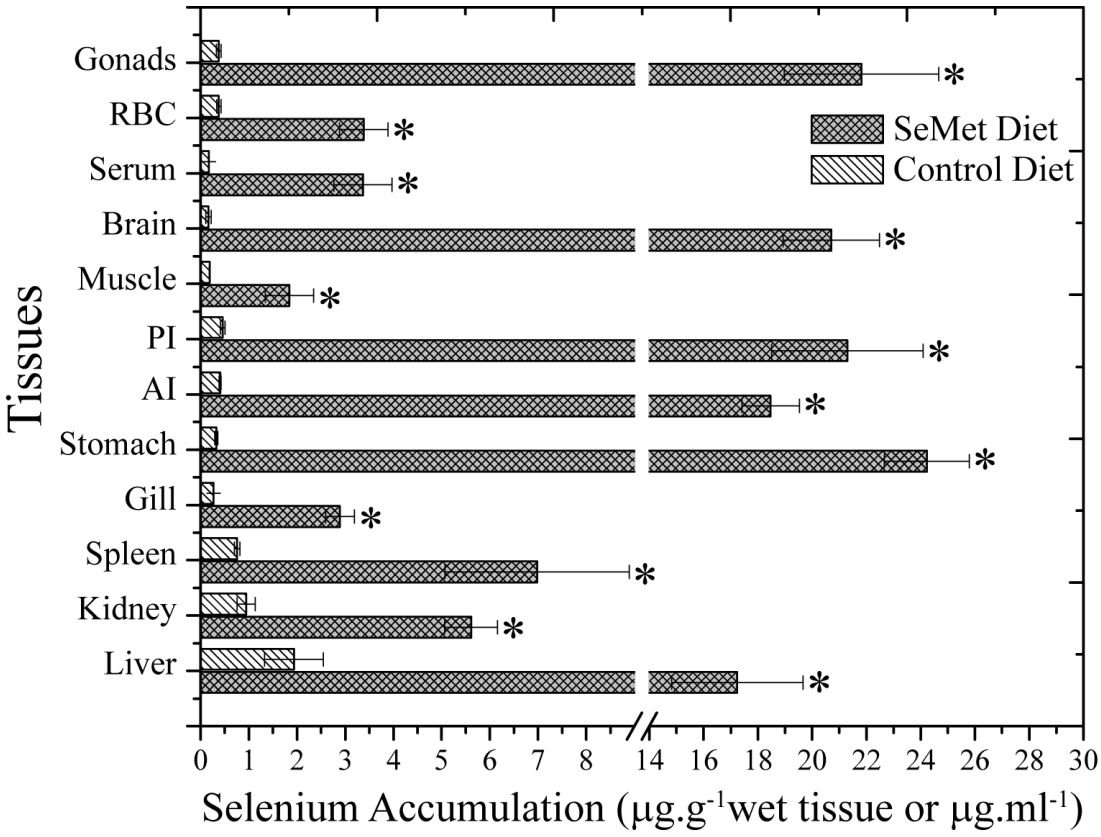

Figure 6.4: Tissue-specific accumulation of selenium in the control and dietary selenomethionine exposed rainbow trout (40 μg $Se.g^{-1}$ dry weight) for 2 weeks. Data from the control and selenomethionine treatment groups were compared using student's t-test or Mann-Whitney Rank Sum Test, as appropriate. Data are presented as mean ± S.E.M. (n=5-6), and significant differences ($p \leq 0.05$) are indicated by the asterisk. The data for serum and RBC are expressed as μg Se. ml^{-1}, and the data for rest of the tissues are presented as μg Se. g^{-1} wet tissue. The abbreviations AI and PI indicate the anterior and posterior intestine, respectively.

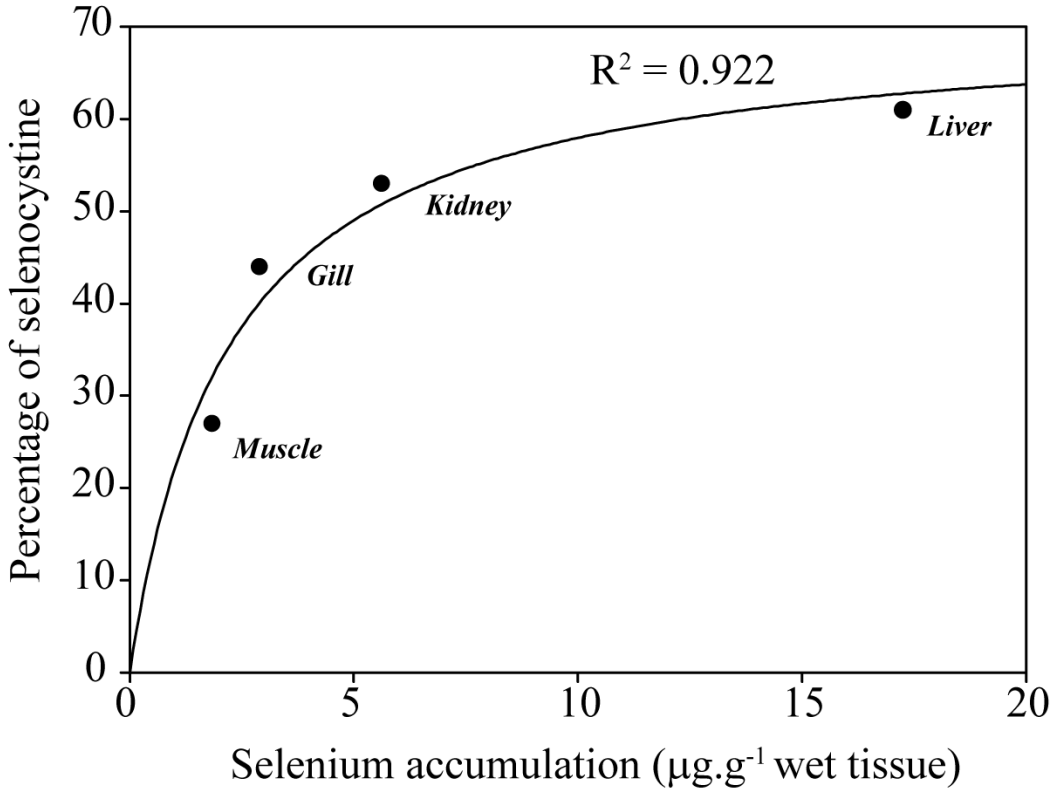

Figure 6.5: Relationship between the total selenium accumulation (wet weight) and percentage of selenocystine in different tissues obtained from fish exposed to dietary selenomethionine (40 µg $Se.g^{-1}$ dry weight) for 2 weeks. The data were plotted by using the ligand binding, one site saturation model in Sigmaplot 11.

6.4 Discussion

A relatively high exposure level of selenium was used in the present study to achieve sufficient selenium accumulation in the target tissues, since it is crucial in obtaining high resolution XANES spectra for the quantitative estimation of selenium speciation. Nevertheless, the selenium exposure level used in this study was comparable to the environmental selenium exposure level recorded in contaminated aquatic systems (Luoma and Presser, 2006).

The present study showed that it is possible to precisely compare the tissue-specific metabolism of selenomethionine using XANES spectroscopy. The obvious tissue-specific differences in the selenium metabolite profile suggest that selenium is handled differently in different tissues. Selenocysteine was found to be present in all of the tissues other than the liver, although its fraction in the excretory tissues (gills and kidney) was about half of that recorded in the muscle and gonads tissues. The fraction of selenomethionine in all the tissues was within the range of 30-40%, with the highest amount being found in the gill. Muscle was the only tissue that showed traces of inorganic form of selenium (selenate). The presence of selenomethionine in the tissues has been reported in previous *in vivo* studies on selenium exposure with rat (Suzuki et al., 2006a) and fish (Phibbs et al., 2011a; Phibbs et al., 2011b) as well as *in vitro* studies with cancer cells lines (Lunøe et al., 2011; Weekley et al., 2011). In our previous experiment, a significant fraction of selenomethionine was also found in rainbow trout hepatocytes exposed to selenomethionine (Misra et al., 2010). All of these observations lead to a common inference that the metabolism of selenomethionine is a relatively slow process.

In mammals, selenomethionine is absorbed and metabolized like its sulphur-analog methionine, and is incorporated into proteins as selenomethionine. The rapid bioaccumulation of high amount of selenomethionine has been observed previously in fish (Maher et al., 2010). Once inside the cell, selenomethionine can be metabolized *via* the *trans*-sulfuration pathway during normal nutritional regime for selenoprotein synthesis (Okuno et al., 2001). However, when the exposure is at a high and potentially toxic level, redox cycling of selenomethionine with glutathione can produce selenomethionine-selenoxide, which is subsequently reduced back to selenomethionine by the intracellular reducing agents such as glutathione, cysteine and

ascorbic acids (Schlenk et al., 2003; Krause and Elfarra, 2009). Alternatively, selenomethionine can be converted to methylselenol through the direct catalysis by the enzyme methionine-γ-lyase (methioninase) (Okuno et al., 2001; Palace et al., 2004; Misra et al., 2010). The latter pathway is considered to become more predominant at a high selenomethionine exposure level (Okuno et al., 2001), and might have played a role in selenomethionine metabolism in trout in the present study. However, with the sampling technique used in the present study, it was not possible to detect any volatile selenium metabolite such as methylselenol in the samples. It was also not clear whether the fraction of selenomethionine detected in the samples was incorporated into the protein structure by methionine replacement or present in the free form. The possibility that all of the selenomethionine was protein bound seems unlikely as the tissue-specific selenium accumulation was too high for that to occur. Interestingly, free selenomethionine has been detected in several tissues of rat using the HPLC-ICPMS technique following an oral administration of selenomethionine (Suzuki et al., 2006a). This observation also supports the argument that a significant fraction of selenomethionine detected in the analyzed samples was probably in its free form.

In the present study, it was observed that all the tissues contained a high amount of selenocystine, ranging from 27-61%. In our previous study with trout hepatocytes exposed to selenomethionine, selenocystine was found to be one of the major components of total selenium (Misra et al., 2010). In the present study, significant fraction of selenocystine in all of the major tissues indicates that selenomethionine was metabolized *via* the *trans*-sulfuration pathway, at least partially, in trout. In this pathway, selenomethionine is metabolized into methyl-selenol *via* an intermediate metabolite, selenocysteine. However, the instability of selenocysteine probably leads to its oxidative conversion into more stable selenocystine (Beld et al., 2007). The fraction of selenocystine correlated well to the total selenium concentration in the liver, kidney, gill and muscle in fish exposed to dietary selenomethionine, although no such trend was found in the gonad tissue. Liver synthesizes selenoprotein P, in which selenium remains in its reduced form of selenocysteine, and thus the absence of selenocysteine in the liver in this study was surprising. However, in such a metabolically active tissue, potential oxidation of the selenol moiety in selenoproteins by selenomethionine-induced generation of the reactive oxygen species is possible (Misra et al., 2010).

The tissue-specific selenium accumulation data in selenomethionine exposed fish showed that selenium is distributed across various tissues in different proportions. All sections of the gastrointestinal tract (stomach as well as intestinal segments) accumulated a very high amount of selenium relative to other tissues. In the stomach, selenium accumulation was about 75 times higher than the control, whereas it was about 45 times higher in the anterior and posterior intestine. Such high distribution of selenium in the gastrointestinal tissue suggests that this epithelium probably acts as a barrier and regulates selenomethionine absorption during elevated exposure regime. Unlike a previous observation in white sturgeon (Tashjian et al., 2006), the total selenium level in the kidney was much lower than that in the liver in the present study. Interestingly, the brain accumulated as much selenium as the liver in fish treated with elevated dietary selenomethionine. This observation suggests that an efficient physiological mechanism exists by which selenium absorbed as selenomethionine can be transported to the brain across the blood-brain barrier. This is consistent with the previous observation that selenium accumulation in the rat brain was about 10-fold higher when the diet was supplemented with selenomethionine as opposed to selenite (both at a concentration of 4.0µg $Se.g^{-1}$ diet) (Whanger and Butler, 1988). Watanabe and Satoh (1994) demonstrated that selenium deficiency can alter the behaviour in mice, however it remains to be investigated whether exposure to high dietary selenomethionine can affect the behaviour in fish. It is interesting to note here Thomas and Janz (2011) recently reported altered swimming behaviour in fish exposed to environmentally relevant dietary selenomethionine, although they argued that it was a consequence of elevated stress response.

Overall, the present study demonstrated that the exposure to elevated dietary selenomethionine causes significant accumulation of selenium in almost all of the vital organs in fish including the brain. It also indicated for the first time that the selenomethionine is metabolized differentially across the major organs in fish, resulting into a tissue-specific pattern of selenium speciation. These findings have important implications for understanding the effects of environmental selenium exposure in feral fish populations.

GENERAL DISCUSSION

7.1 Introduction

Selenium contamination in the natural environment is becoming an emerging global problem (Lemly, 2004). Several reports have documented the consequences of increasing usage and release of selenium in the environment and subsequent toxic effects to resident biota (Hamilton, 2004; Lemly, 1999; Luoma and Presser, 2009). In a recent book entitled "Metal Contamination in Aquatic Environments", Luoma and Rainbow (2008) stated that "for no other trace metal are regulatory approaches as globally incoherent as they are for selenium; and for no other metal do at least some regulations diverge more from the state of knowledge". Such a statement indicates that a great deal of work still needs to be done for bridging the gap between the science and regulation with respect to selenium. The selenium toxicology in aquatic animals is complex. Apart from the exposure routes and levels, diverse chemical speciation of selenium in nature is a major confounding factor in addressing its toxicity. To enhance our understanding of the cause and effect relationship between environmental selenium exposure and effects in biota, a comprehensive knowledge of chemical species-specific selenium uptake, handling and toxicity is required. Unlike many divalent metals, a certain waterborne selenium concentration is not applicable as a single major criterion for assessing toxicity (Hamilton, 2002). Rather, the tissue-specific (e.g., liver, gonads) selenium concentrations have been suggested to be a better predictor of toxicity to biota including fish (Hamilton, 2003). Liver is one of the major organs of selenium accumulation and also the primary site of selenium metabolism in fish, irrespective of the exposure route. Therefore, isolated hepatocytes (functional units of liver) were used as a useful experimental system for investigating the cellular basis of selenium toxicology in fish. It is important to note that toxic effects always initiate at the cellular level, and the integration of effects at multiple cell/tissue types eventually leads to the onset of systemic toxicity.

In the present thesis, *in vitro* experiments were designed to examine the transport, metabolism and toxicity of both inorganic (selenite) and organic selenium (selenomethionine) in fish. The transport experiments were carried out with selenite, while the metabolism and toxicity

studies were carried out with both selenite and selenomethionine. In addition, I examined the tissue-specific differences in selenium (selenomethionine) accumulation and metabolism in fish *in vivo*. In this chapter, the findings of the present work in its entirety have been discussed to explain their significance to the current state of knowledge on selenium exposure and toxicology in fish, along with constraint analysis and future perspectives. The major findings from each chapter of my project and their linkage are presented in a schematic diagram (Figure 7.1).

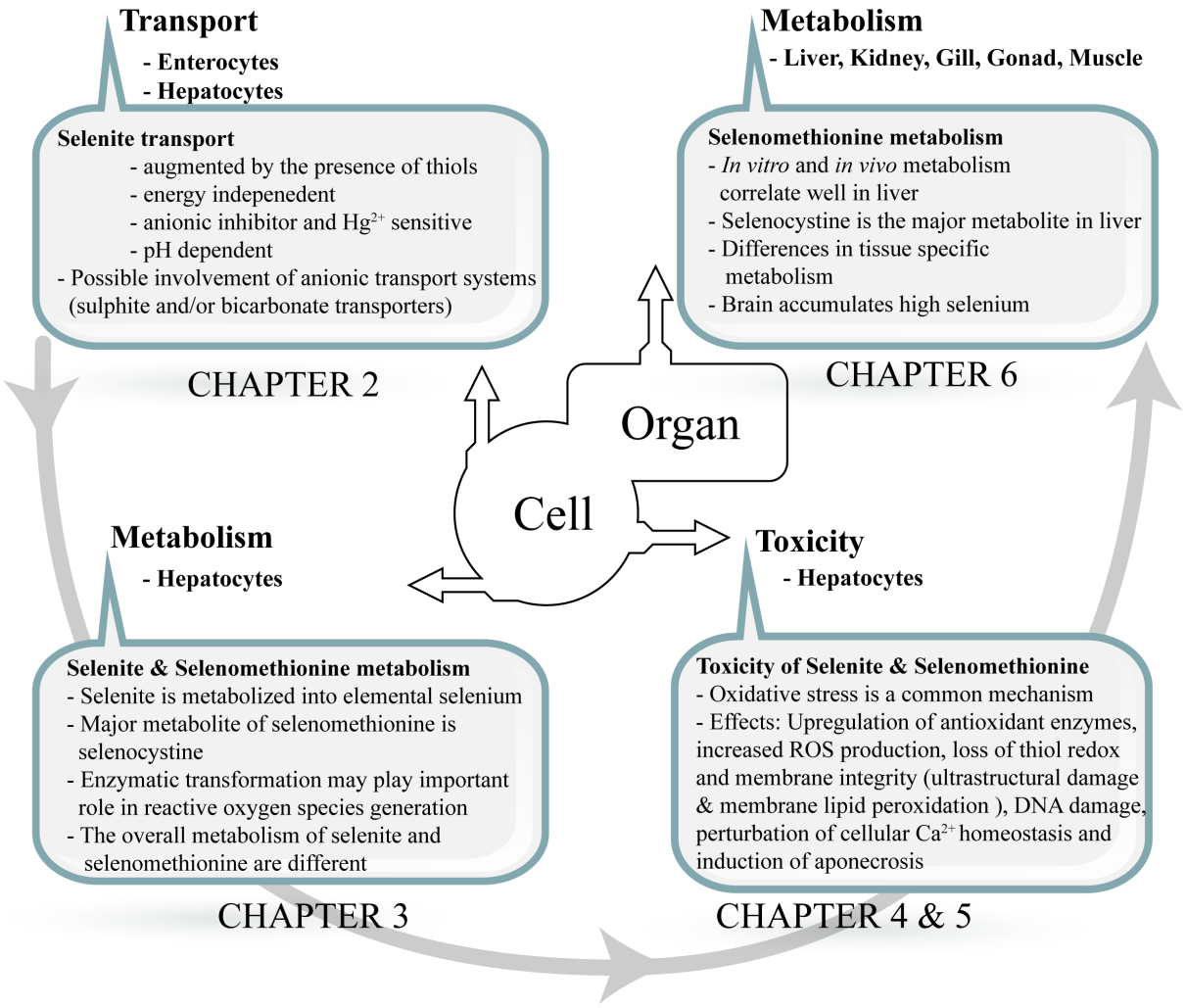

Figure 7.1: Schematic diagram showing the key findings of the present thesis and their linkage.

7.2 Selenium uptake in fish

Very little is known about the selenium uptake mechanisms in fish. It is likely that different transport systems are involved in the uptake of inorganic and organic selenium. Recently, Bakke et al. (2010) suggested that selenomethionine is absorbed by the methionine transporters in fish intestine. To my understanding, the present study is the first one to examine the transport systems involved in the uptake of selenite (the most toxic form of inorganic selenium in the environent) in fish. In general, the uptake of selenite in both enterocytes and hepatocytes of fish appears to be driven by the anionic transport systems (e.g., sulphate/sulphite transporters, bicarbonate transporters), which resembles the characteristics of selenite transport in mammals (Section 2.3.3). The uptake rate of selenite (accumulation/unit time) was higher in hepatocytes relative to that in enterocytes. The selenite transport process was found to be energy independent (Section 2.3.2). Interestingly, the uptake rate was markedly higher in both cell types in the presence of reducing thiols such as GSH and cysteine, suggesting that the reducing equivalents are of particular importance in the accumulation of selenium, when selenite is the chemical form of exposure (section 2.3.1). The magnitude of increase in selenium uptake was higher with cysteine in comparison to GSH. Such differences cannot be explained based on the findings of my study, however molecular size of the reaction products (that are taken up) of selenite and GSH or cysteine may be an important factor. Nevertheless, these findings can explain, at least in part, why liver is one of the major sites of selenium accumulation in fish. Selenium supplementation in the fish diet is a routine practice in commercial aquaculture, and my findings suggest that the use of selenite in conjunction with cysteine can be a cost-effective alternative of more expensive selenomethionine in this context.

The effects of extracellular pH were similar in both enterocytes and hepatocytes, and the uptake of selenite was significantly higher at acidic and circumneutral pH relative to that in alkaline pH (section 2.3.4). Assuming similar transport systems for selenite exist in fish gill epithelial cells as observed in enterocytes or hepatocytes, such observation suggests that selenite may become more bioavailable and toxic to fish in natural waters with relatively low pH. The interactions of selenite with inorganic mercury observed in my study have important implications as well (Section 2.3.5). In both cell types, extracellular Hg^{2+} inhibited selenite transport. In the

presence of GSH, the inhibitory effect remained persistent in enterocytes, whereas an increase in cellular selenium accumulation was found in hepatocytes. From a nutritional perspective, these findings imply that Hg^{2+} can limit the bioavailability of dietary selenium, although it is of marginal significance since selenite is not a major source of dietary selenium in fish. Nevertheless, the interactions of selenite and Hg^{2+} may have ameliorative effects against the waterborne selenite exposure in fish, and future investigations should focus on examining this hypothesis.

Selenium in the environment is mostly concentrated in the fish diet, primarily as selenomethionine; nevertheless selenium exposure *via* water in the form of selenite may still be important. The absorption of selenomethionine occurs in a pulsatile manner (following the digestion of a meal) in fish, and since the assimilation efficiency of selenomethionine is over 50% (Luoma and Rainbow, 2008), about half of the ingested amount is bioavailable. In contrast, the exposure to waterborne selenite *via* the gills is continuous, albeit at a relatively low exposure level, and may contribute a significant proportion to the total selenium body burden over longer exposure period.

7.3 Selenium metabolism and distribution in fish

The metabolism studies were designed to identify the major intermediate metabolites and enzymes associated with selenium biotransformation at cellular and organ level. This approach was an important consideration in linking the cellular transport and toxic effects of selenium in fish. In general, inorganic and organic selenium appeared to be metabolized through different cellular pathways. It was observed that both selenite and selenate were converted into elemental selenium within 6 h of exposure in hepatocytes (Section 3.3). Using XANES spectroscopy, this study provided first experimental evidence suggesting that elemental selenium can be formed intracellularly in fish. Consistent with my finding, Phibbs et al. (2011b) recently reported that elemental selenium can be found in whole fish when exposed to high environmental selenium. In contrast to selenite, selenomethionine metabolism was found to be a much slower process in hepatocytes, and selenocystine was recorded to be the major metabolite in this process. Since the only known pathway of selenocystine biosynthesis is the *trans*-sulfuration pathway, it is

hypothesized that this pathway plays a major role in selenomethionine metabolism in fish. However, my findings indicated that a different pathway exists that comes into play when the exposure concentration of selenomethionine is beyond the nutritional regime or at toxic level. This metabolic pathway involves a direct enzymatic (L-methionine-γ-lyase) catalysis of selenomethionine into methylselenol, which is implicated in redox cycling with GSH and consequent ROS generation. The methodology adopted in the present study provided an indirect evidence for the existence of such a pathway, and more sophisticated approach(es) are required to conclusively establish the role of this enzyme in different tissues of fish, to elucidate whether such transformation is specific to hepatic cells or a common occurrence across many different tissues.

The findings from my *in vivo* selenomethionine accumulation and metabolism study suggested that selenomethionine is distributed and handled differentially across different tissues (Section 6.3). Interestingly, the metabolic profile of selenomethionine exposure *in vivo* in liver validated my observation in hepatocytes, suggesting that selenocystine is the predominant hepatic metabolite of selenomethionine in fish. However, selenocysteine was found in varying proportion in the kidney, gill, muscle and gonad tissues and therefore suggesting obvious differences in the tissue-specific handling of selenomethionine. Phibbs et al. (2011b) have recently reported that the fraction of selenomethionine in the whole body correlates well with the total whole body selenium burden in feral fish exposed to elevated environmental selenium. Apart from selenomethionine, selenocystine was found to be the only other major selenium species in fish tissues (Phibbs et al., 2011b). Although a direct comparison of metabolic profile of selenium between my study and theirs is not practical since they have not examined tissue-specific differences, their results are somewhat similar to my study where selenocystine and selenomethionine were the two most abundant selenium species across all the different tissues examined. It is important to note here that distinct selenium metabolite profile across different tissue samples unravelled in the present work have important implications for understanding tissue-specific selenium toxicity in fish, especially those tissues with high selenocysteine/selenocystine content. This is because such metabolites are redox reactive and can generate ROS following redox cycling with cellular thiols.

Furthermore, one of the other important observations from the tissue-specific distribution of selenium is that brain accumulates a significant amount of selenium in fish exposed to elevated dietary selenomethionine (section 6.3). Since dietary selenomethionine is considered as the major source of selenium in many contaminated aquatic systems, similar consequences might also occur in feral fish and need to be investigated. Because of the ability of selenium to induce oxidative damage in tissues (discussed below), this might cause a broad range of physiological and behavioural effects in fish. Very high accumulation of selenium in the gut of fish exposed to dietary selenomethionine indicates that the gut might have some role in regulating selenium absorption. Since the gut epithelium undergoes a very rapid turnover, the sloughing of intestinal epithelial cells could be an efficient mechanism of selenium excretion in fish during elevated exposure.

7.4 Cellular basis of selenium toxicity in fish

The present study indicated that oxidative stress plays a major role in selenite and selenomethionine toxicity to fish hepatocytes, although the metabolic pathway that leads to the oxidative stress is different for each compound. Both selenite and selenomethionine were found to rapidly increase intracellular ROS generation (Section 4.3.4 and Section 3.3, respectively), and consequently an induction of enzymatic antioxidants (SOD, CAT and GPX) was recorded as a defensive cellular response (Sections 4.3.2 and 5.3.2, respectively). Interestingly, exposure to both selenite and selenomethionine resulted into a steady dose-dependent decrease in intracellular thiol redox (GSH to GSSG ratio) (Sections 4.3.3 and 5.3.3). In addition, exposure to both compounds caused membrane damage, disruption of intracellular calcium balance and DNA damage, which ultimately led to the loss of viability of a significant fraction of cell population *via* aponecrosis at the highest exposure dose examined (Chapters 4 and 5). It is important to note that all of these effects occurred at a 5-10 fold lower exposure dose with selenite compared to selenomethionine, suggesting that the latter is much less toxic to fish hepatocytes than the former. Similar observations have recently been reported in fish adrenocortical cells (Miller and Hontela, 2011) and mammalian hepatic cells (Hoefig et al., 2010). It is important to note here that GSH plays a key role in mediating the toxicity of both selenite and selenomethionine, since

it facilitates the intracellular ROS generation during exposure to these compounds, thereby acting as a prooxidant rather than an antioxidant. It is reasonable to suggest that GSH level could be a major determinant of cell/organ-specific sensitivity to selenium, and thus cells/tissues with higher GSH storage (e.g., hepatocytes/liver) are likely to be more susceptible to selenium toxicity relative to the cells/tissues with lower GSH level. In the same note, differences in GSH storage in the key organs can also explain, the species-specific differences in cytotoxicity of selenium in fish, at least partially, as recently suggested by Miller and Hontela (2011).

My study was designed to assess the mechanisms of selenium toxicity at the cellular level, and therefore the selenium exposure levels used were quite high. It would be difficult as well as unrealistic to extrapolate the implications of current findings to the population level or ecosystem level, since it is unlikely that fish in the natural environment will be exposed to such high levels of selenium. Nevertheless, I believe that an enhanced understanding of the mechanisms of selenium toxicity will help to identify cellular biomarkers (e.g., oxidative stress parameters) that can be employed to assess the health of selenium-impacted feral fish populations. Furthermore, the information generated in my study is also likely to be useful in understanding the influence of selenium speciation on its toxicity to fish. To date, the link between the oxidative stress and physiological consequences (e.g., stress response, fuel and ion homeostasis, metabolic capacity, swimming performance) has rarely been in fish during chronic exposure to selenium, either *via* water or diet. Janz et al. (2010) has recently highlighted the fact that understanding the role of oxidative stress in selenium toxicity has to be one of priority issues in the context of environmental toxicology of selenium, and my study is expected to provide some impetus for future research in that direction.

7.5 Research needs and recommendations

One of the key objectives of my thesis was to examine the properties of transport of selenite in the enterocytes and hepatocytes of fish. This investigation reveals that the cellular transport of selenite and its reduced forms are mainly mediated by anion transport systems. However, the characterization of specific transporters involved was beyond the scope of this investigation. Considering the diversity of anion transport systems in animal systems, future

investigations should focus on identifying the key transporters involved in this process. Similarly, methionine transporters have been implicated in selenomethionine transport in fish intestine (Bakke et al, 2010), however not all of the methionine transporters may have the same specificity for selenomethionine transport and future studies should examine this hypothesis.

My study has provided convincing evidence suggesting oxidative stress is the key mechanism of selenium (both inorganic and organic) toxicity at the cellular level, however it remains to be investigated to what extent that effect translates into adverse consequences at the higher level of biological organization (organismal and/or population). It is becoming increasingly clear that fish at their larval or juvenile stages are much more sensitive to selenium toxicity than at their adult state (reviewed by Janz et al., 2010). Larval deformities have often been reported as one of the common consequences of environmental selenium exposure to fish (Lemly, 1993b; Lemly, 2002; Muscatello et al., 2006). Holm et al. (2005) observed a significant relationship between the maternally transferred selenium in fish eggs and the incidence of developmental abnormalities in hatched embryos. The embryonic exposure mainly occurs from the maternal exposure, and it is likely that fish embryos are mainly exposed to organic forms of selenium (e.g., selenomethionine), which are transferred to the eggs from the liver during yolk formation. Palace et al. (2004) previously suggested that oxidative stress plays an important role in selenomethionine toxicity to fish embryos, however a direct cause-and effect relationship between oxidative stress and larval deformities has yet to be established.

At the early stages of embryonic development, cell death and differentiation play a critical role in subsequent organogenesis. During organogenesis, certain cells develop into their specific fate and are differentiated into different tissues and organs, while others die normally *via* apoptosis. The whole process is highly regulated in such a way that individual cells determine the eventual fate of the overall development process (Kipreos, 2005). Therefore, it is possible that selenium-induced oxidative stress can affect the developmental process of fish embryo by causing unintended death of cells that otherwise are important for proper development. Recent evidences also support the hypothesis that oxidative stress can cause teratogenesis (Dennery, 2007; Hansen, 2006). In addition, the structural integrity of tissues can also be affected by the disruption of events associated with cellular adhesion process (Gumbiner, 1996). The tissue

functionality depends on the complex interaction between the architectural components including collagen, matrix protein and cytoskeletal protein. Two very recent studies have indicated that selenium exposure can influence the structural integrity and functionality of tissues in mammalian systems. Raines and Sunde (2011) reported that exposure to dietary selenite results into the down regulation of extracellular matrix protein 1, collagen (Type XIV alpha) and gap junction protein genes in rat liver. Similarly, Zhang et al. (2011) demonstrated the down-regulation of myoglobin as well as heavy and light chain of myosin in skeletal muscles of mice following exposure to methylseleninic acid, Se-methylselenocysteine, selenomethionine and selenite. Future studies should examine whether selenium exposure can induce similar undesirable effects during the larval development of fish. This is an important issue for the risk assessment of selenium in aquatic ecosystems since disruption of larval development in any fish population would pose serious threat to its long-term sustainability.

LIST OF REFERENCES

Albrecht, R., Pélissier, M.A., and Boisset, M. (**1994**). Excessive dietary selenium decreases the vitamin A storage and the enzymatic antioxidant defence in the liver of rats. **Toxicol Lett** *70*, 291-297.

Andrahennadi, R., Wayland, M., and Pickering, I.J. (**2007**). Speciation of selenium in stream insects using X-ray absorption spectroscopy. **Environ Sci Technol** *41*, 7683-7687.

Anundi, I., Högberg, J., and Ståhl, A. (**1984**). Absorption of selenite in the rat small intestine: interactions with glutathione. **Acta Pharmacol Toxicol (Copenh)** *54*, 273-277.

Ardüser, F., Wolffram, S., Scharrer, E., and Schneider, B. (**1986**). Transport of selenate and selenite across the brush border membrane of rat and sheep small intestine. **Biol Trace Elem Res** *9*, 281-290.

Ari, U., Volkan, M., and Aras, N.K. (**1991**). Determination of selenium in diet by Zeeman effect graphite furnace atomic absorption spectrometry for calculation of daily dietary intakes. **J Agric Food Chem** *39*, 2180-2183.

Arteel, G.E., and Sies, H. (**2001**). The biochemistry of selenium and the glutathione system. **Environ Toxicol Pharmacol** *10*, 153-158.

Arthur, J.R., Nicol, F., and Beckett, G.J. (**1990**). Hepatic iodothyronine 5'-deiodinase. The role of selenium. **Biochem J** *272*, 537-540.

Babich, H., Martin-Alguacil, N., and Borenfreund, E. (**1989**). Arsenic-selenium interactions determined with cultured fish cells. **Toxicol Lett** *45*, 157-164.

Bakke, A.M., Tashjian, D.H., Wang, C.F., Lee, S.H., Bai, S.C., and Hung, S.S.O. (**2010**). Competition between selenomethionine and methionine absorption in the intestinal tract of green sturgeon (*Acipenser medirostris*). **Aquat Toxicol** *96*, 62-69.

Behne, D., Kyriakopoulos, A., Meinhold, H., and Kohrle, J. (**1990**). Identification of type I iodothyronine 5'-deiodinase as a selenoenzyme. **Biochem Biophys Res Commun** *173*, 1143-1149.

Beilstein, M.A., and Whanger, P.D. (**1987**). Metabolism of selenomethionine and effects of interacting compounds by mammalian cells in culture. **Journal of Inorganic Biochemistry** *29*, 137-152.

Beld, J., Woycechowsky, K.J., and Hilvert, D. (**2007**). Selenoglutathione: efficient oxidative protein folding by a diselenide. **Biochemistry (Mosc)** *46*, 5382-5390.

Berzelius, J.J. (**1818**). Lettre de, Berzelius à M Berthollet sur deux métaux nouveaux. **Annales De Chimie Et De Physique** *7*, 199-206.

Besser, J.M., Canfield, T.J., and La Point, T.W. (**1993**). Bioaccumulation of organic and inorganic selenium in a laboratory food chain. **Environ Toxicol Chem** *12*, 57-72.

Bradford, M.M. (**1976**). A rapid and sensitive method for the quantitation of microgram quantities of protein utilizing the principle of protein-dye binding. **Anal Biochem** *72*, 248-254.

Braunbeck, T., and Storch, V. (**1992**). Senescence of hepatocytes isolated from rainbow trout (*Oncorhynchus mykiss*) in primary culture. **Protoplasma** *170*, 138-159.

Brown, K., and Arthur, J. (**2001**). Selenium, selenoproteins and human health: a review. **Public health nutrition** *4*, 593-599.

Buhl, K.J., and Hamilton, S.J. (**1991**). Relative sensitivity of early life stages of arctic grayling, coho salmon, and rainbow trout to nine inorganics. **Ecotoxicol Environ Saf** *22*, 184-197.

Butterman, W.C., and Brown, R.D.J. (**2004**). Mineral commodity profile - Selenium (U.S. Department of Interior, U.S. Geological Survey), pp. 1-20.

Buttke, T.M., and Sandstrom, P.A. (**1994**). Oxidative stress as a mediator of apoptosis. **Immunol Today** *15*, 7-10.

Byers, H.G., and Lakin, H.W. (**1939**). Selenium in Canada. **Canadian Journal of Research** *17b*, 364-369.

Caffrey, P.B., and Frenkel, G.D. (**1992**). Selenite cytotoxicity in drug resistant and nonresistant human ovarian tumor cells. **Cancer Res** *52*, 4812-4816.

Cai, Y., Appelkvist, E.L., and DePierre, J.W. (**1995**). Hepatic oxidative stress and related defenses during treatment of mice with acetylsalicylic acid and other peroxisome proliferators. **J Biochem Toxicol** *10*, 87-94.

Campanucci, V.A., Krishnaswamy, A., and Cooper, E. (**2008**). Mitochondrial reactive oxygen species inactivate neuronal nicotinic acetylcholine receptors and induce long-term depression of fast nicotinic synaptic transmission. **J Neurosci** *28*, 1733-1744.

Celik, H.A., Aydin, H.H., Deveci, R., Terzioglu, E., Karacali, S., Saydam, G., Akarca, U., and Batur, Y. (**2004**). Biochemical and morphological characteristics of selenite-induced apoptosis in human hepatoma Hep G2 cells. **Biol Trace Elem Res** *99*, 27-39.

Chaudiere, J., Courtin, O., and Leclaire, J. (**1992**). Glutathione oxidase activity of selenocystamine: a mechanistic study. **Arch Biochem Biophys** *296*, 328-336.

Chen, C., Zhang, P., Hou, X., and Chai, Z. (**1999**). Investigation of selenium distribution in subcellular fractions of human liver by neutron activation analysis. **Biol Trace Elem Res** *71-72*, 131-138.

Cotter, P.A., Craig, S.R., and McLean, E. (**2008**). Hyperaccumulation of selenium in hybrid striped bass: a functional food for aquaculture? **Aquacult Nutr** *14*, 215-222.

Coughlan, D.J., and Velte, J.S. (**1989**). Dietary toxicity of selenium-contaminated red shiners to striped bass. **Trans Am Fish Soc** *118*, 400-408.

Crompton, M., Palmieri, F., Capano, M., and Quagliariello, E. (**1974**). The transport of sulphate and sulphite in rat liver mitochondria. **Biochemical Journal** *142*, 127.

Deleve, L.D., and Kaplowitz, N. (**1990**). Importance and Regulation of Hepatic Glutathione. **Semin Liver Dis** *10*, 251,266.

Dennery, P.A. (**2007**). Effects of oxidative stress on embryonic development. **Birth Defects Res C Embryo Today Rev** *81*, 155-162.

Diplock, A.T. (**1976**). Metabolic aspects of selenium action and toxicity. **CRC Crit Rev Toxicol** *4*, 271-329.

Dong, Z., Saikumar, P., Weinberg, J.M., and Venkatachalam, M.A. (**2006**). Calcium in cell injury and death. **Annual Review of Pathology: Mechanisms of Disease** *1*, 405-434.

Dudley, H.C. (**1936a**). Toxicology of selenium. I. A study of the distribution of selenium in acute and chronic cases of selenium poisoning. **Am J Epidemiol** *23*, 169-180.

Dudley, H.C. (**1936b**). Toxicology of selenium. II. The urinary excretion of selenium. **Am J Epidemiol** *23*, 181-186.

Ellis, M., Motley, H., Ellis, M., and Jones, R. (**1937**). Selenium poisoning in fishes. **Proc Soc Exp Biol Med** *36*, 519-522.

Elmore, S. (**2007**). Apoptosis: A Review of Programmed Cell Death. **Toxicol Pathol** *35*, 495.

Esaki, N., Nakamura, T., Tanaka, H., and Soda, K. (**1982**). Selenocysteine lyase, a novel enzyme that specifically acts on selenocysteine. Mammalian distribution and purification and properties of pig liver enzyme. **J Biol Chem** *257*, 4386-4391.

Fan, T.W.M., Teh, S.J., Hinton, D.E., and Higashi, R.M. (**2002**). Selenium biotransformations into proteinaceous forms by foodweb organisms of selenium-laden drainage waters in California. **Aquat Toxicol** *57*, 65-84.

Flohé, L., Gunzler, W.A., and Schock, H.H. (**1973**). Glutathione peroxidase: a selenoenzyme. **FEBS Lett** *32*, 132-134.

Formigli, L., Papucci, L., Tani, A., Schiavone, N., Tempestini, A., Orlandini, G., Capaccioli, S., and Zecchi Orlandini, S. (**2000**). Aponecrosis: morphological and biochemical exploration of a syncretic process of cell death sharing apoptosis and necrosis. **J Cell Physiol** *182*, 41-49.

Franke, K.W., Moxon, A.L., Poley, W.E., and Tully, W.C. (**1936**). Monstrosities produced by the injection of selenium salts into hens' eggs. **The Anatomical Record** *65*, 15-22.

Franz, E.D., Wiramanaden, C.I.E., Janz, D.M., Pickering, I.J., and Liber, K. (**2011**). Selenium bioaccumulation and speciation in *Chironomus dilutus* exposed to water-borne selenate, selenite, or seleno-DL-methionine. **Environ Toxicol Chem**, Article in Press.

Frost, D.V., and Olson, O.E. (**1972**). The two faces of selenium - can selenophobia be cured? **Crit Rev Toxicol** *1*, 467-514.

Gabel-Jensen, C., Lunoe, K., and Gammelgaard, B. (**2010**). Formation of methylselenol, dimethylselenide and dimethyldiselenide in *in vitro* metabolism models determined by headspace GC-MS. **Metallomics** *2*, 167-173.

Gad, M.A., and Abd El-Twab, S.M. (**2009**). Selenium toxicosis assessment (*in vivo* and *in vitro*) and the protective role of vitamin B_{12} in male quail (*Coturnix coturnix*). **Environ Toxicol Pharmacol** *27*, 7-16.

Gagné, F., Blaise, C., VanAggelen, G., Boivin, P., Martel, P., Chong-Kit, R., Jonczyk, E., Marion, M., Kennedy, S.W., Legault, R.*, et al.* (**1999**). Intercalibration study in the evaluation of toxicity with rainbow trout hepatocytes. **Environ Toxicol** *14*, 429-437.

Galanter, W.L., Hakimian, M., and Labotka, R.J. (**1993**). Structural determinants of substrate specificity of the erythrocyte anion transporter. **American Journal of Physiology-Cell Physiology** *265*, C918.

Gammelgaard, B., Cornett, C., Olsen, J., Bendahl, L., and Hansen, S.H. (**2003**). Combination of LC-ICP-MS, LC-MS and NMR for investigation of the oxidative degradation of selenomethionine. **Talanta** *59*, 1165-1171.

Gammelgaard, B., Gabel-Jensen, C., Stürup, S., and Hansen, H.R. (**2008**). Complementary use of molecular and element-specific mass spectrometry for identification of selenium compounds related to human selenium metabolism. **Anal Bioanal Chem** *390*, 1691-1706.

Gammelgaard, B., Jackson, M., and Gabel-Jensen, C. (**2011**). Surveying selenium speciation from soil to cell—forms and transformations. **Anal Bioanal Chem** *399*, 1743-1763.

Ganther, H.E. (**1968**). Selenotrisulfides. Formation by the reaction of thiols with selenious acid. **Biochemistry (Mosc)** *7*, 2898-2905.

Ganther, H.E. (**1971**). Reduction of the selenotrisulfide derivative of glutathione to a persulfide analog by gluthathione reductase. **Biochemistry (Mosc)** *10*, 4089-4098.

Ganyc, D., and Self, W.T. (**2008**). High affinity selenium uptake in a keratinocyte model. **FEBS Lett** *582*, 299-304.

Garberg, P., Stahl, A., Warholm, M., and Hogberg, J. (**1988**). Studies of the role of DNA fragmentation in selenium toxicity. **Biochem Pharmacol** *37*, 3401-3406.

George, G., and Pickering, I. (**2007**). X-ray absorption spectroscopy in biology and chemistry. In Brilliant Light in Life and Material Sciences, V. Tsakanov, and H. Wiedemann, eds. (Springer Netherlands), pp. 97-119.

Gill, T.A., Sundeen, G.B., Richards, J.F., and Bragg, D.B. (**1980**). The effects of dietary selenium and vitamin E on avian white muscle disease as measured by both chemical and physical parameters. **Poult Sci** *59*, 2088-2097.

Guillouzo, A. (**1998**). Liver cell models in *in vitro* toxicology. **Environ Health Perspect** *106*, 511-532.

Gumbiner, B.M. (**1996**). Cell adhesion: The molecular basis of tissue architecture and morphogenesis. **Cell** *84*, 345-357.

Gunter, K.K., Miller, L.M., Aschner, M., Eliseev, R., Depuis, D., Gavin, C.E., and Gunter, T.E. (**2002**). XANES Spectroscopy: A Promising Tool for Toxicology: A Tutorial. **Neurotoxicology** *23*, 127-146.

Haddoub, R., Rützler, M., Robin, A., and Flitsch, S.L. (**2009**). Design, Synthesis and Assaying of Potential Aquaporin Inhibitors. In Aquaporins, E. Beitz, ed. (Springer Berlin Heidelberg), pp. 385-402.

Halestrap, A.P., and Price, N.T. (**1999**). The proton-linked monocarboxylate transporter (MCT) family: structure, function and regulation. **Biochemical Journal** *343*, 281-293.

Halestrap, A.P., and Meredith, D. (**2004**). The SLC16 gene family-from monocarboxylate transporters (MCTs) to aromatic amino acid transporters and beyond. **Pflugers Arch** *447*, 619-628.

Hamilton, S.J., Palmisano, A.M., Wedemeyer, G.A., and Yasutake, W.T. (**1986**). Impacts of selenium on early life stages and smoltification of fall chinook salmon. In Transactions of the 51st North American Wildlife and Natural Resources Conference, R.E. McCabe, ed. (Wildlife Management Institute, Washington D.C.), pp. 343–356.

Hamilton, S.J., and Buhl, K.J. (**1990**). Acute toxicity of boron, molybdenum, and selenium to fry of chinook salmon and coho salmon. **Arch Environ Contam Toxicol** *19*, 366-373.

Hamilton, S.J., Buhl, K.J., Faerber, N.L., Wiedmeyer, R.H., and Bullard, F.A. (**1990**). Toxicity of organic selenium in the diet to chinook salmon. **Environ Toxicol Chem** *9*, 347-358.

Hamilton, S.J. (**2002**). Rationale for a tissue-based selenium criterion for aquatic life. **Aquat Toxicol** *57*, 85-100.

Hamilton, S.J. (**2003**). Review of residue-based selenium toxicity thresholds for freshwater fish. **Ecotoxicol Environ Saf** *56*, 201-210.

Hamilton, S.J. (**2004**). Review of selenium toxicity in the aquatic food chain. **Sci Total Environ** *326*, 1-31.

Hansen, J.M. (**2006**). Oxidative stress as a mechanism of teratogenesis. **Birth Defects Res C Embryo Today Rev** *78*, 293-307.

Haratake, M., Hongoh, M., Ono, M., and Nakayama, M. (**2009**). Thiol-Dependent Membrane Transport of Selenium through an Integral Protein of the Red Blood Cell Membrane. **Inorg Chem** *48*, 7805-7811.

Heald, S.M. (**1988**). Design of a EXAFS experiment. In X-ray Absorption: Principles, Applications Techniques of EXAFS, SEXAFS and XANES, D.C. Koningsberger, and R. Prins, eds. (Eindhoven, John Willey and Sons), pp. 87-118.

Hengartner, M.O. (**2000**). The biochemistry of apoptosis. **Nature** *407*, 770-776.

Hicks, B.D., Hilton, J.W., and Ferguson, H.W. (**1984**). Influence of dietary selenium on the occurrence of nephrocalcinosis in the rainbow trout, *Salmo gairdneri* Richardson. **J Fish Dis** *7*, 379-389.

Hilton, J.W., Hodson, P.V., and Slinger, S.J. (**1980**). The requirement and toxicity of selenium in rainbow trout (*Salmo gairdneri*). **J Nutr** *110*, 2527.

Hilton, J.W., and Hodson, P.V. (**1983**). Effect of increased dietary carbohydrate on selenium metabolism and toxicity in rainbow trout (*Salmo gairdneri*). **The Journal of Nutrition** *113*, 1241-1248.

Hissin, P.J., and Hilf, R. (**1976**). A fluorometric method for determination of oxidized and reduced glutathione in tissues. **Anal Biochem** *74*, 214-226.

Hodson, P.V., Spry, D.J., and Blunt, B.R. (**1980a**). Effects on rainbow trout (*Salmo gairdneri*) of a chronic exposure to waterborne selenium. **Can J Fish Aquat Sci** *37*, 233-240.

Hodson, P.V., Spry, D.J., and Blunt, B.R. (**1980b**). Effects on rainbow trout (*Salmo gairdneri*) of a chronic exposure to waterborne selenium. **Can J Fish Aquat Sci** *37*, 233-240.

Hodson, P.V., and Hilton, J.W. (**1983**). The nutritional requirements and toxicity to fish of dietary and waterborne selenium. **Ecological Bulletins**, 335-340.

Hoefig, C.S., Renko, K., Köhrle, J., Birringer, M., and Schomburg, L. (**2010**). Comparison of different selenocompounds with respect to nutritional value vs. toxicity using liver cells in culture. **The Journal of Nutritional Biochemistry** *In Press, Corrected Proof*.

Holm, J., Palace, V., Siwik, P., Sterling, G., Evans, R., Baron, C., Werner, J., and Wautier, K. (**2005**). Developmental effects of bioaccumulated selenium in eggs and larvae of two salmonid species. **Environ Toxicol Chem** *24*, 2373-2381.

Huber, R.E., and Criddle, R.S. (**1967**). The isolation and properties of β-galactosidase from *Escherichia coli* grown on sodium selenate. **Biochimica et Biophysica Acta (BBA) - General Subjects** *141*, 587-599.

Inoue, H., Inagaki, K., Sugimoto, M., Esaki, N., Soda, K., and Tanaka, H. (**1995**). Structural analysis of the L-methionine γ-lyase gene from *Pseudomonas putida*. **J Biochem** *117*, 1120-1125.

Izawa, S., Inoue, Y., and Kimura, A. (**1996**). Importance of catalase in the adaptive response to hydrogen peroxide: analysis of acatalasaemic *Saccharomyces cerevisiae*. **Biochem J** *320*, 61.

Jacob, C., Giles, G.I., Giles, N.M., and Sies, H. (**2003**). Sulfur and Selenium: The Role of Oxidation State in Protein Structure and Function. **Angew Chem Int Ed** *42*, 4742-4758.

Janz, D., DeForest, D., Brooks, M., Chapman, P., Gilron, G., Hoff, D., Hopkins, W., G., McIntyre, D., Mebane, C., Palace, V*., et al.* (**2010**). Selenium toxicity to aquatic organisms. In Ecological assessment of selenium in the aquatic environment (CRC Press), pp. 141-231.

Janz, D.M. (**2011**). Selenium. In Fish Physiol, C.M. Wood, A.P. Farrell, and C.J. Brauner, eds. (Academic Press), pp. 327-374.

Kelly, S.A., Havrilla, C.M., Brady, T.C., Abramo, K.H., and Levin, E.D. (**1998**). Oxidative stress in toxicology: established mammalian and emerging piscine model systems. **Environ Health Perspect** *106*, 375-384.

Kennedy, C.J., McDonald, L.E., Loveridge, R., and Strosher, M.M. (**2000**). The effect of bioaccumulated selenium on mortalities and deformities in the eggs, larvae, and fry of a wild population of cutthroat Trout (*Oncorhynchus clarki lewisi*). **Arch Environ Contam Toxicol** *39*, 46-52.

Kice, J.L., Lee, T.W.S., and Pan, S.-T. (**1980**). Mechanism of the reaction of thiols with selenite. **J Am Chem Soc** *102*, 4448-4455.

Kiersztan, A., Lukasinska, I., Baranska, A., Lebiedzinska, M., Nagalski, A., Derlacz, R.A., and Bryla, J. (**2007**). Differential effects of selenium compounds on glucose synthesis in rabbit kidney-cortex tubules and hepatocytes. *In vitro* and *in vivo* studies. **J Inorg Biochem** *101*, 493-505.

Kim, T.-s., Jeong, D.-w., Yun, B.Y., and Kim, I.Y. (**2002**). Dysfunction of rat liver mitochondria by selenite: induction of mitochondrial permeability transition through thiol-oxidation. **Biochem Biophys Res Commun** *294*, 1130-1137.

Kipreos, E.T. (**2005**). *C. elegans* cell cycles: invariance and stem cell divisions. **Nat Rev Mol Cell Biol** *6*, 766-776.

Kitahara, J., Seko, Y., and Imura, N. (**1993**). Possible involvement of active oxygen species in selenite toxicity in isolated rat hepatocytes. **Arch Toxicol** *67*, 497-501.

Kleinow, K.M., and Brooks, A.S. (**1986a**). Selenium-compounds in the fathead minnow (*Pimephales promelas*) .1. Uptake, distribution, and elimination of orally-administered selenate, selenite and L-selenomethionine. **Comparative Biochemistry and Physiology C - Pharmacology Toxicology & Endocrinology** *83*, 61-69.

Kleinow, K.M., and Brooks, A.S. (**1986b**). Selenium compounds in the fathead minnow (*Pimephales promelas*) .2. Quantitative approach to gastrointestinal absorption, routes of elimination and influence of dietary pretreatment. **Comparative Biochemistry and Physiology C - Pharmacology Toxicology & Endocrinology** *83*, 71-76.

Krause, R.J., and Elfarra, A.A. (**2009**). Reduction of l-methionine selenoxide to seleno-l-methionine by endogenous thiols, ascorbic acid, or methimazole. **Biochem Pharmacol** *77*, 134-140.

Kremer, D., Ilgen, G., and Feldmann, J. (**2005**). GC–ICP–MS determination of dimethylselenide in human breath after ingestion of ^{77}Se-enriched selenite: monitoring of *in-vivo* methylation of selenium. **Anal Bioanal Chem** *383*, 509-515.

Kryukov, G.V., and Gladyshev, V.N. (**2000**). Selenium metabolism in zebrafish: multiplicity of selenoprotein genes and expression of a protein containing 17 selenocysteine residues. **Genes Cells** *5*, 1049-1060.

Kryukov, G.V., Castellano, S., Novoselov, S.V., Lobanov, A.V., Zehtab, O., Guigo, R., and Gladyshev, V.N. (**2003**). Characterization of mammalian selenoproteomes. **Science** *300*, 1439-1443.

Kuchan, M.J., Fico Santoro, M., and Milner, J.A. (**1990**). Consequences of selenite supplementation on the growth and metabolism of cultures of canine mammary cells. **The Journal of Nutritional Biochemistry** *1*, 478-483.

Kuchan, M.J., and Milner, J.A. (**1991**). Influence of supplemental glutathione on selenite-mediated growth inhibition of canine mammary cells. **Cancer Lett** *57*, 181-186.

Kwong, R.W., Andres, J.A., and Niyogi, S. (**2010**). Molecular evidence and physiological characterization of iron absorption in isolated enterocytes of rainbow trout (*Oncorhynchus mykiss*): implications for dietary cadmium and lead absorption. **Aquat Toxicol** *99*, 343-350.

Labotka, R.J., Galanter, W., and Misiewicz, V.M. (**1989**). Erythrocyte bisulfite transport. **Biochimica et Biophysica Acta (BBA) - Biomembranes** *981*, 358-362.

Lalitha, K., Rani, P., and Narayanaswami, V. (**1994**). Metabolic relevance of selenium in the insect (*Corcyra cephalonica*). **Biol Trace Elem Res** *41*, 217-233.

Lavado, R., Shi, D., and Schlenk, D. (**2011**). Effects of salinity on the toxicity and biotransformation of L-selenomethionine in Japanese medaka (*Oryzias latipes*) embryos: mechanisms of oxidative stress. **Aquat Toxicol** *In Press, Accepted Manuscript*.

Lemly, A.D. (**1993a**). Metabolic stress during winter increases the toxicity of selenium to fish. **Aquat Toxicol** *27*, 133-158.

Lemly, A.D. (**1993b**). Teratogenic effects of selenium in natural populations of freshwater fish. **Ecotoxicol Environ Saf** *26*, 181-204.

Lemly, A.D. (**1997**). A teratogenic deformity index for evaluating impacts of selenium on fish populations. **Ecotoxicol Environ Saf** *37*, 259-266.

Lemly, A.D. (**1999**). Selenium impacts on fish: An insidious time bomb. **Human and Ecological Risk Assessment (HERA)** *5*, 1139-1151.

Lemly, A.D. (**2002**). Symptoms and implications of selenium toxicity in fish: the Belews Lake case example. **Aquat Toxicol** *57*, 39-49.

Lemly, A.D. (**2004**). Aquatic selenium pollution is a global environmental safety issue. **Ecotoxicol Environ Saf** *59*, 44-56.

Letavayová, L., Vlcková, V., and Brozmanová, J. (**2006**). Selenium: From cancer prevention to DNA damage. **Toxicology** *227*, 1-14.

Lin, Y., and Spallholz, J.E. (**1993**). Generation of reactive oxygen species from the reaction of selenium compounds with thiols and mammary tumor cells. **Biochem Pharmacol** *45*, 429-437.

Lobanov, A., Fomenko, D., Zhang, Y., Sengupta, A., Hatfield, D., and Gladyshev, V. (**2007**). Evolutionary dynamics of eukaryotic selenoproteomes: large selenoproteomes may associate with aquatic life and small with terrestrial life. **Genome Biol** *8*, R198.

Lobanov, A., Hatfield, D., and Gladyshev, V. (**2008**). Reduced reliance on the trace element selenium during evolution of mammals. **Genome Biol** *9*, R62.

Lobinski, R., Edmonds, J., Suzuki, K., and Uden, P. (**2000**). Species-selective determination of selenium compounds in biological materials. **Pure Appl Chem** *72*, 447-462.

Lorentzen, M., Maage, A., and Julshamn, K. (**1994**). Effects of dietary selenite or selenomethionine on tissue selenium levels of Atlantic salmon (*Salmo salar*). **Aquaculture** *121*, 359-367.

Lu, J., and Holmgren, A. (**2009**). Selenoproteins. **J Biol Chem** *284*, 723-727.

Lunøe, K., Gabel-Jensen, C., Stűrup, S., Andresen, L., Skov, S., and Gammelgaard, B. (**2011**). Investigation of the selenium metabolism in cancer cell lines. **Metallomics** *3*, 162-168.

Luoma, S.N., and Presser, T. (**2006**). Forecasting selenium discharges to the San Francisco Bay-Delta Estuary: ecological effects of a proposed San Luis drain extension (Reston, Virginia, US Dept. of the Interior, US Geological Survey), pp. 1-209.

Luoma, S.N., and Rainbow, P.S. (**2008**). Selenium: dietary exposure, trophic transfer and food web effects. In Metal contamination in aquatic enviroments: science and lateral management (Cambridge, Cambridge University Press), pp. 327-353.

Luoma, S.N., and Presser, T.S. (**2009**). Emerging opportunities in management of selenium contamination. **Environ Sci Technol** *43*, 8483-8487.

Madison, T.C. (**1860**). U.S. Congress 36th Session. In Senate Ex Document (Washington D.C.), pp. 37-41.

Maher, W., Roach, A., Doblin, M., Fan, T., Foster, S., Garrett, R., Möller, G., Oram, L., and Wallschläger, D. (**2010**). Environmental Sources, Speciation, and Partitioning of Selenium. In Ecological Assessment of Selenium in the Aquatic Environment, P.M. Chapman, Adams, William J., Brooks, Marjorie L., Delos, Charles G., Luoma, Samuel N., Maher, William A., Ohlendorf, Harry M., Presser, Theresa S. and Shaw, D. Patrick ed. (CRC Press), pp. 47-92.

Maier, K.J., and Knight, A.W. (**1994**). Ecotoxicology of selenium in freshwater systems. **Rev Environ Contam Toxicol** *134*, 31-48.

Martin, A.J., Simpson, S., Fawcett, S., Wiramanaden, C.I.E., Pickering, I.J., Belzile, N., Chen, Y.W., London, J., and Wallschläger, D. (**2011**). Biogeochemical mechanisms of selenium exchange between water and sediments in two contrasting lentic environments. **Environ Sci Technol** *45*, 2605-2612.

McConnell, K.P., and Cho, G.J. (**1965**). Transmucosal movement of selenium. **Am J Physiol** *208*, 1191-1195.

McDermott, J.R., Rosen, B.P., and Liu, Z.J. (**2010**). Jen1p: A high affinity selenite transporter in Yeast. **Mol Biol Cell** *21*, 3934-3941.

Michiels, C., Raes, M., Toussaint, O., and Remacle, J. (**1994**). Importance of Se-glutathione peroxidase, catalase, and Cu/Zn-SOD for cell survival against oxidative stress. **Free Radical Biol Med** *17*, 235-248.

Miller, L.L., Wang, F., Palace, V.P., and Hontela, A. (**2007**). Effects of acute and subchronic exposures to waterborne selenite on the physiological stress response and oxidative stress indicators in juvenile rainbow trout. **Aquat Toxicol** *83*, 263-271.

Miller, L.L., Rasmussen, J.B., Palace, V.P., and Hontela, A. (**2009a**). Physiological stress response in white suckers from agricultural drain waters containing pesticides and selenium. **Ecotoxicol Environ Saf** *72*, 1249-1256.

Miller, L.L., Rasmussen, J.B., Palace, V.P., and Hontela, A. (**2009b**). The physiological stress response and oxidative stress biomarkers in rainbow trout and brook trout from selenium-impacted streams in a coal mining region. **J Appl Toxicol** *29*, 681-688.

Miller, L.L., and Hontela, A. (**2011**). Species-specific sensitivity to selenium-induced impairment of cortisol secretion in adrenocortical cells of rainbow trout (*Oncorhynchus mykiss*) and brook trout (*Salvelinus fontinalis*). **Toxicol Appl Pharmacol** *253*, 137-144.

Mills, G.C. (**1959**). The purification and properties of glutathione peroxidase of erythrocytes. **J Biol Chem** *234*, 502-506.

Misra, S., and Niyogi, S. (**2009**). Selenite causes cytotoxicity in rainbow trout (*Oncorhynchus mykiss*) hepatocytes by inducing oxidative stress. **Toxicol In Vitro** *23*, 1249-1258.

Misra, S., Peak, D., and Niyogi, S. (**2010**). Application of XANES spectroscopy in understanding the metabolism of selenium in isolated rainbow trout hepatocytes: insights into selenium toxicity. **Metallomics** *2*, 710-717.

Moroder, L. (**2005**). Isosteric replacement of sulfur with other chalcogens in peptides and proteins. **J Pept Sci** *11*, 187-214.

Moulis, J.M., and Meyer, J. (**1982**). Characterization of the selenium-substituted 2[4Fe-4Se] ferredoxin from *Clostridium pasteurianum*. **Biochemistry (Mosc)** *21*, 4762-4771.

Mount, D.B., and Romero, M.F. (**2004**). The SLC26 gene family of multifunctional anion exchangers. **Pflugers Arch** *447*, 710-721.

Moxon, A.L., and Rhian, M. (**1943**). Selenium poisoning. **Physiol Rev** *23*, 305-337.

Muscatello, J.R., Bennett, P.M., Himbeault, K.T., Belknap, A.M., and Janz, D.M. (**2006**). Larval deformities associated with selenium accumulation in northern pike (*Esox lucius*) exposed to metal mining effluent. **Environ Sci Technol** *40*, 6506-6512.

Muth, O.H., Oldfield, J.E., Remmert, L.F., and Schubert, J.R. (**1958**). Effects of selenium and vitamin-E on white muscle disease. **Science** *128*, 1090-1090.

Muth, O.H., Oldfield, J.E., Schubert, J.R., and Remmert, L.F. (**1959**). White muscle disease (myopathy) in lambs and calves .6. Effects of selenium and vitamin-E on lambs. **Am J Vet Res** *20*, 231-234.

Mykkanen, H.M., and Wasserman, R.H. (**1989**). Uptake of ^{75}Se-selenite by brush border membrane vesicles from chick duodenum stimulated by vitamin D. **The Journal of Nutrition** *119*, 242.

Nickel, A., Kottra, G., Schmidt, G., Danier, J., Hofmann, T., and Daniel, H. (**2009**). Characteristics of transport of selenoamino acids by epithelial amino acid transporters. **Chem-Biol Interact** *177*, 234-241.

Nicotera, P., McConkey, D., Svensson, S.-Å., Bellomo, G., and Orrenius, S. (**1988**). Correlation between cytosolic Ca^{2+} concentration and cytotoxicity in hepatocytes exposed to oxidative stress. **Toxicology** *52*, 55-63.

NRC (**1980**). Mineral tolerance of domestic animals. (Washington, D.C, National Research Council, National Academy of Sciences).

Nuttall, K.L. (**1985**). Elemental selenium and glutathione reductase. **Medical Hypotheses** *16*, 155-158.

Okuno, T., Kubota, T., Kuroda, T., Ueno, H., and Nakamuro, K. (**2001**). Contribution of enzymic α,γ-elimination reaction in detoxification pathway of selenomethionine in mouse liver. **Toxicol Appl Pharmacol** *176*, 18-23.

Olin, Å., Noläng, B., Osadchii, E.G., Öhman, L.-O., and Rosén, E. (**2005**). **Chemical thermodynamics of selenium** (Amsterdam, Elsevier B.V.).

Orme-Johnson, W.H., Hansen, R.E., Beinert, H., Tsibris, J.C., Bartholomaus, R.C., and Gunsalus, I.C. (**1968**). On the sulfur components of iron-sulfur proteins. I. The number of acid-labile sulfur groups sharing an unpaired electron with iron. **Proceedings of the National Academy of Sciences** *60*, 368-372.

Orun, I., Ates, B., Selamoglu, Z., Yazlak, H., Ozturk, E., Yi, dotover, and lmaz, I. (**2005**). Effects of various sodium selenite concentrations on some biochemical and haematological parameters of rainbow trout (*Oncorhynchus mykiss*). **Fresenius Environ Bull** *14*, 18-22.

Pain, A. (**2000**). Dietary reference intakes for vitamin C, vitamin E, selenium, and carotenoids: a report of the Panel on Dietary Antioxidants and Related Compounds, Subcommittees on Upper Reference Levels of Nutrients and of Interpretation and Use of Dietary Reference Intakes, and the Standing Committee on the Scientific Evaluation of Dietary Reference Intakes, Food and Nutrition Board, Institute of Medicine. (Washington D.C., National Acdemy Press).

Painter, E.P. (**1941**). The chemistry and toxicity of selenium compounds, with special reference to the selenium problem. **Chem Rev** *28*, 179-213.

Palace, V.P., Spallholz, J.E., Holm, J., Wautier, K., Evans, R.E., and Baron, C.L. (**2004**). Metabolism of selenomethionine by rainbow trout (*Oncorhynchus mykiss*) embryos can generate oxidative stress. **Ecotoxicol Environ Saf** *58*, 17-21.

Papp, L.V., Lu, J., Holmgren, A., and Khanna, K.K. (**2007**). From selenium to selenoproteins: synthesis, identity, and their role in human health. **Antioxidants & redox signaling** *9*, 775-806.

Park, Y.-C., and Whanger, P.D. (**1995**). Toxicity, metabolism and absorption of selenite by isolated rat hepatocytes. **Toxicology** *100*, 151-162.

Patterson, E.L., Milstrey, R., and Stokstad, E.L.R. (**1957**). Effect of selenium in preventing exudative diathesis in chicks. **Proc Soc Exp Biol Med** *95*, 617-620.

Penner-Hahn, J.E. (**2003**). X-ray Absorption Spectroscopy. In Comprehensive Coordination Chemistry II, J.A. McCleverty, and T.J. Meyer, eds. (Oxford, Pergamon), pp. 159-186.

Pesonen, M., and Andersson, T.B. (**1997**). Fish primary hepatocyte culture; an important model for xenobiotic metabolism and toxicity studies. **Aquat Toxicol** *37*, 253-267.

Phibbs, J., Franz, E., Hauck, D., Gallego, M., Tse, J.J., Pickering, I.J., Liber, K., and Janz, D.M. (**2011a**). Evaluating the trophic transfer of selenium in aquatic ecosystems using caged fish, X-ray absorption spectroscopy and stable isotope analysis. **Ecotoxicol Environ Saf***, In Press, Corrected Proof*.

Phibbs, J., Wiramanaden, C.I.E., Hauck, D., Pickering, I.J., Liber, K., and Janz, D.M. (**2011b**). Selenium uptake and speciation in wild and caged fish downstream of a metal mining and milling discharge. **Ecotoxicol Environ Saf** *74*, 1139-1150.

Pickering, I.J., Brown, G.E., and Tokunaga, T.K. (**1995**). Quantitative speciation of selenium in soils using X-ray absorption spectroscopy. **Environ Sci Technol** *29*, 2456-2459.

Pickering, I.J., Prince, R.C., Salt, D.E., and George, G.N. (**2000**). Quantitative, chemically specific imaging of selenium transformation in plants. **Proceedings of the National Academy of Sciences of the United States of America** *97*, 10717-10722.

Pinsent, J. (**1954**). The need for selenite and molybdate in the formation of formic dehydrogenase by members of the coli-aerogenes group of bacteria. **Biochem J** *57*, 10.

Porter, E.K., Karle, J.A., and Shrift, A. (**1979**). Uptake of selenium-75 by human lymphocytes *in vitro*. **The Journal of nutrition** *109*, 1901-1908.

Poston, H.A., Combs, G.F., and Leibovitz, L. (**1976**). Vitamin E and selenium interrelations in the diet of atlantic salmon (*Salmo salar*): gross, histological and biochemical deficiency signs. **The Journal of Nutrition** *106*, 892-904.

Presser, T., and Barnes, I. (**1984**). **Dissolved constituents including selenium in waters in the vicinity of Kesterson National wildlife refuge and the west grassland, Fresno and Merced counties, California** (Menlo Park, California, United States Geological Survey).

Pritchard, J.B., and Renfro, J.L. (**1983**). Renal sulfate transport at the basolateral membrane is mediated by anion exchange. **Proceedings of the National Academy of Sciences of the United States of America** *80*, 2603 - 2607.

Raines, A., and Sunde, R. (**2011**). Selenium toxicity but not deficient or super-nutritional selenium status vastly alters the transcriptome in rodents. **BMC Genomics** *12*, 26.

Rayman, M.P. (**2005**). Selenium in cancer prevention: a review of the evidence and mechanism of action. **Proc Nutr Soc** *64*, 527-542.

Roberge, M.T., Borgerding, A.J., and Finley, J.W. (**2003**). Speciation of selenium compounds from high selenium broccoli is affected by the extracting solution. **J Agric Food Chem** *51*, 4191-4197.

Rodríguez-Fuentes, G., Aparicio-Fabre, R., Li, Q., and Schlenk, D. (**2008**). Osmotic regulation of a novel flavin-containing monooxygenase in primary cultured cells from rainbow trout (*Oncorhynchus mykiss*). **Drug Metab Disposition** *36*, 1212-1217.

Romero, M.F., Fulton, C.M., and Boron, W.F. (**2004**). The SLC4 family of HCO_3^- transporters. **Pflugers Arch** *447*, 495-509.

Rong, Y., and Distelhorst, C.W. (**2008**). Bcl-2 protein family members: versatile regulators of calcium signaling in cell survival and apoptosis. **Annu Rev Physiol** *70*, 73-91.

Rotruck, J.T., Pope, A.L., Ganther, H.E., Swanson, A.B., Hafeman, D.G., and Hoekstra, W.G. (**1973**). Selenium: Biochemical role as a component of glutathione peroxidase. **Science** *179*, 588-590.

Rouached, H., Berthomieu, P., El Kassis, E., Cathala, N., Catherinot, V., Labesse, G., Davidian, J.-C., and Fourcroy, P. (**2005**). Structural and functional analysis of the C-terminal STAS (Sulfate transporter and anti-sigma antagonist) domain of the *Arabidopsis thaliana* sulfate transporter SULTR1.2. **Journal of Biological Chemistry** *280*, 15976-15983.

Ryser, A.L., Strawn, D.G., Marcus, M.A., Fakra, S., Johnson-Maynard, J.L., and Moller, G. (**2005**). Microscopically focused synchrotron X-ray investigation of selenium speciation in soils developing on reclaimed mine lands. **Environ Sci Technol** *40*, 462-467.

Sarret, G., Avoscan, L., Carriere, M., Collins, R., Geoffroy, N., Carrot, F., Coves, J., and Gouget, B. (**2005**). Chemical forms of selenium in the metal-resistant bacterium *Ralstonia metallidurans* CH34 exposed to selenite and selenate. **Appl Environ Microbiol** *71*, 2331.

Sathiyaa, R., Campbell, T., and Vijayan, M.M. (**2001**). Cortisol modulates HSP90 mRNA expression in primary cultures of trout hepatocytes. **Comparative Biochemistry and Physiology Part B: Biochemistry and Molecular Biology** *129*, 679-685.

Sato, T., Ose, Y., and Sakai, T. (**1980**). Toxicological effect of selenium on fish. **Environmental Pollution Series a-Ecological and Biological** *21*, 217-224.

Scharrer, E., Senn, E., and Wolffram, S. (**1992**). Stimulation of mucosal uptake of selenium from selenite by some thiols at various sites of rat intestine. **Biol Trace Elem Res** *33*, 109-120.

Schlenk, D., Zubcov, N., and Zubcov, E. (**2003**). Effects of salinity on the uptake, biotransformation, and toxicity of dietary seleno-L-methionine to rainbow trout. **Toxicol Sci** *75*, 309-313.

Schwarz, K., Bieri, J.G., Briggs, G.M., and Scott, M.L. (**1957**). Prevention of exudative diathesis in chicks by factor-3 and selenium. **Proc Soc Exp Biol Med** *95*, 621-625.

Schwarz, K., and Foltz, C.M. (**1957**). Selenium as an integral part of factor 3 against dietary necrotic liver degeneration. **J Am Chem Soc** *79*, 3292-3293.

Segner, H. (**1998**). Fish cell lines as a tool in aquatic toxicology. In Fish Ecotoxicology, T. Braunbeck, B. Streit, and D.E. Hinton, eds. (Basel, Switzerland, Birkhauser), pp. 1-38.

Seko, Y., Saito, Y., Kitahara, J., and Imura, N. (**1989**). Active oxygen generation by the reaction of selenite with reduced glutathione *in vitro*. In Selenium in Biology and Medicine, A. Wendel, ed. (Berlin, Springer-Verlag), pp. 70-73.

Shamberger, R.J., and Frost, D.V. (**1969**). Possible protective effect of selenium against human cancer. **Can Med Assoc J** *100*, 682.

Shen, H.-M., Yang, C.-F., Liu, J., and Ong, C.-N. (**2000**). Dual role of glutathione in selenite-induced oxidative stress and apoptosis in human hepatoma cells. **Free Radical Biol Med** *28*, 1115-1124.

Shen, H.M., Yang, C.F., and Ong, C.N. (**1999**). Sodium selenite-induced oxidative stress and apoptosis in human hepatoma $HepG_2$ cells. **Cancer** *81*, 820-828.

Ship, S., Shami, Y., Breuer, W., and Rothstein, A. (**1977**). Synthesis of tritiated 4,4'-diisothiocyano-2,2'-stilbene disulfonic acid ([^{3}H]DIDS) and its covalent reaction with sites related to anion transport in human red blood cells. **J Membr Biol** *33*, 311-323.

Sies, H. (**1986**). Biochemistry of oxidative stress. **Angewandte Chemie International Edition in English** *25*, 1058-1071.

Soda, K. (**1968**). Microdetermination of D-amino acids and D-amino acid oxidase activity with 3-methyl-2-benzothiazolone hydrazone hydrochloride. **Anal Biochem** *25*, 228-235.

Sopjani, M., Föller, M., Gulbins, E., and Lang, F. (**2008**). Suicidal death of erythrocytes due to selenium-compounds. **Cell Physiol Biochem** *22*, 387-394.

Sorensen, E.M., and Bauer, T.L. (**1983**). Hematological dyscrasia in teleosts chronically exposed to selenium-laden effluent. **Arch Environ Contam Toxicol** *12*, 135-141.

Sorensen, E.M.B., Cumbie, P.M., Bauer, T.L., Bell, J.S., and Harlan, C.W. (**1984**). Histopathological, hematological, condition-factor, and organ weight changes associated with selenium accumulation in fish from Belews Lake, North Carolina. **Arch Environ Contam Toxicol** *13*, 153-162.

Sorensen, E.M.B. (**1988**). Selenium accumulation, reproductive status, and histopathological changes in environmentally exposed redear sunfish. **Arch Toxicol** *61*, 324-329.

Spallholz, J.E. (**1994**). On the nature of selenium toxicity and carcinostatic activity. **Free Radical Biol Med** *17*, 45-64.

Spallholz, J.E. (**1997**). Free radical generation by selenium compounds and their prooxidant toxicity. **Biomed Environ Sci** *10*, 260.

Spallholz, J.E., Shriver, B.J., and Reid, T.W. (**2001**). Dimethyldiselenide and methylseleninic acid generate superoxide in an *in vitro* chemiluminescence assay in the presence of glutathione: implications for the anticarcinogenic activity of L-selenomethionine and L-Se-methylselenocysteine. **Nutr Cancer** *40*, 34-41.

Spallholz, J.E., and Hoffman, D.J. (**2002**). Selenium toxicity: cause and effects in aquatic birds. **Aquat Toxicol** *57*, 27-37.

Stewart, M.S., Spallholz, J.E., Neldner, K.H., and Pence, B.C. (**1999**). Selenium compounds have disparate abilities to impose oxidative stress and induce apoptosis. **Free Radical Biol Med** *26*, 42-48.

Stewart, R., Grosell, M., Buchwalter, D., Fisher, N., Luoma, S., Mathews, T., Orr, P., and Wang, W.-X., eds. (**2010**). Bioaccumulation and Trophic Transfer of Selenium (Boca raton, FL, CRC Press).

Sunde, R.A. (**1997**). Selenium. In Handbook of nutritionally essential minerals, B.O. O'Dell, and R.A. Sunde, eds. (New York, NY, USA, Marcel Dekker), pp. 493–557.

Suzuki, K.T., Itoh, M., and Ohmichi, M. (**1995**). Selenium distribution and metabolic profile in relation to nutritional selenium status in rats. **Toxicology** *103*, 157-165.

Suzuki, K.T., and Itoh, M. (**1997**). Metabolism of selenite labelled with enriched stable isotope in the bloodstream. **Journal of Chromatography B: Biomedical Sciences and Applications** *692*, 15-22.

Suzuki, K.T., Shiobara, Y., Ishiwata, K., and Ohmichi, M. (**1997**). Speciation by HPLC/ICP-MS with use of stable isotpes: Chemical reactions in the metabolism of selenium administered as selenite. **Journal of Inorganic Biochemistry** *67*, 21-56.

Suzuki, K.T., Doi, C., and Suzuki, N. (**2006a**). Metabolism of ^{76}Se-methylselenocysteine compared with that of ^{77}Se-selenomethionine and ^{82}Se-selenite. **Toxicol Appl Pharmacol** *217*, 185-195.

Suzuki, K.T., Kurasaki, K., Ogawa, S., and Suzuki, N. (**2006b**). Metabolic transformation of methylseleninic acid through key selenium intermediate selenide. **Toxicol Appl Pharmacol** *215*, 189-197.

Suzuki, K.T., Ohta, Y., and Suzuki, N. (**2006c**). Availability and metabolism of ^{77}Se-methylseleninic acid compared simultaneously with those of three related selenocompounds. **Toxicol Appl Pharmacol** *217*, 51-62.

Suzuki, K.T., Kurasaki, K., and Suzuki, N. (**2007**). Selenocysteine [beta]-lyase and methylselenol demethylase in the metabolism of Se-methylated selenocompounds into selenide. **Biochimica et Biophysica Acta (BBA) - General Subjects** *1770*, 1053-1061.

Sze, G., Kaplowitz, N., Ookhtens, M., and Lu, S.C. (**1993**). Bidirectional membrane transport of intact glutathione in Hep G2 cells. **Am J Physiol** *265*, G1128-1134.

Tarze, A., Dauplais, M., Grigoras, I., Lazard, M., Ha-Duong, N.-T., Barbier, F., Blanquet, S., and Plateau, P. (**2007**). Extracellular production of hydrogen selenide accounts for thiol-assisted toxicity of selenite against *Saccharomyces cerevisiae*. **J Biol Chem** *282*, 8759-8767.

Tashjian, D.H., Teh, S.J., Sogomonyan, A., and Hung, S.S.O. (**2006**). Bioaccumulation and chronic toxicity of dietary L-selenomethionine in juvenile white sturgeon (*Acipenser transmontanus*). **Aquat Toxicol** *79*, 401-409.

Teh, S.J., Deng, X., Deng, D.F., Teh, F.C., Hung, S.S.O., Fan, T.W.M., Liu, J., and Higashi, R.M. (**2004**). Chronic effects of dietary selenium on juvenile Sacramento splittail (*Pogonichthys macrolepidotus*). **Environ Sci Technol** *38*, 6085-6093.

Terada, A., Yoshida, M., Seko, Y., Kobayashi, T., Yoshida, K., Nakada, M., Nakada, K., Echizen, H., Ogata, H., and Rikihisa, T. (**1999**). Active oxygen species generation and cellular damage by additives of parenteral preparations: selenium and sulfhydryl compounds. **Nutrition** *15*, 651-655.

Thisse, C., Degrave, A., Kryukov, G.V., Gladyshev, V.N., Obrecht-Pflumio, S., Krol, A., Thisse, B., and Lescure, A. (**2003**). Spatial and temporal expression patterns of selenoprotein genes during embryogenesis in zebrafish. **Gene Expression Patterns** *3*, 525-532.

Thomas, J.K., and Janz, D.M. (**2011**). Dietary selenomethionine exposure in adult zebrafish alters swimming performance, energetics and the physiological stress response. **Aquat Toxicol** *102*, 79-86.

Thorvaldson, T., and Johnson, L.R. (**1940**). The selenium content of Saskatchewan wheat. **Canadian Journal of Research** *18b*, 138-150.

Tournaire-Roux, C., Sutka, M., Javot, H., Gout, E., Gerbeau, P., Luu, D.-T., Bligny, R., and Maurel, C. (**2003**). Cytosolic pH regulates root water transport during anoxic stress through gating of aquaporins. **Nature** *425*, 393-397.

Van Cruchten, S., and Van Den Broeck, W. (**2002**). Morphological and biochemical aspects of apoptosis, oncosis and necrosis. **Anat Histol Embryol** *31*, 214-223.

Vanvleet, J.F., Carlton, W., and Olander, H.J. (**1970**). Hepatosis dietetica and mulberry heart disease associated with selenium deficiency in indiana swine. **J Am Vet Med Assoc** *157*, 1208-&.

Vickerman, D.B., Trumble, J.T., George, G.N., Pickering, I.J., and Nichol, H. (**2004**). Selenium biotransformations in an insect ecosystem: effects of insects on phytoremediation. **Environ Sci Technol** *38*, 3581-3586.

Vidal, D., Bay, S.M., and Schlenk, D. (**2005**). Effects of dietary selenomethionine on larval rainbow trout (*Oncorhynchus mykiss*). **Arch Environ Contam Toxicol** *49*, 71-75.

Watanabe, C., and Satoh, H. (**1994**). Brain selenium status and behavioral development in selenium-deficient preweanling mice. **Physiol Behav** *56*, 927-932.

Weekley, C.M., Aitken, J.B., Vogt, S., Finney, L.A., Paterson, D.J., de Jonge, M.D., Howard, D.L., Musgrave, I.F., and Harris, H.H. (**2011**). Uptake, distribution and speciation of selenoamino acids by human cancer cells: X-ray absorption and fluorescence methods. **Biochemistry (Mosc)** *50*, 1641-1650.

Weiller, M., Latta, M., Kresse, M., Lucas, R., and Wendel, A. (**2004**). Toxicity of nutritionally available selenium compounds in primary and transformed hepatocytes. **Toxicology** *201*, 21-30.

Whanger, P., and Butler, J. (**1988**). Effects of various dietary levels of selenium as selenite or selenomethionine on tissue selenium levels and glutathione peroxidase activity in rats. **The Journal of Nutrition** *118*, 846.

Whanger, P.D., Weswig, P.H., Schmitz, J.A., and Oldfield, J.E. (**1977**). Effects of selenium and vitamin-E on blood selenium levels, tissue glutathione peroxidase activities and white muscle disease in sheep fed purified or hay diets. **J Nutr** *107*, 1298-1307.

Williams, K.T., and Byers, H.G. (**1935**). Occurrence of selenium in the Colorado River and some of its tributaries. **Industrial and Engineering Chemistry - Analytical Edition** *7*, 0431-0432.

Wiseman, S., Thomas, J.K., Higley, E., Hursky, O., Pietrock, M., Raine, J.C., Giesy, J.P., Janz, D.M., and Hecker, M. (**2011**). Chronic exposure to dietary selenomethionine increases gonadal steroidogenesis in female rainbow trout. **Aquat Toxicol***, In Press, Accepted Manuscript*.

Wolffram, S., Arduser, F., and Scharrer, E. (**1985**). *In vivo* intestinal absorption of selenate and selenite by rats. **J Nutr** *115*, 454.

Wolffram, S., Anliker, E., and Scharrer, E. (**1986**). Uptake of selenate and selenite by isolated intestinal brush border membrane vesicles from pig, sheep, and rat. **Biological Trace Element Research** *10*, 293-306.

Wu, J., Lyons, G.H., Graham, R.D., and Fenech, M.F. (**2009**). The effect of selenium, as selenomethionine, on genome stability and cytotoxicity in human lymphocytes measured using the cytokinesis-block micronucleus cytome assay. **Mutagenesis** *24*, 225-232.

Wu, S., Oldfield, J., Whanger, P., and Weswig, P. (**1973**). Effect of selenium, vitamin E, and antioxidants on testicular function in rats. **Biol Reprod** *8*, 625-629.

Würmli, R., Wolffram, S., Stingelin, Y., and Scharrer, E. (**1989**). Stimulation of mucosal uptake of selenium from selenite by L-cysteine in sheep small intestine. **Biol Trace Elem Res** *20*, 75-85.

Xu, X.M., Carlson, B.A., Irons, R., Mix, H., Zhong, N., Gladyshev, V.N., and Hatfield, D.L. (**2007**). Selenophosphate synthetase 2 is essential for selenoprotein biosynthesis. **The Biochemical journal** *404*, 115-120.

Yan, L., and Spallholz, J.E. (**1992**). Generation of reactive oxygen species from the reaction of selenium compounds with thiols and mammary tumor cells. **Biochem Pharmacol** *45*, 429-437.

Yu-Feng, L., Xiaoyan, W., Liming, W., Bai, L., Yuxi, G., and Chunying, C. (**2010**). Direct quantitative speciation of selenium in selenium-enriched yeast and yeast-based products by X-ray absorption spectroscopy confirmed by HPLC-ICP-MS. **J Anal At Spectrom** *25*, 426-430.

Zahn, T., and Braunbeck, T. (**1993**). Isolated fish hepatocytes as a tool in aquatic toxicology: sublethal effects of dinitro-o-cresol and 2,4-dichlorophenol. **Sci Total Environ** *134*, 721-734.

Zareh, M.M., Amin, A.S., and Abdel-Aziz, M. (**1995**). New polycrystalline solid state responsive electrodes for the determination of the selenite ion. **Electroanalysis** *7*, 587-590.

Zhang, J., Wang, L., Li, G., Anderson, L.B., Xu, Y., Witthuhn, B., and Lü, J. (**2011**). Mouse prostate proteomes are differentially altered by supranutritional intake of four selenium compounds. **Nutr Cancer** *63*, 778-789.

Zhuang, S., Demirs, J.T., and Kochevar, I.E. (**2001**). Protein kinase C inhibits singlet oxygen-induced apoptosis by decreasing caspase-8 activation. **Oncogene** *20*, 6764-6776.

Zinoni, F., Birkmann, A., Stadtman, T.C., and Böck, A. (**1986**). Nucleotide sequence and expression of the selenocysteine-containing polypeptide of formate dehydrogenase (formate-hydrogen-lyase-linked) from *Escherichia coli*. **Proceedings of the National Academy of Sciences of the United States of America** *83*, 4650.

Znidaric, M., Falnoga, I., Skreblin, M., and Turk, V. (**2006**). Induction of metallothionein-like proteins by mercury and distribution of mercury and selenium in the cells of hepatopancreas and gill tissues in mussel (*Mytilus galloprovincialis*). **Biol Trace Elem Res** *111*, 121-135.

APPENDIX[6]

---

[6] Supplementary data are included in this chapter. The figure number is presented as Cx.Sy format, where 'Cx' indicates Chapter number; 'Sy' indicates individual figure.

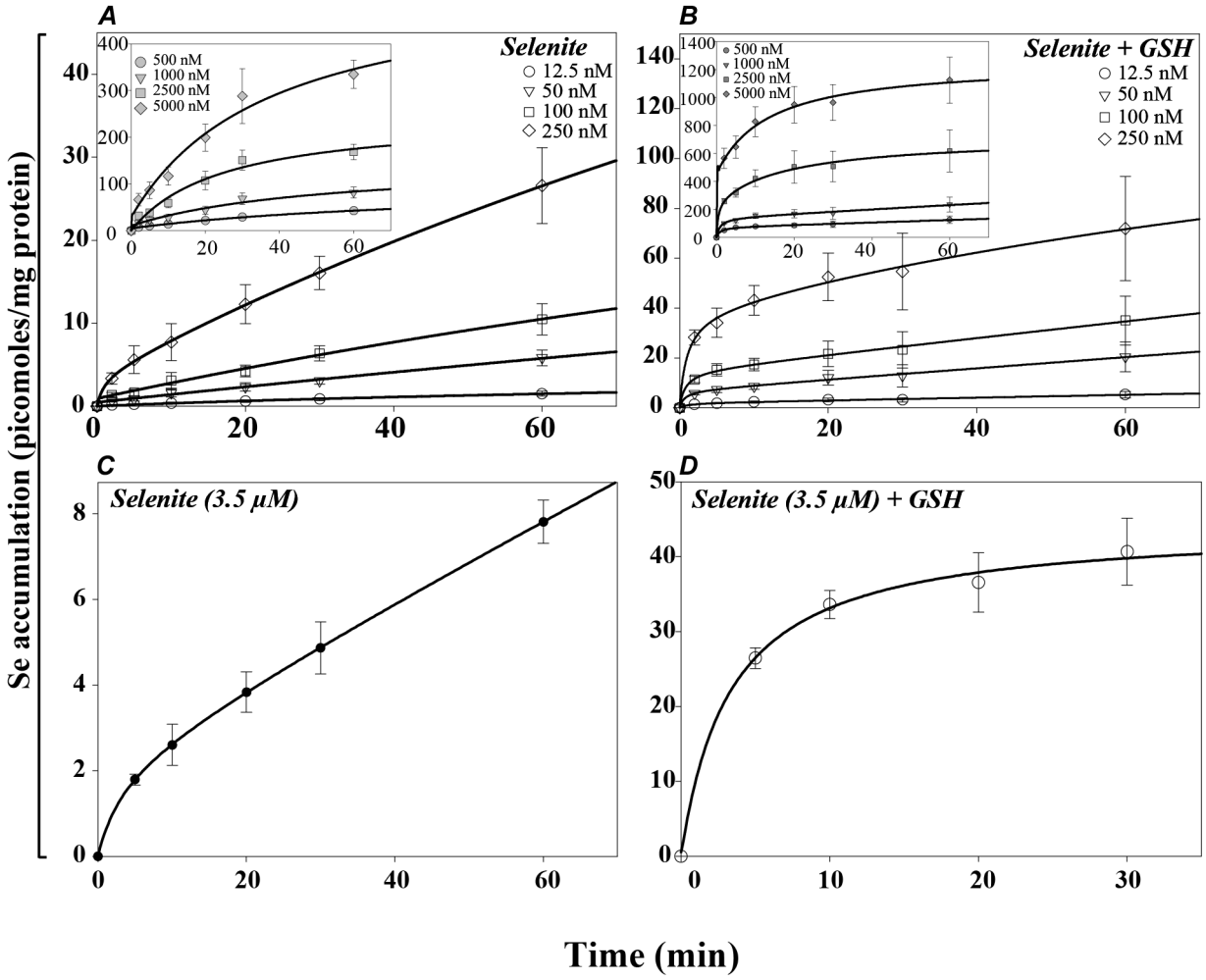

Figure C2.S1: Time-dependent uptake of selenite and its reduced form(s). The uptake of [^{75}Se]-selenite reached a steady state in hepatocytes (Figure S1A) within 30 minutes, but not in enterocytes (Figure S1C). However, in the presence of GSH, steady state was reached within 10 minutes both in hepatocytes (Figure S1B) and in enterocytes (Figure S1D). Insets (Figures S1A and S1B) show cellular accumulation of selenium in hepatocytes at higher concentration of selenite. Data are presented as mean ± S.E.M. (n=4-5), where n represents the number of independent measurements using cells from as many fish.

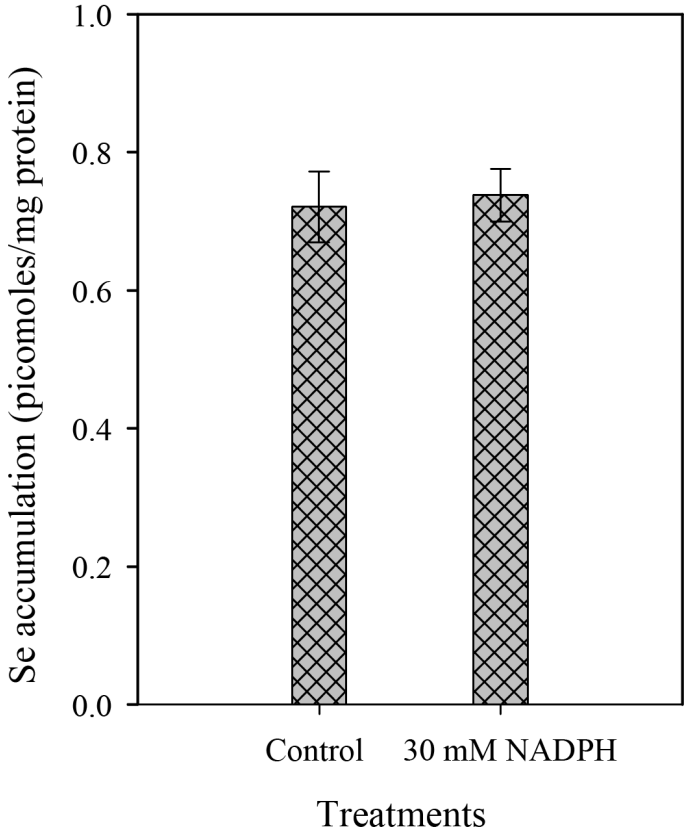

Figure C2.S2: The uptake of [^{75}Se]-selenite in hepatocytes remained unchanged when [^{75}Se]-selenite was pre-incubated with 30 μM NADPH for 20 minutes (Student's t-test, $p < 0.05$). Data are presented as mean ± S.E.M. (n=8), where n represents the number of independent measurements using cells from as many fish.

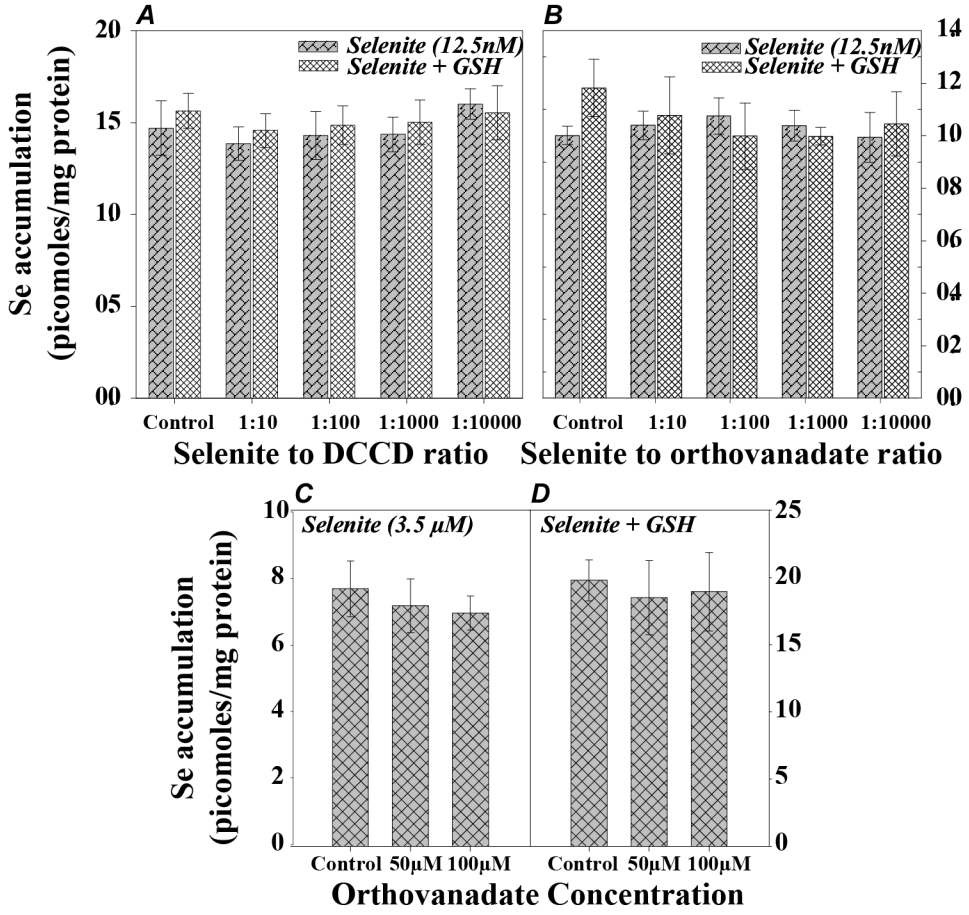

Figure C2.S3: Selenium transport is energy independent. The uptake of [^{75}Se]-selenite and its reduced form(s) was insensitive to DCCD (Figure S2A) and orthovanadate (Figure S2B) in hepatocytes (n=6). A similar response for orthovanadate (Figure S2C) was also found in enterocytes (n=5) demonstrating energy independence of the transport process. Data are presented as mean ± S.E.M. and n represents the number of independent measurements using cells from as many fish. The statistical significance in respective treatments was analyzed by One Way ANOVA ($p < 0.05$).

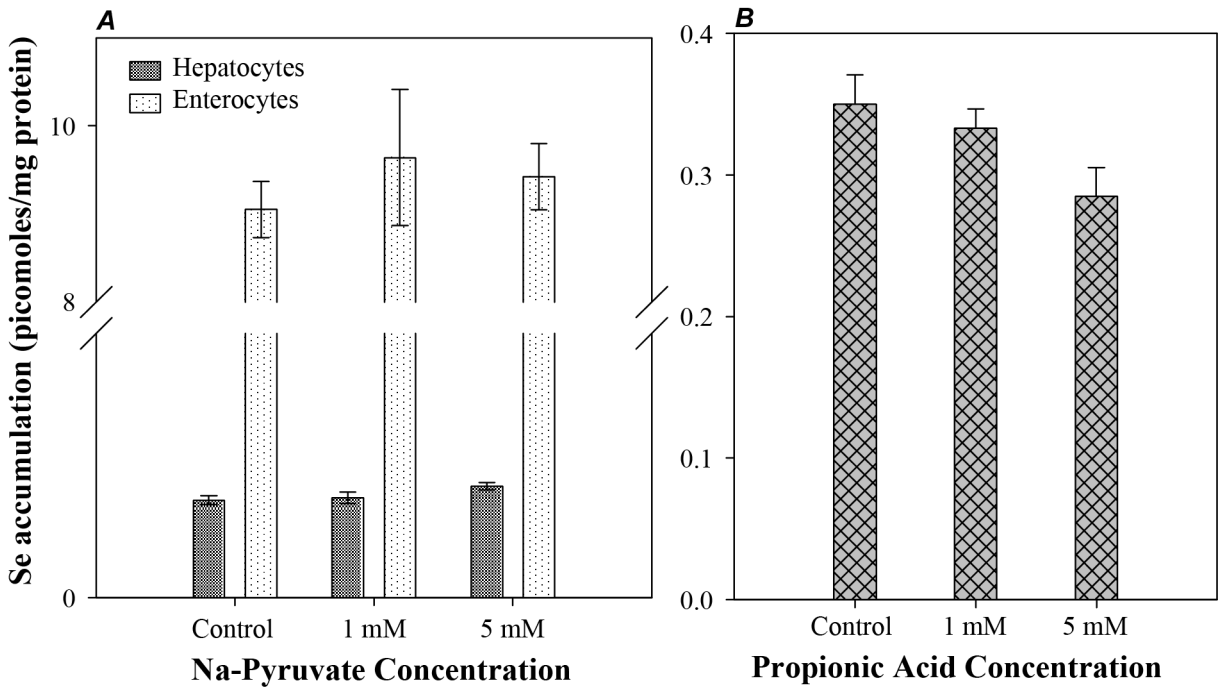

Figure C2.S4: Na-pyruvate did not inhibit [^{75}Se]-selenite transport either in hepatocytes or enterocytes (Figure S4A). Final selenite exposure concentration was 0.0125 μM for experiments with hepatocytes and 3.5 μM for enterocytes. In hepatocytes, propionic acid did not inhibit the uptake of [^{75}Se]-selenite. Data are presented as mean ± S.E.M. (n=5), where n represents the number of independent measurements using cells from as many fish. The statistical significance in respective treatments was analyzed by One Way ANOVA ($p < 0.05$).

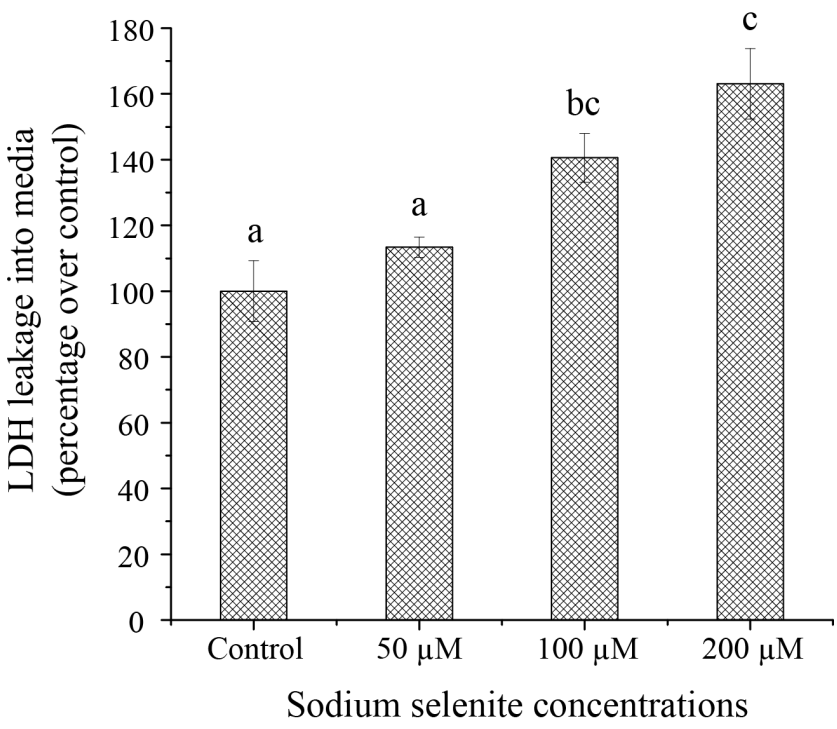

Figure C4.S1: LDH leakage into the exposure media from hepatocytes exposed to selenite (0 – 200µM) for 24 h. Significant difference in LDH leakage (One way ANOVA, $p \leq 0.01$) was recorded only at the highest exposure dose after 24 h, compared to the control. The data are presented as the mean ± S.E.M. of 4 – 5 independent observations, where each observation represents cells isolated from an individual fish.

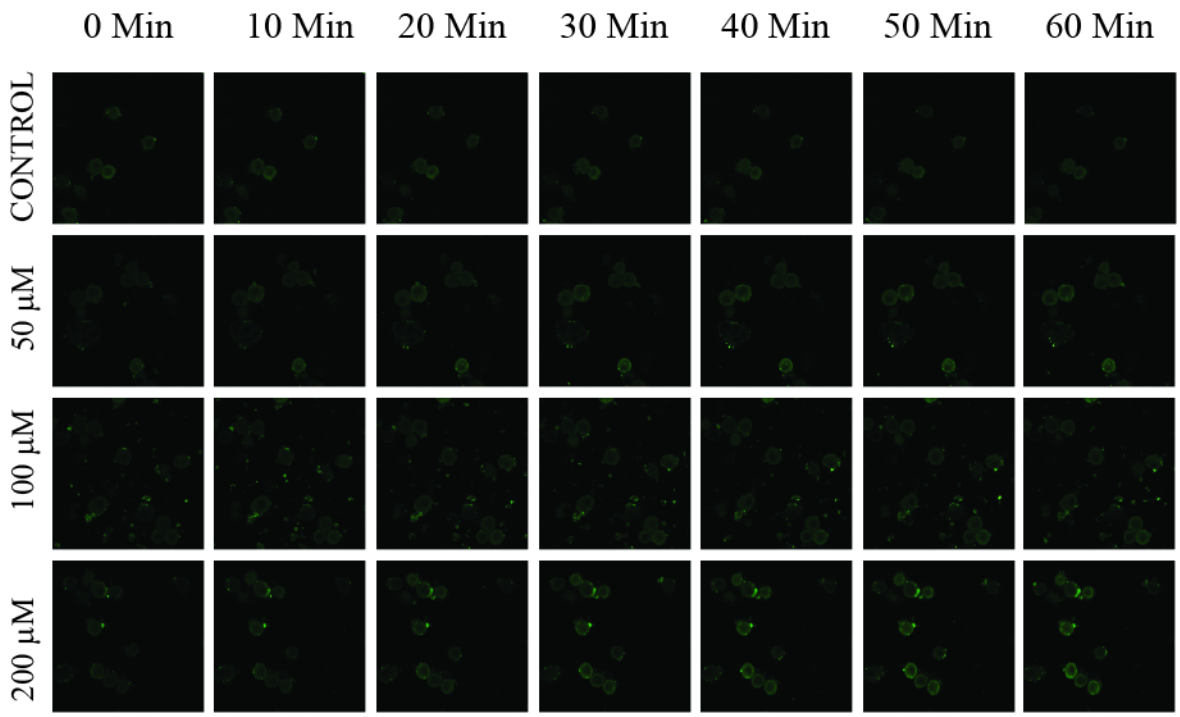

Figure C4.S2: Confocal images of hepatocytes showing time-dependent changes in $[Ca^{2+}]_i$ following short-term (60 min) exposure to 0 – 200µM selenite. Time '0' indicates the initiation of time series image capture that took about 5 min (sample processing) from the initiation of exposure. A rapid increase in the $[Ca^{2+}]_i$ was recorded over time in hepatocytes following exposure to selenite. The images shown here are representative of 2 independent experiments, and each experiment was conducted using cells isolated from an individual fish.

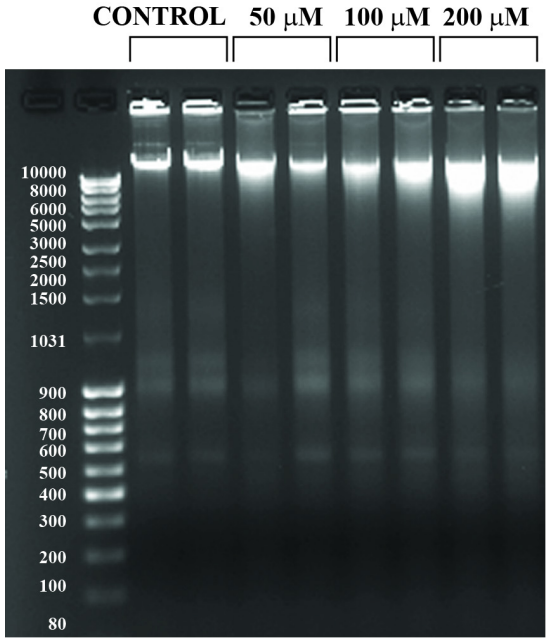

Figure C4.S3: Ethidium bromide stained gel was used to demonstrate the effect of selenite exposure for 24 h on the integrity of genomic DNA in hepatocytes. The left most panel shows the molecular weight markers that correspond to their molecular weight (kb). The smearing pattern at the highest exposure dose (200μM) indicates DNA damage. Two lanes for each dose are the representative of genomic DNA isolated from 2 independent experiments, and each experiment was conducted using cells isolated from an individual fish.

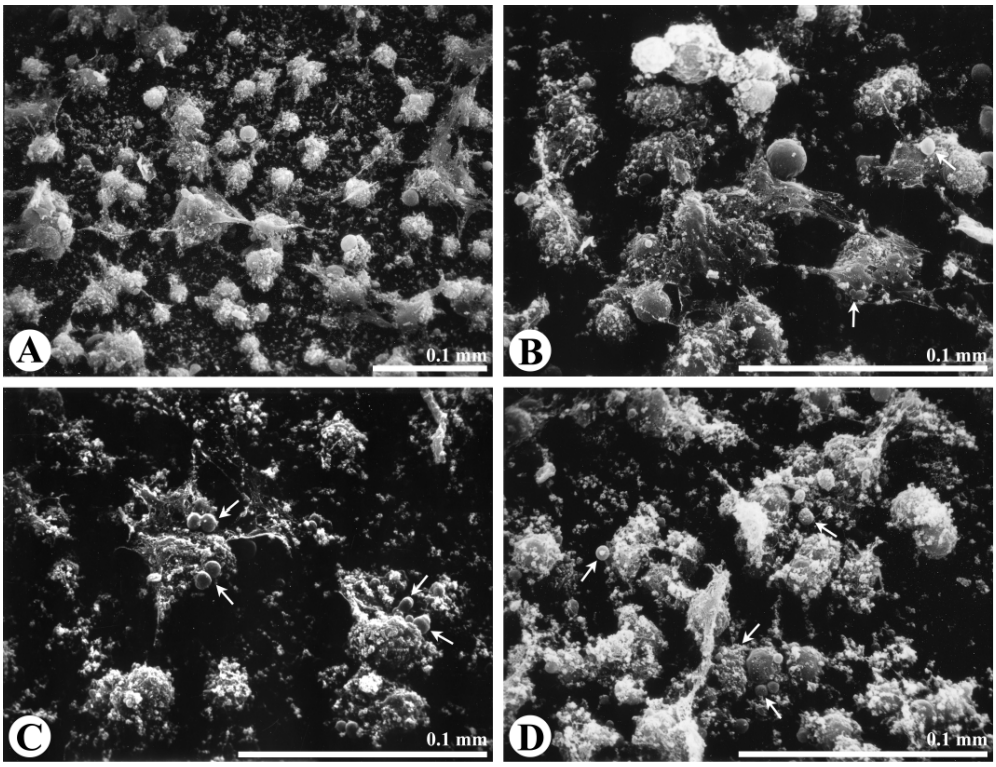

Figure C4.S3: Scanning Electron Microscope (SEM) images of trout hepatocytes exposed to different doses of selenite (A – Control, B – 50µM, C – 100µM and D – 200µM) for 24 hrs. The arrows show bleb formation in the plasma membrane of exposed hepatocytes, indicating typical morphological changes associated with apoptosis. The images shown here are the representative of 2 independent experiments, and each experiment was conducted using cells isolated from an individual fish.